

Cristiana Andreia Vieira Torres

Mestre

**Engineering of Bacterial Exopolysaccharides:
From Synthesis to Properties**

Dissertação para obtenção do Grau de Doutor em Engenharia
Química e Bioquímica

Orientadora: Professora Doutora Maria d'Ascensão C. F. Miranda Reis
Co-orientador: Doutora Maria Filomena Andrade de Freitas
Co-orientador: Doutor Vítor Manuel Delgado Alves

Júri:

Presidente: Professora Doutora Maria Elvira Fortunato

Arguentes: Doutor Bruno Sommer Ferreira

Professora Doutora Isabel Maria Nunes de Sousa

Vogais: Professor Doutor Arsénio Mendes Fialho

Professora Doutora Margarida Moldão Martins

Doutor Christophe François Aimé Roca

Dezembro, 2012

Engineering of Bacterial Exopolysaccharides: From Synthesis to Properties

Copyright © Cristiana Andreia Vieira Torres, Faculdade de Ciências e Tecnologia, Universidade Nova de Lisboa.

A Faculdade de Ciências e Tecnologia e a Universidade Nova de Lisboa têm o direito, perpétuo e sem limites geográficos, de arquivar e publicar esta dissertação através de exemplares impressos reproduzidos em papel ou de forma digital, ou por qualquer outro meio conhecido ou que venha a ser inventado, e de a divulgar através de repositórios científicos e de admitir a sua cópia e distribuição com objectivos educacionais ou de investigação, não comerciais, desde que seja dado crédito ao autor e editor. Note-se que o conteúdo de alguns capítulos, quando devidamente assinalados, fazem parte integral ou parcial de publicações em revistas científicas, que detêm os direitos de autor, embora prevendo o direito à sua reprodução em teses ou trabalhos académicos.

Agradecimentos

Em primeiro lugar, gostaria de agradecer à minha orientadora, Maria Ascensão Reis, por esta oportunidade, pelo entusiasmo transmitido, pelas interessantes discussões e por nos momentos mais difíceis ter tido disponibilidade para me ouvir.

Aos meus co-orientadores Filomena Freitas e Vítor Alves um muito obrigada! Obrigada pela disponibilidade, por todas as discussões motivantes, por toda a partilha de conhecimento e acima de tudo obrigada pela amizade!

À Professora Ana Ramos, uma das principais responsáveis pela minha iniciação no mundo da investigação, um muito obrigado por toda simpatia e toda a disponibilidade demonstrada sempre que precisei de usar o GPC.

À Madalena Cruz, Rodolfo Marques e Sílvia Antunes, quero agradecer por toda a ajuda no trabalho laboratorial e também pela amizade.

À Carla Portugal agradeço a ajuda na diafiltração e também os momentos de boa disposição.

À Professora Maria João Melo agradeço toda a ajuda na utilização do FTIR.

Não posso também deixar de agradecer a simpatia com que todos me receberam ao longo das minhas temporadas no CEER (Centro de Engenharia dos Biosistemas) do Instituto Superior de Agronomia. Tendo que destacar, a Professora Isabel Sousa por toda a disponibilidade demonstrada e também por toda a simpatia.

Agradeço à SGC Energia – Biovegetal – o fornecimento do glicerol (subproduto do biodiesel).

Aos meus colegas do grupo BPEG agradeço o espírito de entreatajuda ao longo destes anos. Mas acima de tudo, não posso deixar de salientar que tem sido uma experiência única trabalhar com todos vocês, a qual me enriqueceu bastante a nível pessoal e profissional. Tenho contudo que dar especial destaque a algumas pessoas, Luísa Neves, Joana Pais, Mónica Carvalheira, Carla Daniel, Rita Ferreira e Nuno Costa, a todos agradeço os

momentos de boa disposição, o apoio e por todos os momentos partilhados ao longo destes anos.

À minha amiga Joana, provavelmente a grande responsável por eu ter enveredado no mundo da investigação, um muito obrigada por todo o interesse, toda a cumplicidade e todo o apoio.

Aos meus pais por um muito obrigada por todo o apoio e motivação!

Ao Filipe um obrigado muito especial por tudo, o interesse demonstrado pelo meu trabalho, a ajuda, o apoio, o carinho e a paciência.

À Fundação para a Ciência e Tecnologia agradeço o financiamento da bolsa.

Resumo

O trabalho realizado nesta tese centra-se na produção e caracterização de um novo exopolissacárido (EPS) bacteriano de alto valor acrescentado, denominado por FucoPol. Neste processo utilizou-se como substrato o subproduto da indústria do biodiesel – glicerol. A bactéria produtora de EPS, isolada de uma solução de glicerol contaminada, foi caracterizada morfológica, bioquímica e geneticamente e denominada por *Enterobacter* estirpe A47.

A produção do exopolissacárido pela *Enterobacter* A47 foi realizada em condições controladas de temperatura e pH (30.0 °C e 6.80). O FucoPol apresenta um elevado peso molecular ($\sim 5.0 \times 10^6$) e é rico em fucose, uma característica interessante, uma vez que a fucose é um dos açúcares raros e difíceis de obter na natureza. Tipicamente, o FucoPol é composto por açúcares, nomeadamente, fucose (32 – 36 %mol), galactose (25 – 26 %mol), glucose (28 – 34 %mol) e ácido glucorónico (9 – 10 %mol), e grupos acilo, particularmente acetato (3 – 5 wt.%), piruvato (13 – 14 wt.%) e succinato (3 wt.%).

De modo a otimizar a produção de FucoPol, foi estudado o impacto da temperatura (15.6 – 44.1 °C) e pH (5.6 – 8.4) no crescimento celular e produção de EPS. Para tal foram utilizadas ferramentas estatísticas, tais como a metodologia de superfície de resposta e o desenho compósito central. Os resultados mostraram que *Enterobacter* A47 tem a capacidade de sintetizar diferentes heteropolissacáridos em função do pH e temperatura, uma característica que pode ser explorada de modo a obter polímeros com composições em função das aplicações desejadas. Para além disso, a produção de polímeros com elevado conteúdo em fucose foi estável para uma larga gama de valores de pH (6.0 – 8.0) e de temperatura (25 – 35 °C), o que é importante para o desenvolvimento do processo tendo em vista uma aplicação industrial.

Estudou-se também, em dois grupos de experiências, a influência da concentração de glicerol e azoto. No primeiro grupo, foi avaliado o efeito da concentração inicial de glicerol e azoto na fase “batch” e no segundo grupo o impacto de usar soluções de

alimentação com diferentes concentrações de glicerol e azoto na fase “fed-batch”. A bactéria *Enterobacter* A47 teve um desempenho semelhante numa vasta gama de concentrações iniciais de glicerol e azoto (25 – 50 e 0.68 – 1.05 g L⁻¹, respectivamente), tanto para a produção (~8 g L⁻¹) como para a composição do EPS (idêntica à composição típica). Utilizando uma solução de alimentação com uma concentração de glicerol (400 g L⁻¹) e de azoto (9 g L⁻¹) obteve-se a maior síntese de EPS (10.16 g L⁻¹), a maior produtividade volumétrica (5.52 g L⁻¹ d⁻¹) e o maior conteúdo em fucose (41 %mol).

Foram estudadas as propriedades do FucoPol em solução, de modo a perceber o seu potencial de aplicação. O FucoPol apresenta uma viscosidade intrínseca de cerca de 8 dL g⁻¹ e as suas soluções aquosas apresentam um comportamento reofluidificante. Verificou-se que, tanto o valor da viscosidade intrínseca como o comportamento reofluidificante se mantêm numa gama alargada de valores de pH e força iónica (3.5 – 8.0 e 0.05-0.50 M NaCl, respectivamente). O FucoPol apresentou uma capacidade de espessamento semelhante à demonstrada pela goma guar. Verificou-se ainda que as soluções de FucoPol mantêm a sua viscosidade aparente e as suas propriedades viscoelásticas à temperatura de 25 °C, após ciclos consecutivos de aquecimento (até T=80°C) e arrefecimento, indicando uma boa estabilidade térmica quando sujeitas a flutuações de temperatura. Estas propriedades indiciam que o FucoPol poderá ser utilizado como agente espessante em soluções aquosas que sofram variações de pH, força iónica e temperatura.

Foi também realizado um estudo preliminar sobre a capacidade do FucoPol formar e estabilizar emulsões de compostos hidrofóbicos em água, demonstrando um bom potencial para vários compostos, em particular para óleos alimentares (índice de emulsão, E₂₄ > 60%). Esta capacidade é similar à de outros polissacáridos comerciais (ex. xantano e pectina). A sua capacidade de floculação foi também avaliada, demonstrando ser semelhante a alguns produtos já comercializados (ex. xantano e carboximetilcelulose)

As propriedades apresentadas pelo FucoPol, nomeadamente as propriedades reológicas, assim como a capacidade de formar e estabilizar emulsões e a sua actividade floculante, conferem-lhe grande potencial para ser utilizado em várias aplicações (ex.: produtos alimentares, cosméticos e farmacêuticos; detergentes, fluídos de perfuração).

Abstract

This thesis is focused on the production and characterisation of a novel value added bacterial exopolysaccharide (EPS), named FucoPol, using glycerol byproduct from the biodiesel industry as carbon source. The EPS producing bacterium was isolated from a contaminated glycerol solution. It was morphologically, biochemically and genetically characterized and named *Enterobacter* A47.

Exopolysaccharide production by *Enterobacter* A47 was performed under controlled temperature and pH (30.0°C and 6.80, respectively). FucoPol has a high molecular weight ($\sim 5.0 \times 10^6$) and was rich in fucose, which is very interesting, since fucose is one of the rare sugars difficult to obtain in Nature. Typically, FucoPol is composed of sugar monomers, namely, fucose (32 – 36 %mol), galactose (25 – 26 %mol), glucose (28 – 34 %mol) and glucuronic acid (9 – 10 %mol); and acyl group substituents, namely, acetyl (3 – 5 wt%), pyruvyl (13 – 14 wt%) and succinyl (3 wt%).

In order to optimize FucoPol production the impact of temperature (15.6 to 44.1 °C) and pH (5.6 to 8.4) on cellular growth and EPS production was assessed using statistical tools (response surface methodology and central composite design). *Enterobacter* A47 revealed the ability to synthesize different heteropolysaccharides as a function of pH and temperature, a feature that can be exploited to obtain tailored polymer compositions. Moreover, the synthesis of high fucose content EPS was stable for wide pH (6.0 – 8.0) and temperature (25 – 35 °C) ranges, which is important for the envisaged industrial development of the bioprocess.

Afterwards, the influence of glycerol and nitrogen concentration was also evaluated in two sets of experiments. In the first set, the effect of the initial nitrogen and glycerol concentrations was assessed, while in the second the impact of using different glycerol and nitrogen concentrations in the feeding solution was studied. *Enterobacter* A47 demonstrated to have a stable performance, both in terms of EPS production ($\sim 8.00 \text{ g L}^{-1}$) and in EPS composition, within initial glycerol and nitrogen concentrations of 25 – 50 and

0.68 – 1.05 g L⁻¹, respectively. On the other hand, the highest EPS synthesis (10.16 g L⁻¹), volumetric productivity (5.52 g L⁻¹ d⁻¹), and fucose content (41 %mol) were reached when the feeding solution had a higher glycerol concentration (400 g L⁻¹) and a nitrogen concentration of 9 g L⁻¹.

In order to understand the potential for FucoPol's industrial applicability, its solution properties were studied. FucoPol had an intrinsic viscosity of ~8.00 dL g⁻¹ and produced viscous aqueous solutions with a shear thinning behaviour. Both intrinsic viscosity and shear thinning behaviour were maintained under a wide range of pH and ionic strength values (3.5 – 8.0 and 0.05 – 0.50 M NaCl, respectively). The thickening capacity of FucoPol was similar to that of commercial guar gum. The influence of temperature on steady shear and oscillatory data was also evaluated in the temperature range from 15 to 65 °C. FucoPol has shown to form high viscosity solutions with a shear-thinning behaviour. Moreover, the viscous and viscoelastic properties at 25 °C were maintained after consecutive heating (up to 80°C) and cooling cycles, indicating a good thermal stability under temperature fluctuations. Therefore, the application of FucoPol as thickening agent is foreseen in aqueous solutions with variations of pH, ionic strength as well as temperature.

A preliminary study about the FucoPol's emulsion forming and stabilizing capacity, as well as flocculating activity were performed. FucoPol has shown a good emulsion forming and stabilizing capacity for hydrophobic compounds, especially for food grade oils (emulsification index, E₂₄ > 60%), similar to some commercial polysaccharides (e.g. xanthan and pectin). Furthermore, FucoPol has also demonstrated good flocculating capacity (28%), in the same range of some commercially available products (e.g. xanthan and carboxymethylcellulose).

The main properties of FucoPol, namely, rheological properties in aqueous medium, emulsion forming and stabilizing capacity, and flocculating capacity, make it a promising alternative to be used in several industrial applications (food processing, detergents, oil drilling fluids). On the other hand, the presence of fucose renders it an enormous potential for use in pharmaceutical and cosmetic formulations, wherein it may be used alone or blended with other polymers (e.g. chitosan).

Nomenclature

Abbreviations

ANOVA	Analysis of Variance
CCRD	Central Composite Rotatable Design
CDW	Cell Dry Weight
CMC	Carboxymethylcellulose
DO	Dissolved Oxygen
DSMZ	Deutsche Sammlung von Mikroorganismen und Zellkulture
EMBL	European Molecular Biology Laboratory
EPS	Exopolysaccharide
FT-IR	Fourier Transform Infra-Red spectroscopy
GRAS	Generally Recognized As Safe
HMO	Human Milk Oligosaccharides
HPLC	High Performance Liquid Chromatography
IS	Ionic Strength
MLR	Multiple Linear Regression
O/W	Oil/Water
PCR	Polymerase Chain Reaction
PD	Polydispersity
RDP	Ribosomal Database Program
RSM	Response Surface Methodology

SEC-MALLS	Size Exclusion Chromatography – Multi-Angle Laser Light Scattering
SS	Sum of Squares
TCA	Trichloroacetic Acid
TFA	Trifluoroacetic Acid

Variables

A	Pre-exponential factor
A	Optical density of the control in flocculating activity determination
Acet	Acetyl content (wt.%)
a_T	Temperature-dependent shift factor
B	Optical density of the sample in flocculating activity determination
b_0	Coefficient estimate for interception
b_i	Coefficient estimate for linear correlation
b_{ij}	Coefficient estimate for quadratic correlation
b_T	Temperature density ratio
C	FucoPol concentration
C:N ratio	Carbon to nitrogen ratio (w/w)
D	Dilution rate (h^{-1})
dn/dc	Refractive index increment (mL g^{-1})
E_{24}	Emulsification index after 24 hours (%)
E_a	Activation energy (kJ mol^{-1})

EPS_{\max}	Maximum EPS concentration (g L^{-1})
F	Inlet feed rate in the fed-batch phase (L h^{-1})
F	Frequency (Hz)
Fuc	Fucose content (%mol)
G'	Storage modulus (Pa)
G''	Loss modulus (Pa)
Gal	Galactose content (%mol)
Glc	Glucose content (%mol)
GlcA	Glucuronic acid content (%mol)
GlcN	Glucosamine content (%mol)
h_e	Height of the emulsion layer (mm)
h_t	Overall height of mixture (mm)
K	Consistency index (Pa s^{-1})
K_d	Specific death rate (h^{-1})
k_H	Huggins coefficient (dimensionless)
k_k	Kramer coefficient (dimensionless)
K_M	Martin polymer-polymer interaction parameter (dimensionless)
K_N	Nitrogen half saturation constant (g L^{-1})
K_S	Glycerol half saturation constant (g L^{-1})
M	Dimensionless constant related to the exponent of the power law
m_S	Maintenance coefficient on glycerol ($\text{g g}^{-1} \text{h}^{-1}$)
Mn	Number average molecular weight
Mw	Weight average molecular weight

N	Nitrogen concentration (g L^{-1})
N	Power law index
N_0	Inlet nitrogen concentration (g L^{-1})
P	EPS concentration (g L^{-1})
pH	pH (dimensionless)
Pyr	Pyruvyl content (wt.%)
q_p	Specific productivity ($\text{gEPS gCDW}^{-1} \text{d}^{-1}$)
R	Gas constant ($\text{kJ mol}^{-1} \text{K}^{-1}$)
Rha	Rhamnose content (%mol)
r_p	EPS volumetric productivity ($\text{g L}^{-1} \text{d}^{-1}$)
Succ	Succinyl content (wt.%)
S	Glycerol concentration (g L^{-1})
S_0	Inlet glycerol concentration (g L^{-1})
T	Time (d)
T	Temperature ($^{\circ}\text{C}$)
T_0	Reference temperature ($^{\circ}\text{C}$)
V	Volume (L)
v_s	Specific rate of glycerol uptake ($\text{g g}^{-1} \text{h}^{-1}$)
v_N	Specific rate of nitrogen uptake ($\text{g g}^{-1} \text{h}^{-1}$)
v_p	Specific rate of EPS production ($\text{g g}^{-1} \text{h}^{-1}$)
X	Biomass concentration (g L^{-1})
X_i	Experimental variables in RSM
Y_i	Observed responses in RSM

$Y_{X/S}$	Yield of biomass on glycerol (g g^{-1})
$Y_{P/S}$	Yield of EPS on glycerol (g g^{-1})
$Y_{X/N}$	Yield of biomass on nitrogen (g g^{-1})
Y_p	Predicted responses in RSM

Greek letters

α	Axial level in RSM
α	Yield of product synthesis per biomass produced (g g^{-1})
α	Pre-exponential factor of the power law regression
B	Specific rate of non-growth associated product synthesis ($\text{g g}^{-1} \text{h}^{-1}$)
B	Exponent in the power law regression
$\dot{\gamma}$	Shear rate (s^{-1})
$[\eta]$	Intrinsic viscosity (dL g^{-1})
η_0	Zero-shear rate viscosity (Pa s)
η_a	Apparent viscosity (Pa s)
η_{sp}	Specific viscosity (dimensionless)
η_{rel}	Relative viscosity (dimensionless)
η^*	Complex viscosity (Pa s)
η'	Dynamic viscosity (Pa s)
η''	Out-of-phase viscosity (Pa s)
μ	Specific growth rate (h^{-1})

μ_{\max}	Maximum specific growth rate (h^{-1})
T	Shear stress (Pa)
T	Time constant for Eq. 2.18 (s)

Table of Contents

1. Background and Motivation	1
1.1. Polysaccharides	2
1.2. Fermentative Exopolysaccharides Production	8
1.3. Motivation	11
1.4. Thesis Outline	11
2. FucoPol Standard Bioprocess Operation and Polymer Characterisation	13
2.1. Summary	14
2.2. Introduction	15
2.3. Materials and Methods	18
2.3.1. FucoPol Production	18
2.3.2. Culture Broth Characterization	24
2.3.3. FucoPol Characterization	25
2.4. Results and Discussion	27
2.4.1. Identification and Characterization of the Microorganism	27
2.4.2. FucoPol Production Process	32
2.4.3. Characterization of the Culture Broth	36
2.4.4. FucoPol Characterization	46
2.5. Conclusions	55
3. Optimization of FucoPol Production: Study of the Interactive Effect of	57

Temperature and pH using Multivariate Statistical Analysis	
3.1. Summary	58
3.2. Introduction	59
3.3. Material and Methods	60
3.3.1. FucoPol Production	60
3.3.2. FucoPol Characterization	61
3.3.3. Experimental Design	62
3.4. Results and Discussion	63
3.4.1. Standard Conditions for EPS Production	64
3.4.2. Influence of Temperature and pH: Response Analysis	64
3.4.3. RSM Modelling	68
3.5. Conclusions	76
4. FucoPol: Impact of glycerol and nitrogen concentration	77
4.1. Summary	78
4.2. Introduction	79
4.3. Materials and Methods	80
4.3.1. FucoPol Production	80
4.4. Results and Discussion	81
4.4.1. Effect of Initial Glycerol and Nitrogen Concentration	82
4.4.2. Effect of Changing Glycerol and Nitrogen Concentration in the Feeding Solution	87
4.4.3. EPS Physical-chemical Characterization	90
4.5. Conclusions	93

5. FucoPol: Properties in aqueous solutions	95
5.1. Summary	96
5.2. Introduction	96
5.3. Materials and Methods	98
5.3.1. Preparation of FucoPol Aqueous Solutions	98
5.3.2. Rheological Measurements	98
5.3.3. Experimental Design	100
5.4. Results and Discussion	101
5.4.1. Intrinsic Viscosity	101
5.4.2. Rheological Properties under Steady and Dynamic Shear	106
5.4.3. Concentration Regimes	125
5.5. Conclusions	127
6. FucoPol: Emulsifying and Flocculating Capacity	129
6.1. Summary	130
6.2. Introduction	131
6.3. Material and Methods	133
6.3.1. Emulsion forming and stabilizing capacity	133
6.3.2. Flocculating activity	134
6.4. Results and discussion	135
6.4.1. Emulsion forming and stabilizing capacity	135
6.4.2. Flocculating activity	143
6.5. Conclusions	144
7. General Conclusions and Future Work	147

7.1. General Conclusions	148
7.2. Future Work	150
Bibliography	151

List of Figures

- Figure 2.1 Flow behaviour – Newtonian and shear-thinning – at logarithmic scale. 17
- Figure 2.2 Phylogenetic analysis based on 16S rRNA gene sequences available from 31 European Molecular Biology Laboratory (EMBL), Ribosomal Database Program (RDP) and DSMZ databases (accession numbers are given in brackets). The scale bar below the dendrograms indicates 1 nucleotide substitutions per 100 nucleotides.
- Figure 2.3 Time course of the cultivation of *Enterobacter* A47 on glycerol byproduct: 33 (□) glycerol, (×) ammonium, (⊠) CDW and (▲) EPS. (a) Initial glycerol and nitrogen concentration of 25 and 0.7 g L⁻¹, respectively; (b) Initial glycerol and nitrogen concentration of 40 and 1.1 g L⁻¹, respectively.
- Figure 2.4 Experimental (symbols) and modelling results (continuous lines) showing 35 the (□) glycerol, (×) ammonia, (⊠) biomass and (▲) EPS kinetics with time. The mean square errors were 0.194 g L⁻¹, 4.09 g L⁻¹, 0.020 g L⁻¹ and 0.181 g L⁻¹ for biomass, glycerol, ammonia and EPS respectively.
- Figure 2.5 Microscopic observations of *Enterobacter* A47 broth samples at different 38 cultivation times: 1.0 day (upper images: A and B), 3.0 days (middle images: C and D) and end of cultivation run (lower images: E and F), observed in phase contrast (left images) and after staining with China ink (right images).
- Figure 2.6 Flow curves for culture broth samples at different cultivation times: (Δ) 0 40 days, (-) 1.0 days, (×) 2.0 days, (■) 4.0 days, (⊠) 5.0 days, (◇) 6.0 days and (▲) 7.0 days. The measurements were made at 30 °C.
- Figure 2.7 Steady-state (A) and oscillatory data (B) of the culture broth at day 7.0 (■), 42 and of an aqueous solution in deionised water of the purified EPS taken at day 7.0 (▲), both samples having the same effective polymer concentration (0.81 wt%). G' (full symbols), G'' (open symbols).

Figure 2.8 Storage (■) and loss modulus (□) for broth samples taken at different 45
cultivation times: (a) 4.0 days; (b) 5.0 days; (c) 6.0 days and (d) 7.0 days.

Figure 2.9 Cox–Merz plots for the broth samples isolated at days 4.0 and 7.0: (-) 46
apparent viscosity; (○) complex viscosity and (●) dynamic viscosity.

Figure 2.10 Profile of the FucoPol neutral sugar composition ((×) glucose; (□) 47
galactose; (●) fucose) (A) and acyl groups ((■) succinyl; (○) pyruvyl and (△) acetyl)
(B) along the cultivation run.

Figure 2.11 Resumed diagram of nucleotide biosynthetic pathway involved in bacterial 48
EPS synthesis by Gram- negative bacteria. NDP, nucleoside diphosphate; UDP,
uridine diphosphate; GDP, guanosine diphosphate (adapted from Freitas et al.,
2011a).

Figure 2.12 Comparative FT-IR spectra of polysaccharides: (a) FucoPol, (b) Fucogel, (c) 51
alginate and (d) guar gum.

Figure 2.13 (a) Evolution of FucoPol's average molecular weight (Ж) and 52
polydispersity (■) along the cultivation run. (b) Variation of the intrinsic viscosity over
time.

Figure 2.14 Mw chromatogram profiles for different cultivation times. 53

Figure 3.1 Response surface of specific growth rate (a); EPS concentration (b) and 72
specific productivity (c) as a function of temperature and pH.

Figure 3.2 Response surface of fucose (a); galactose (b) glucose (c); glucuronic acid (d); 73
rhamnose (e) and glucosamine (f) as a function of temperature and pH.

Figure 3.3 Response surface of acyl groups total content (% wt.) as a function of 74
temperature and pH.

Figure 3.4 Response surface of molecular weight as a function of temperature and pH. 75

Figure 4.1 Impact of initial glycerol and nitrogen concentrations on cell growth and 84
EPS production across the different cultivation runs (a) Run 1; (b) Run 2 and (c) Run

3. Profile of cultivation runs: (▲) EPS (g L^{-1}); (◻) CDW (g L^{-1}); (*) N-NH_4^+ (g L^{-1}); (□) glycerol (g L^{-1}).

Figure 4.2 Impact of nitrogen concentration on biomass (●) and EPS production (▲), 85 for all the 5 runs (Stdr 1 and 2 and runs 1 to 3).

Figure 4.3 Impact of glycerol and nitrogen concentrations in the feeding solution. 89 Time course of the cultivation runs: (a) Run 4, (b) Run 5 and (c) Run6 ((▲) EPS (g L^{-1}); (◻) CDW (g L^{-1}); (*) N-NH_4^+ (g L^{-1}); (□) glycerol (g L^{-1})).

Figure 5.1 (a) Reduced viscosity as a function of FucoPol concentration in salt free 102 solution; (b) determination of the intrinsic viscosity in 0.1 M NaCl using the Huggins (□) and (■) Kraemer equations.

Figure 5.2 Response surface plot of intrinsic viscosity $[\eta]$ as a function of pH and NaCl 105 concentration.

Figure 5.3 Shear rate dependence of viscosity for different concentrations of FucoPol. 107 (▲) 0.20 wt.%; (○) 0.35 wt.%; (□) 0.45 wt.%; (*) 0.50 wt.%; (◇) 0.60 wt.%; (◻) 0.80 wt.%; (x) 0.90 wt.%; (▪) 1.0 wt.%; (◆) 1.2 wt. %. Lines represented the fitted Cross equation.

Figure 5.4 Master curve obtained shifting vertically dividing by η_0 , and horizontally 109 multiplying by relaxation time (τ). Inset: τ as a function of FucoPol concentration.

Figure 5.5 Comparative flow curves of polysaccharides (C=1%wt, 0.1M NaCl): (■) 110 FucoPol; (□) Fucogel; (x) xanthan; (○) guar gum; (◻) CMC; (▲) pectin and (◆) alginate.

Figure 5.6 Mechanical spectra (G' (■); G'' (□)) of FucoPol aqueous solution at 111 different concentrations in 0.1 M NaCl. (a) 0.6 wt.%; (b) 0.8 wt.%; (c) 1 wt.% and (d) 1.2 wt.%.

Figure 5.7 Apparent viscosity and complex viscosity (FucoPol solution 1.0 wt.%) as a 112 function of the shear rate and angular frequency, respectively.

Figure 5.8 Effect of ionic strength NaCl (M) and pH on FucoPol's shear rate 114
dependency on viscosity. (◆) 0.15M NaCl - pH 4.5; (■) 0.65 M NaCl – pH 4.5; (△)
0.15 M NaCl – pH 9.5; (×) 0.65 M NaCl – pH 9.5; (✱) 0.40 M NaCl – pH 7.0; (⊠) 0.40 M
NaCl – pH 7.0; (+)0.40 M NaCl – pH 7.0; (*) 0.05M NaCl – pH 7.00; (•) 0.75 M NaCl –
pH 7.00; (◇) 0.40 M NaCl – pH 3.47; (□) 0.40 M NaCl – pH 10.54. Lines represent the
fitted model.

Figure 5.9 Response surface of zero-shear viscosity (η_0) as a function of pH and NaCl 115
concentration.

Figure 5.10 Mechanical spectra for FucoPol solutions with different ionic strength and 116
pH values, G' (full symbols) and G'' (empty symbols). (a) (● and ○) 0.75 M NaCl – pH
7.00; (▲ and △) 0.05 M NaCl – pH 7.00; (b) (■ and □) 0.40 M NaCl – pH 7.00; (c) (●
and ○) 0.40 M NaCl – pH 3.45; (▲ and △) 0.40 M NaCl – pH 10.54.

Figure 5.11 Flow curves for a 0.81 wt.% FucoPol solution at different temperatures: 117
(◆) 15°C; (○) 25°C; (▲) 30°C; (■) 45°C; (✱) 55°C; (+) 65°C.

Figure 5.12 (a) Mechanical spectra of 0.81wt.% FucoPol solution at 15 °C (squares) 120
and 65 °C (triangles), G' - full symbols; G'' - open symbols. (b) Dynamic viscosity η' (full
symbols) and out of phase viscosity η'' (open symbols) as a function of the applied
frequency for 15 °C (squares), 45 °C (bullets) and 65 °C (triangles).

Figure 5.13 Frequency and temperature superposition of the loss (G'') and storage 121
(G') moduli. The solid line represents the data for the reference temperature (25 °C)
and the symbols correspond to the other temperatures: (△) 15 °C; (■) 30 °C; (●) 45
°C; (◆) 55 °C; (□) 65 °C.

Figure 5.14 Temperature dependence of: apparent viscosity at shear rate 5 s^{-1} (●) and 123
 13 s^{-1} (■); zero-shear rate viscosity estimated by the Carreau model (◇). The lines
correspond to Arrhenius equation.

Figure 5.15 Data measured at 25 °C before (open symbols) and after (full symbols) the 124
temperature cycles: (a) flow curves; (b) dynamic moduli and (c) dynamic (η') and out

of phase (η'') viscosities.

Figure 5.16 Apparent viscosity η (lines), and complex viscosity $|\eta^*|$ (symbols), as a function of the shear rate and angular frequency, respectively. 125

Figure 5.17 Concentration dependence of zero-shear specific viscosity for FucoPol samples. Dotted line: Martin model 126

Figure 6.1 Flow curves of emulsions prepared with different polymer concentrations ((a) 0.50 wt.%; (b) 1.00 wt.% and (c) 1.50 wt.%) and different oil-water proportions: 20/80 (diamonds); 40/60 (bullets); 60/40 (squares); 80/20 (triangles). 139

Figure 6.2 Mechanical spectra showing the frequency dependence of G' (full symbols) and G'' (open symbols). (a) 0.50 wt.% (b) 1.00 wt.% (c) 1.50 wt.%. O/W ratios: 20/80 (diamonds); 40/60 (bullets); 60/40 (squares); 80/20 (triangles). 141

Figure 6.3 Mechanical spectra showing the frequency dependence of G' (full symbols) and G'' (open symbols). (a) 20/80 (b) 40/60 (c) 60/40 (d) 80/20. FucoPol wt.%: 0.5 (triangles); 1.0 (bullets); 1.5 (diamonds.). 142

Figure 6.4 Flocculating activity of FucoPol in comparison with commercially available flocculants 143

List of Tables

Table 2.1 Biochemical and physiological characteristics of <i>Enterobacter</i> A47 in comparison with related species type strains <i>Enterobacter pyrinus</i> KCTC 2520T, <i>E. hormaechei</i> ATCC 49162T and <i>E. asburiae</i> ATCC 35953T	29
Table 2.2 16SrDNA gene sequence of the bacterium <i>Enterobacter</i> A47 (DSM 23139)	30
Table 2.3 Maximum yields and Michaelis-Menten constant for glycerol uptake	36
Table 2.4 Power Law parameters for <i>Enterobacter</i> A47 broth samples taken at different cultivation times	41
Table 2.5 Cross model parameters for <i>Enterobacter</i> A47 broth samples taken at different cultivation times	44
Table 3.1 Central composite rotatable design (CCRD) with two independent variables, X_1 (Temperature, T) and X_2 (pH), and the observed responses studied, Y_i (μ , specific growth rate; EPS_{max} , maximum EPS concentration; qP , specific productivity; Fuc, fucose; Gal, galactose; Glc, glucose; Rha, rhamnose; GlcN, glucosamine; Pyr, pyruvyl; Succ; succinyl; Acet, acetyl; Mw, average molecular weight)	67
Table 3.2 Model and lack of fit p-values (significance levels) and R^2 values for the analysis of variance (ANOVA) for the responses of the central composite design	69
Table 3.3 Constants and coefficients of polynomial models and p-values for both linear and quadratic effects and interaction of temperature and pH for the several responses (Y_n)	71
Table 4.1 Kinetic parameters during batch and fed batch phase, as well as global values for the standard cultivation runs (section 2.4.2 – Chapter 2) and for runs 1 – 6	86
Table 4.2 Physical-chemical EPS characterization: sugar composition (%mol); acyl groups content (wt.%) and average molecular weight	92
Table 5.1 Central composite rotatable design (CCRD) with two independent variables	103

X_1 (Ionic Strength, IS) and X_2 (pH), and the observed responses studied Y_1 (intrinsic viscosity, $[\eta]$) and Y_2 (zero-shear rate viscosity, η_0)

Table 5.2 Analysis of variance of the second order model for parameter $[\eta]$ (intrinsic viscosity) 104

Table 5.3 Cross model parameters estimated for different FucoPol concentrations 108

Table 5.4 Analysis of variance of the second order model for parameter η_0 (zero shear viscosity from Cross model fitting) 115

Table 5.5 Parameters of Carreau model for the range of temperatures studied 118

Table 5.6 Shift factors of Time-Temperature Superposition 121

Table 6.1 Emulsification index (E_{24}) for FucoPol and commercially available emulsion forming and stabilizing agents against several hydrophobic compounds. All emulsions were prepared by mixing a 0.5wt% aqueous solution with each of the hydrophobic compound (3:2 v/v ratio) and left at room temperature for 24 h to determine E_{24} 136

Table 6.2 Emulsification index (E_{24}) for FucoPol against sunflower oil and apparent viscosity at a shear rate 1 s^{-1} for FucoPol solutions and emulsions with different O/W proportions 137

Table 6.3 β values of the power law regression for the different emulsions 140

Chapter 1

Background and Motivation

Polysaccharides have a wide spectrum of applications due to their functional properties (e.g. thickening, emulsifying, stabilizing and/or gelling capacity). Indeed, polysaccharides are currently used in all sectors of human activity, namely food and feed products, personal care products, medicine, pharmaceuticals, paper, oil drilling and paints, among others (Elnashar, 2011). Even when present at low concentrations (less than 1%), polysaccharides may have a significant influence on the products textural properties and on the efficiency of industrial processes (Phillips and Williams, 2009).

Being materials obtained from living organisms, natural polysaccharides are usually non-toxic and biodegradable, a feature that turns them into attractive biomaterials for sustainable development. Polysaccharides are widely distributed in nature: they can be found in plants, animals, algae and microorganisms, performing different fundamental biological functions (Reis et al., 2011; Elnashar, 2011).

Microbial polysaccharides often have improved or new properties, comparing to polysaccharides from other natural sources (e.g. plants and algae). Hence, in the last years, the demand for novel microbial polysaccharides with interesting properties for industrial applications has greatly increased.

1.1. Polysaccharides

Polysaccharides are high molecular weight ($10^4 - 10^7$) polymeric biomaterials with a large structural diversity, being composed of one or more monosaccharides joined by glycosidic bonds, often forming repeating units and presenting different degrees of branching (Sutherland, 2001; Reis et al., 2008). They are mainly composed of carbohydrates, such as neutral sugars (e.g. galactose, glucose), acidic sugars (e.g. glucuronic acid, galacturonic acid) and amino sugars (e.g. N-acetyl-glucosamine, N-acetyl-galactosamine). Furthermore, many polysaccharides possess non sugar substituents,

namely organic acyl groups (e.g. acetyl, succinyl and pyruvyl) and inorganic groups (e.g. sulphate, phosphate) (Sutherland, 1982). The presence of some acyl groups (e.g. succinyl and pyruvyl), as well as acidic or amino sugars, confers the polymers a polyelectrolyte character (Freitas et al., 2011).

Polysaccharides may be composed of a unique sort of monosaccharide (homopolysaccharides) or comprise two or more different monosaccharides (heteropolysaccharides). Besides that, in some cases, single polysaccharide chains may associate with each other through intra or intermolecular non-covalent bonds, conferring to the macromolecule a certain geometry and rigidity, which will determine the polymer's properties both in solid state and in solution (Kumar et al., 2007; Reis et al., 2011).

In Nature, polysaccharides can be obtained from plants (e.g. starch, guar gum, pectin), animals (e.g. chitin), algae (e.g. carrageenan, alginate, agar) and microorganisms (e.g. xanthan, gellan, pullulan). They present diverse physiological roles, functioning as structural elements, maintaining mechanical shape and rigidity of the living cells (e.g. cellulose and pectin in plant cell wall; chitin in arthropod exoskeletons and yeast and fungi cell walls), as energy reserve substances (e.g. starch or inulin in plants; glycogen in animals and microorganisms), or as adhesion and protective barriers (microorganisms) (Kaplan, 1998; Kumar et al., 2007; Elnashar, 2011).

Their ability to change the physical-chemical properties of aqueous solutions (e.g. thickening, emulsifying and stabilizing capacity), allows their application on several products and processes, namely in the food, pharmaceutical, cosmetic, paper, paint and oil drilling sectors. Beyond that, the capacity to form biodegradable films shown by some polysaccharides (e.g. starch, alginate, pullulan, cellulose derivatives) enables their use in packaging (e.g. vessels and sheets for several agro-food applications), pharmaceuticals and other industrial applications. Their biocompatibility also enables their use in medical applications (e.g. as scaffolds or matrices for tissue engineering, wound dressing and drug delivery) (Rehm, 2010).

Nowadays, the polysaccharides market is still dominated by products obtained from plants and algae (e.g. starch, galactomannans, pectin, carrageenan and alginate), while microbial polysaccharides represent only a small fraction of the market (e.g. xanthan) (Canilha et al., 2005). In 2008, the total market value was > 4 million US\$, with xanthan being the only significant microbial polysaccharide, which accounted for 6% of the total market value (Imeson, 2010; Freitas et al., 2011).

Microbial polysaccharides can be divided into intracellular (e.g. glycogen), structural cell wall components (e.g. chitin) and extracellular polysaccharides. Extracellular polysaccharides or exopolysaccharides (EPS) are polymers secreted by the cells, either as a capsule that remains associated with the cell surface (e.g. K30 antigens) or as a slime that is loosely bound to the cell surface (e.g. xanthan, gellan, hyaluronic acid) (Kumar et al., 2007; Rehm, 2010). Several different EPS (e.g. dextran, xanthan, gellan) have been extensively studied over the last decades. The research on many exopolysaccharides has relied on their biological functions, namely as reserve materials or as part of bacterial cell protective structure, providing an advantage under certain environmental conditions. Although the factors leading to EPS synthesis are still not clearly elucidate, it is thought to be a response of the microbial strains to environmental stress conditions (e.g. pH, temperature, light intensity) (Sutherland, 1998; Kumar et al., 2007; Rehm, 2010; Donot et al., 2012).

Some microbial EPS can replace polysaccharides extracted from plants (e.g. guar gum or pectin) or algae (e.g. carrageenan or alginate) in traditional applications, due to their improved physical properties (e.g. xanthan or gellan gum). On the other hand, other microbial EPS possess unique and superior properties that enable the development of new commercial opportunities (Freitas et al., 2011). For this reason, in recent years, there has been an increasing demand for the identification and isolation of new microbial polysaccharides that can compete with traditional polymers due to their improved physical and chemical properties: higher emulsifying and flocculating activities; resistance to solvents; biological activity (e.g. anticarcinogenic and immunoenhancing effects); and rheological characteristics (e.g. higher viscosity for lower polymer concentrations and

greater stability to a wide ranges of temperature, pH and ionic strength) (Kumar et al., 2007; Sutherland, 2001).

Furthermore, microbial polysaccharides production is advantageous comparing with that of plant and algae-derived polysaccharides, since it is usually more productive and less resource intensive, and relies on controlled fermentation processes, with more degrees of freedom to control product composition, yield and productivity (Moreno et al., 1998). On the other hand, plants, algae and animals have life cycles of months or years, being the production cycle usually seasonal. Moreover, they are subjected to climatic and environmental impact, such as pollution, which causes great variability in the quantity and quality of the final products.

However, for new microbial polysaccharides to conquer the market as commodity products, it is crucial to lower their production costs (Rehm, 2010), which can be performed by: (i) using low cost substrates, (ii) improving product yield by optimizing fermentation conditions, (iii) developing higher yielding strains (e.g. by mutagenesis or genetic manipulation), and (iv) optimizing downstream processing. The great opportunity to bacterial EPS to be developed at industrial scale and commercialized relies on high value market niches (e.g. cosmetics, pharmaceuticals and biomedicine), since microbial polysaccharides may present the desired degree of purity and functional properties that the traditional polysaccharides obtained from plants and algae may not have. In this case, the potential designed characteristics and quality of the product will exceed production costs and product yield issues (Freitas et al., 2011).

Table 1 summarizes the main characteristics of some of the microbial polysaccharides that are currently commercialized. Dextran was the first microbial polysaccharide to be commercialized and approved for food applications by FDA (US Food and Drug Administration). Nowadays, xanthan, produced by *Xantomonas campestris*, is the most widely accepted microbial polysaccharide. It has been granted a GRAS (Generally Recognized as Safe) status, and is used in many manufactured foods, as well as in cosmetics and personal care products. Xanthan has a huge thickening and suspending capacity with

high stability under a large range of pH and temperature conditions (Garcia-Ochoa et al., 2000; Sutherland, 2002; Freitas et al., 2011). Gellan is another GRAS polysaccharide produced by *Sphingomonas paucimobilis*. It is mainly used in food applications due to its great gelling capacity that allows it to be used at a much lower concentration than agar (Sutherland, 2002; Bajaj et al., 2007; Freitas et al., 2011).

Bacterial cellulose is a high-value product, produced by *Acetobacter* sp.. Its purity and fibres orientation makes them very suitable to form audio membranes with great quality. Bacterial cellulose is also known to be an immune stimulant and tumour suppressive agent (Sutherland, 2002; Chawla et al., 2009). Other commercial polysaccharides with interesting properties are hyaluronic acid and succinoglycan, which have found medical, pharmaceutical and cosmetic applications due to their resemblance to eukaryotic polymers (Sutherland, 2001; Freitas et al., 2011).

Table 1.1 Commercial microbial polysaccharides, their properties and main applications

Polysaccharide	Microorganism	Composition	Main properties	Main applications	References
Xanthan	<i>Xanthomonas campestris</i>	Glucose	High viscosity	Foods	Sanford et al. (1984)
		Mannose	Stability over a wide range of temperatures and pH	Petroleum Industry	Garcia-Ochoa et al. (2000)
Gellan	<i>Sphingomonas paucimobilis</i>	Glucuronic acid	Emulsifier	Pharmaceuticals	Sutherland (2002)
		Acetate		Cosmetic and personal care products	Rehm (2010)
		Pyruvate		Drilling muds	Freitas et al. (2011)
		Glucose	Stability over a wide range of pH	Foods	Sutherland (2002)
Dextran	<i>Leuconostoc mesenteroides</i> <i>Streptococcus sp.</i>	Rhamnose	Gelling capacity	Pharmaceuticals	Bajaj et al. (2007)
		Glucuronic acid	Thermoreversible gels	Pet foods	Banik et al. (2007)
		Acetate		Plant biotechnology	Rehm (2010)
		Glycerate			Freitas et al. (2011)
Cellulose	<i>Acetobacter sp.</i>	Glucose	Good stability	Foods	Qader et al. (2005)
			Newtonian fluid behaviour	Pharmaceutical industry: blood-plasma volume expander	Rehm (2010)
				Chromatographic media	Freitas et al. (2011)
Hyaluronan	<i>Pseudomonas aeruginosa</i> <i>Streptococcus sp.</i>	Glucose	High crystallinity	Audio Systems	Sutherland (2002)
			Insolubility in most solvents	Biomedical: wound healing; tissue engineered blood vessels	Chawla et al. (2009)
			High tensile strength		Rehm (2010)
			Moldability		Freitas et al. (2011)
Succinoglycan	<i>Agrobacterium sp.</i> <i>Alcaligenes spp.</i> <i>Pseudomonas sp.</i> <i>Rhizobium sp.</i>	Glucuronic acid	Biocompatible	Medicine	Rinaudo (2008)
		N-acetyl-glucosamine	Biological activity	Cosmetic	Liu et al. (2009)
			Highly hydrophilic	Solid culture media	Rehm (2010)
			Viscous shear-thinning aqueous solution	Food	Sutherland (2002)
			Stability in acidic condition	Oil recovery	Rehm (2010)
					Freitas et al. (2011)

1.2. Fermentative exopolysaccharides production

In the design of any microbial process it is necessary to take into account the type of product that is to be produced. Hence, certain EPS are growth associated products (e.g. bacterial alginate), being synthesized only during the cell growth phase, while others are growth dissociated products, which are synthesized only in the post-stationary growth phase (e.g. curdlan). On the other hand, many microorganisms show a partially growth-associated EPS production trend, with polymer synthesis being initiated during the exponential growth phase and proceeding with identical production rate when cell growth is restricted.

Furthermore, there are no standard operational conditions for bacterial EPS production. In fact, EPS-producing microorganisms differ widely in their carbon and nitrogen source utilization, oxygen and mineral requirements, optimal temperature and pH. The amount of EPS produced is strongly influenced by the nutritional and environmental conditions (Sutherland, 2001; Donot et al., 2011), which may be manipulated to achieve improved production (Kumar et al., 2007). Usually, polysaccharides production processes require excess of carbon source, concomitant with limitation of another nutrient (e.g. nitrogen or phosphate) (Bajaj et al., 2007, Rehm, 2010; Freitas et al., 2011). Most microbial EPS are produced under aerobic conditions. However, some EPS-producing strains need maximal aeration (e.g. *Xanthomonas* sp.), while for others the production is maximized under microaerophilic conditions (e.g. *Azotobacter vinelandii*) (Peña et al., 2000; Rehm, 2010). Production is also frequently favoured under sub-optimal incubation temperatures (Sutherland, 2001) and pH (Kumar et al., 2007). Furthermore, in some cases the production is stimulated by supplementation of the production medium with surfactants (e.g. Triton X-100), vitamins and aminoacids (e.g. tryptophan) and cations (e.g. Ca^{2+} and Mg^{2+}) (Bajaj et al., 2007; Kumar et al., 2007; Freitas et al., 2011).

For most of the EPS-producing microorganisms, the growth conditions do not influence the basic carbohydrate EPS composition (Rosalam and England, 2006; Freitas et

al., 2011). However, their content in substituent groups can vary extensively, which greatly affects polymer properties. An exception has to be made for some EPS-producing organisms (e.g. *Rhizobium* and *Pseudomonas*), for which EPS composition may be affected by medium composition, as well as incubation conditions (Freitas et al., 2011). Thus, bioprocesses based on those bacteria can be used for the production of tailor made polymers.

Many EPS producers are also able to accumulate variable amounts of intracellular storage products (e.g. glycogen or polyhydroxyalkanoates), thus reducing their full potential for EPS production. *Xanthomonas* sp. is an exception to this, since those bacteria do not produce significant amounts of other bioproducts, which allows achieving very high substrate conversion into xanthan (Rehm, 2010).

Most EPS-producing microorganisms use substrates with a high degree of purity, which increases the production costs. The most common carbon sources used to produce microbial polysaccharides are sugars, mainly glucose, but also fructose, sucrose, lactose, maltose, mannitol and sorbitol (Bajaj et al., 2007; Kumar et al., 2007; Reis et al., 2008).

In order to reduce polysaccharide production costs it is desirable to use abundant and less expensive carbon sources, such as agro-food and industrial wastes and byproducts. A large amount of wastes/byproducts are generated by several agricultural activities and industrial processes, such as sugarcane molasses, cheese whey and glycerol from the biodiesel industry. Several byproducts and wastes (e.g. sugar cane molasses, cheese whey, waste sugar beet pulp, peach pulp) have been tested as substrates for xanthan production, achieving competitive results. Nevertheless, the industrial process is still based on glucose and sucrose due to the higher production yields and product quality they enable (Kalogiannis et al., 2003; Rosalam and England, 2006; Silva et al., 2009). Cheese whey and molasses, that have high sugar contents, have also been successfully tested as raw materials for the fermentative production of gellan (Fialho et al., 1999; Banik et al., 2007).

In the bio-combustible industry, the biodiesel byproduct, rich in glycerol, has become a stream for which there is an urgent need of alternative applications, in order to reduce its industrial stocks and make biodiesel production a more cost effective process. Biodiesel is made through a chemical catalysed reaction, transesterification, which occurs between oils or fats and an alcohol, usually methanol, with the production of glycerol as a byproduct (10% of the total biodiesel produced) (Temudo et al., 2008).

As such, glycerol is being generated in large quantities (~2.1million tons/year), far beyond current consumption in traditional applications, thus making it a product for which interesting applications are lacking. Pure glycerol is used for different industrial applications, such as soaps, paints, foods, pharmaceuticals (Temudo et al., 2008). However, glycerol byproduct from the biodiesel industry contains residual methanol, NaOH, carry-over fat/oil, some esters, and low amounts of sulphur compounds, proteins and minerals (Thompson et al., 2006), which make it inadequate for use in many of the traditional glycerol applications (e.g. food, pharmaceutical, and cosmetic industries), unless costly purification steps are performed (Freitas et al., 2009a).

The use of glycerol byproduct as a carbon source in microbial processes is a good way to increase its consumption and valorisation. It has been tested in fermentation processes to produce several microbial products, such as lipids (Papanikolau et al., 2002), pigments (Narayan et al., 2005) and ethanol, succinate, acetate, lactate and hydrogen (Dharmadi et al., 2006). Furthermore, glycerol is a potential carbon source for protein production by *Pichia pastoris* (Çelik et al., 2008) and for the production of polymers, namely PHA (Ashby et al., 2005), exopolysaccharides (Freitas et al., 2009a) and chitin-glucan complex (Roca et al., 2012), thus opening the possibility of new markets for glycerol.

1.3. Motivation

Bearing in mind that renewable resources, like industrial wastes/byproducts, may be regarded as potential alternative substrate sources for biopolymers production, in this PhD thesis, a process was studied to valorise glycerol byproduct from the biodiesel industry with the production of a novel value-added bacterial fucose-rich exopolysaccharide (Reis et al., 2008) that was named FucoPol.

The following main objectives were envisaged:

1. Setting the standard cultivation process and optimization of bioreactor operation, by studying the effect of environmental conditions (pH and temperature) and nutrient concentration (nitrogen and glycerol) aiming at maximizing FucoPol productivity.
2. Polymer characterisation, in terms of its chemical composition (sugars and substituent groups); molecular weight; rheology and functional properties (emulsion forming and stabilizing ability and flocculating capacity).

1.4. Thesis outline

This thesis is divided into seven chapters, describing the work performed during this PhD project. The methodology used in each individual chapter is detailed in the context of the respective subject and, when applicable, is related to that used in previous chapters. Chapters 2, 3 and 4 are dedicated to FucoPol production and process optimization. Chapters 5 and 6 describe FucoPol's properties. The work performed during this PhD resulted in five scientific papers, which have been published in international scientific publications, while one more manuscript is being prepared.

Chapter 1 introduces the subject of this thesis, by presenting the context and motivation for this PhD work.

Chapter 2 presents the morphological, physiological and genetic characterisation of the strain, which was named *Enterobacter* strain A47 and deposited at DSMZ with accession number 23139, under the Budapest Treaty. It also describes the standard cultivation for FucoPol production and its physical-chemical characterisation, as well as the morphological and rheological characterisation of the fermentation broth.

Chapter 3 and Chapter 4 describe the studies performed for the optimization of FucoPol production. Chapter 3 focused on the interactive effect of temperature and pH using multivariate statistical analysis, while in Chapter 4, the effect of glycerol and nitrogen concentration on FucoPol production was studied.

Chapter 5 describes FucoPol's behaviour in aqueous solution, in a diluted regime (intrinsic viscosity) and in a concentrated regime: steady shear and viscoelastic properties. The effect of salt concentration, pH and temperature, on such properties, was assessed by using statistical tools.

Chapter 6 presents a preliminary study of the emulsion forming and stabilizing ability of FucoPol, as well as its flocculating capacity, in order to better understand the FucoPol's potential applications, namely in the cosmetic, food and pharmaceutical industry.

The main conclusions obtained in this PhD thesis are presented in Chapter 7. Some suggestions for future research are also proposed.

Chapter 2

FucoPol

Standard Bioprocess Operation and Polymer Characterisation

The results presented in this chapter were published in three peer reviewed papers.

Alves, V.D., Freitas, F., Torres, C.A.V., Cruz, M., Marques, R., Grandfils, C., Gonçalves, M.P., Oliveira, R., Reis, M.A.M., 2010. *Rheological and morphological characterization of the culture broth during exopolysaccharide production by Enterobacter sp.* Carbohydrate Polymers, 81, 758-764.

Freitas, F., Alves, V.D., Torres C.A.V., Cruz, M., Sousa, I., Melo, M.J., Ramos, A.M., Reis, M.A.M., 2011. *Fucose-containing exopolysaccharide produced by the newly isolated Enterobacter strain A47 DSM 23139.* Carbohydrate polymers, 83, 159-165.

Torres, C.A.V., Marques, R., Antunes, S., Alves, V.D., Sousa, I., Ramos, A.M., Oliveira, R., Freitas, F., Reis, M.A.M., 2011. *Kinetics of production and characterization of the fucose-containing exopolysaccharide from Enterobacter A47.* Journal of Biotechnology, 156, 4, 261-267.

2.1 Summary

A fucose-containing exopolysaccharide (EPS) – FucoPol – was produced by the bacterium *Enterobacter* A47 using glycerol byproduct from the biodiesel industry. Kinetic parameter values estimated by a MATLAB model were in agreement with experimental data and suggested that EPS synthesis was partially growth associated. The culture broth was characterized in terms of its morphological and rheological properties throughout the cultivation run. Microscopic observations revealed the formation of cell aggregates surrounded by the EPS at the beginning of the cultivation run, while, at the end, aggregates were reduced and an EPS matrix with the cells embedded in it was observed. The apparent viscosity of the culture broth increased over time, which was attributed to the increase of the FucoPol concentration in the first period of the cultivation run. However, in the final stage, the creation of new polymer interactions within the complex culture broth was likely the reason for the viscosity increase observed, since there was not a significant variation of the FucoPol concentration, average molecular weight or chemical composition. The broth presented a Newtonian behavior at the beginning of the run, changing to shear thinning as the EPS concentration increased, and revealed to follow the Cox–Merz rule.

FucoPol was composed by neutral sugars, namely fucose (32 – 36 %mol), galactose (25 – 26 %mol) and glucose (28 – 34 %mol), and acidic sugar, glucuronic acid (9 – 10 %mol). It had also acyl groups substituents, acetyl (3 – 5 wt.%), pyruvyl (13 – 14 wt.%) and succinyl (2 wt%). The neutral sugars relative proportion was measured throughout the cultivation run and a considerably variation was observed. At the beginning (1 day), glucose was the main component (83 %mol), while at the end (4 days) it was composed of 32 % mol fucose, 25 %mol galactose and 34 %mol glucose. The acyl groups content and composition have also changed. Moreover, the molecular weight has increased linearly during the run (from 8×10^5 to 5×10^6). The changes observed in EPS composition and molecular weight had also had an impact upon the polymer's intrinsic viscosity, as shown by its linear increase from 3.95 to 10.72 dL g^{-1} . The results suggest that the culture might have synthesized at least two distinct EPS, with different sugar composition and average molecular weight, which predominated at different cultivation stages.

2.2. Introduction

Although the interesting physical properties that microbial polysaccharides may present, certain microbial exopolysaccharide (EPS) have an increased value due to their content in some rare sugars, such as fucose or rhamnose, which occur rarely in Nature and are difficult to obtain (Vanhooren and Vandamme, 2000). One of those rare sugars is fucose. Fucose-containing polymers are particularly interesting due to their biological properties. It has been reported that preparations with fucose-containing oligo- and polysaccharides, as well as fucose monomers, have biological properties that potentiate their therapeutic use, for example, as anti-carcinogenic and anti-inflammatory agents, in the treatment of rheumatoid arthritis, in age-related pathologies accompanied by tissue loss, in the acceleration of wound healing and as hydrating and anti-aging additives (Cescutti et al., 2005; Péterszegi et al., 2003). There is also a growing interest in the use of fucose or fucoligosaccharides for the synthesis of human milk oligosaccharides (HMO) that are used as additives in infant formulae. HMOs are important for enhancing the protection of infants against enteric and other pathogens, especially in early development (Chaturvedi et al., 2001; Coppa et al., 2006; Romeo et al., 2010).

Oligo- and polysaccharides containing fucose may be found in microorganisms, plants, seaweeds and animals (Vanhooren & Vandamme, 1999). Microorganisms producing exopolysaccharides rich in fucose include a wide range of bacteria, fungi and microalgae. Extensively studied bacterial fucose-containing extracellular polysaccharides include colanic acid, fucogel and clavan. Colanic acid is a polysaccharide composed of fucose, glucose, galactose and glucuronic acid, and the acyl groups pyruvyl and acetyl (Grant et al., 1969). It is commonly produced by many members of the family *Enterobacteriaceae*, including *Escherichia*, *Salmonella* and *Klebsiella* strains (Ratto et al., 2006). Fucogel is a polysaccharide produced by *Klebsiella pneumoniae* I-1507, composed of galactose, 4-*O*-acetyl-galacturonic acid and fucose (Guetta et al., 2003). It has been successfully commercialized by Solabia BioEurope, France (www.solabia.com), for the cosmetic industry (Paul et al., 1999). Clavan is composed of glucose, galactose, fucose and pyruvyl, being produced by *Clavibacter michiganensis* strains (van den Bulk et al., 1991; Vanhooren & Vandamme, 2000).

Among the genus *Enterobacter*, several species have been reported to secrete exopolysaccharides containing fucose. Examples include: *Enterobacter* sp. CNCM 1-2744 that produces an EPS in which fucose, galactose, glucose and glucuronic acid monomers are present in a ratio of 2:2:1:1 (Philbe, 2002), *Enterobacter* sp. SSYL (KCTC 0687BP) that produces an EPS in which fucose represents 8-10% of the sugar content, being glucuronic acid the main component (40-70%) (Yang, 2002), *Enterobacter sakazakii*, strains ATCC 53017, ATCC 29004 and ATCC 12868 that produce an EPS in which fucose represents 13-22% (Harris & Oriol, 1989) and *Enterobacter amnigenus* that produces a heteropolymer containing glucose, galactose, fucose, mannose, glucuronic acid and pyruvate (Cescutti et al., 2005). More recently, an *E. ludwigii* strain isolated from the Chernobyl exclusion zone has also been reported to synthesize a fucose-containing EPS (Pawlicki-Julian et al., 2010). This polymer is composed by neutral sugars and uronic acids in a ratio of 90/10, the neutral sugars are fucose, galactose and glucose in a molar ratio of 2:1:1.

The maximum possible productivity and product concentration that can be obtained in any biochemical process are limited by microbial kinetics and by mass transport phenomena occurring during it. The latter is influenced by the mixing degree and hydrodynamic conditions in the process. These parameters are related to the fluid flow characteristics that determine mass (oxygen, carbon source and other nutrients) and heat transfer rates in bioreactors (Bandaipheth & Prasertsan, 2006). Hence, the study of the rheological properties of culture broths is one of the keys to improved yield of the desired microbial products.

Cultivation broths containing unicellular microorganisms of simple shape should behave as Newtonian fluids. However, in many microbial cultivation the broths are much more complex and deviations from Newtonian behaviour are significant. The broths may exhibit different types of behaviour, depending on their stage of development during the cultivation. In a number of industrially important cultivation processes the broth develops shear thinning behaviour (Figure 2.1). Examples of such behaviour include industrially important microbial polysaccharides, such as xanthan gum that is produced by *Xanthomonas campestris* (Candia & Deckwer, 1999), pullulan that is produced by *Aureobasidium pullulans* (Furuse et al., 2002) and dextran that is produced by *Leuconostoc mesenteroides* (Landon et al., 1993). Rheological properties provide a sensitive analytical means for the

characterisation of cellular mass changes and provide a clue to the relationship between cellular structure and biochemical activity in a microbial cultivation.

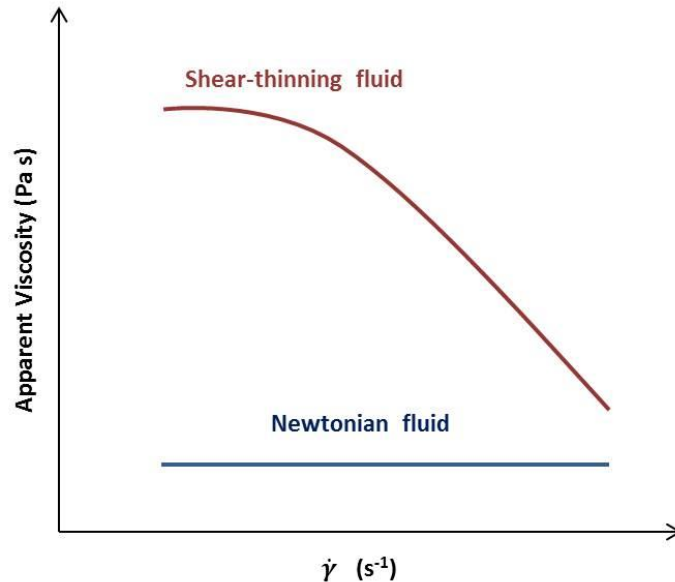


Figure 2.1 Flow behaviour – Newtonian and shear-thinning – at logarithmic scale.

The viscosity of microbial culture broths may be influenced by physical, as well as biological parameters, including the cultivation medium, the size of both cells and cell aggregates formed, biomass concentration, morphological parameters and the products being secreted into the solution (Al-Asheh et al., 2002). However, in most cases, the change in flow behaviour in such microbial processes is attributed to the increasing extracellular polymer concentration being produced, with negligible contribution from the cells (Landon et al., 1993).

In this chapter, a newly isolated EPS-producing microorganism, was identified and named *Enterobacter* A47. This culture was grown on glycerol byproduct from the biodiesel industry as the sole carbon source for EPS production. A kinetic model has been developed with the objective of describing the behaviour of the culture during its growth on glycerol and EPS synthesis. Furthermore, the polymer was characterized in terms of its chemical composition and average molecular weight and intrinsic viscosity along the cultivation run. The culture broth was characterized regarding its rheological and morphological properties throughout the cultivation run. A special attention was driven to evaluate the changes experienced by the bacterial cells during growth and EPS production on glycerol byproduct.

In addition, the culture broth rheology was related to polymer concentration, composition and average molecular weight, as well as to the cell concentration and morphology.

2.3. Material and Methods

2.3.1. FucoPol Production

Microorganism

The strain used in this work was isolated from a contaminated glycerol byproduct aqueous solution. *Enterobacter* A47 (DSM 23139) was characterised morphologically and biochemically (biochemical and physiological tests - Table 2.1). The 16S rRNA gene sequence was determined by direct sequencing of PCR-amplified 16S rDNA. Genomic DNA extraction, PCR (Polymerase Chain Reaction) mediated amplification of the 16S rDNA and purification of the PCR product was carried out as described by Rainey et al. (1996). Purified PCR products were sequenced using the CEQTMDTCS-Quick Start Kit (Beckman Coulter) as directed in the manufacturer's protocol. Sequence reactions were electrophoresed using the CEQTM8000 Genetic Analysis System. The resulting sequence data was put into alignment editor ae2 (Maidak et al., 1999). For comparison 16S sequences were obtained from the EMBL, RDP or DSMZ databases.

The phylogenetic dendogram of the bacteria *Enterobacter* A47 was constructed using the ARB package (Pruesse et al., 2007). Based on the evolutionary distance values, the phylogenetic tree was constructed by neighbor-joining method (Jukes and Cantor, 1969), using the correlations of Saitou and Nei (1987). The root of the tree was determined by including the 16S rRNA gene sequence of *Klebsiella pneumoniae* into the analysis.

Enterobacter A47 aliquots were preserved in glycerol 20% and stored at -80 °C.

Media

In all experiments, *Enterobacter* A47 was grown on a slightly modified Medium E* (pH 7.0) (Brandl et al., 1988), with the following composition (per liter): $(\text{NH}_4)_2\text{HPO}_4$, 3.3 g; K_2HPO_4 , 5.8 g; KH_2PO_4 , 3.7 g; 10 mL of a 100 mM MgSO_4 solution and 1 mL of a micronutrient solution. The micronutrient solution had the following composition (per liter of 1N HCl): $\text{FeSO}_4 \cdot 7\text{H}_2\text{O}$, 2.78 g; $\text{MnCl}_2 \cdot 4\text{H}_2\text{O}$, 1.98 g; $\text{CoSO}_4 \cdot 7\text{H}_2\text{O}$, 2.81 g; $\text{CaCl}_2 \cdot 2\text{H}_2\text{O}$, 1.67 g; $\text{CuCl}_2 \cdot 2\text{H}_2\text{O}$, 0.17 g; $\text{ZnSO}_4 \cdot 7\text{H}_2\text{O}$, 0.29 g. (pH 7.0). Glycerol byproduct was added to give a concentration between 25 and 50 g L⁻¹. Glycerol byproduct (with a glycerol content ca. 89%) was supplied by SGC Energia, SGPS, SA, Portugal.

Bioreactor Operation

EPS production was performed in a 2 and 10 L bioreactors (BioStat Bplus, Sartorius), with initial working volumes of 1.8 or 8 L, respectively. Inocula for bioreactor experiments (20%, v/v) were prepared by incubating the culture in Medium E* supplemented with glycerol byproduct, in shake flasks, for 72 h at 30 °C, in an incubator shaker (150 rpm).

The temperature and the pH were controlled at 30.0 ± 0.1 °C and 6.80 ± 0.05 , respectively. The initial glycerol and ammonium concentration were 25 – 40 and 0.7 – 1.1 g L⁻¹, corresponding to a C:N ratio of 14:1 (w/w). After initial nitrogen depletion, a feeding solution composed of Medium E* supplemented with 200 g L⁻¹ of glycerol byproduct was fed to the bioreactor at a constant rate (5 and 20 mL h⁻¹ for the 2 and 10 L bioreactors, respectively). The aeration rate (0.4 and 1.0 L/min, in the 2 and 10 L bioreactors, respectively) was kept constant throughout the cultivation, and the dissolved oxygen concentration (DO) was controlled by the automatic variation of the stirrer speed (300–800 rpm) provided by two six-blade impellers. During the fed-batch phase, the DO was maintained below 10%.

Culture broth samples taken periodically during the cultivation runs were centrifuged at $13\,000 \times g$, for 15 min, for cell separation. The cell-free supernatant was stored at – 20 °C for the determination of glycerol and ammonium concentrations, and for the quantification of the EPS produced, while the cell pellet was used for the determination of the cell dry weight (CDW).

Analytical Techniques

The CDW was determined by gravimetry, after washing the cell pellet with deionized water (resuspension in water, centrifugation at $13\ 000 \times g$, for 15 min, and, finally, resuspension in water and filtration through $0.20\ \mu\text{m}$ filters) and dried at $100\ ^\circ\text{C}$, for 24 h.

Glycerol concentration in the cell-free supernatant was determined by high performance liquid chromatography (HPLC) with an Aminex HPX-87H column (BioRad), coupled to a refractometer. The cell-free supernatant samples were diluted in H_2SO_4 0.01 N and filtered with Vectra Spin Micro Polysulphone filters ($0.2\ \mu\text{m}$), at 10 000 rpm, for 10 min. The analysis was performed at $50\ ^\circ\text{C}$, with sulphuric acid (H_2SO_4 0.01N) as eluent, at a flow rate of $0.6\ \text{mL min}^{-1}$. An external standard calibration curve was constructed using glycerol (Sigma – Aldrich 99%) solutions in concentrations within 1000 and 10 ppm.

Ammonium concentration was determined with a potentiometric sensor (Thermo Electron Corporation, Orion 9512). Cell-free supernatant samples (1 mL) were mixed with 20 μL of ISA (Ionic Strength Adjuster) reagent, and the electric potential was measured within 5 minutes. An external standard calibration curve was constructed using NH_4Cl (Panreac) solutions (50 – 0.02 mM).

EPS Extraction

Culture broth samples were diluted with deionised water for viscosity reduction and centrifuged at $13\ 000 \times g$ for 1 h. Two methods were used for the recovery of the EPS from the cell-free supernatant, namely:

1- Solvent precipitation with acetone

The cell-free supernatant was subjected to protein denaturation by the addition of trichloroacetic acid (TCA) at a final concentration of 10% (reaction at $4\ ^\circ\text{C}$ for 15 min), followed by their separation by centrifugation ($13\ 000 \times g$, 1 h). The polymer was then precipitated from the supernatant by the addition of cold acetone (3:1) and separated by centrifugation ($10\ 000 \times g$, 15 min). The pellet was dissolved in deionised water and freeze dried.

2- Dialysis

The cell-free supernatant was subjected to thermal treatment (70 °C, 1 h) to inactivate bacterial enzymes that might cause polymer degradation during the subsequent purification steps. The treated supernatant was centrifuged (13 000 × g, 1 h) to remove any remaining cell debris and denatured proteins. Finally, it was dialyzed with a 10 000 MWCO membrane (SnakeSkin™ Pleated Dialysis Tubing, Thermo Scientific), against deionized water (48 h, 4 °C) and freeze dried.

Calculus

The specific growth rate (μ , h⁻¹) was determined using the follow equation:

$$\ln\left(\frac{x}{x_0}\right) = \mu t \quad \text{Eq. 2.1}$$

where x_0 (g L⁻¹) is the cell concentration in the beginning of the run.

The yields of biomass on substrate ($Y_{X/S}$, g.g⁻¹) and EPS on substrate ($Y_{P/S}$, g.g⁻¹) were determined by using the following equations:

$$Y_{X/S} = \frac{\Delta x}{\Delta s} \quad \text{Eq. 2.2}$$

$$Y_{P/S} = \frac{\Delta P}{\Delta s} \quad \text{Eq. 2.3}$$

where Δx and ΔP are the biomass and EPS produced, respectively, and Δs is the substrate uptake.

The EPS volumetric productivity (rP , g L⁻¹d⁻¹) was determined as following:

$$rP = \frac{dP}{dt} \quad \text{Eq. 2.4}$$

where P corresponds to the product, EPS (g L^{-1}) at time $t(\text{days})$.

EPS specific production rate was determined by dividing the volumetric rate by cell concentration in terms of cell dry weight.

$$q_P = \frac{r_P}{d_{CDW}} \quad \text{Eq. 2.5}$$

Kinetic Modelling

Growth kinetics was assumed to follow the Monod model with potential limitation of glycerol (S) and ammonia (N).

$$\mu = \mu_{max} \cdot \frac{S}{K_S+S} \cdot \frac{N}{K_N+N} \quad \text{Eq. 2.6}$$

Overall glycerol consumption results from glycerol taken up for biomass synthesis ($\mu/Y_{X/S}$), glycerol taken up for EPS synthesis ($v_P/Y_{P/S}$) and energy spent for maintenance processes (m_S).

$$v_S = \frac{\mu}{Y_{X/S}} + \frac{v_P}{Y_{P/S}} + m_S \quad \text{Eq. 2.7}$$

EPS synthesis is assumed to be partially associated to cell growth and described by the following equation:

$$v_P = Y_{P/X} \cdot \mu + q_P \quad \text{Eq. 2.8}$$

Finally, ammonia uptake is associated with biomass synthesis

$$v_N = \frac{\mu}{Y_{X/N}} \quad \text{Eq. 2.9}$$

These kinetic equations result into the following set of material balance equations for a stirred-tank bioreactor operated in batch/fed-batch mode:

$$\frac{dX}{dt} = (\mu - K_d - D) \cdot X - \quad \text{Eq. 2.10}$$

$$\frac{dS}{dt} = -v_S \cdot X + D \cdot (S_0 - S) \quad \text{Eq. 2.11}$$

$$\frac{dN}{dt} = -v_N \cdot X + (N_0 - N) \quad \text{Eq. 2.12}$$

$$\frac{dP}{dt} = v_P \cdot X - D \cdot P \quad \text{Eq. 2.13}$$

$$\frac{dV}{dt} = D \cdot V \quad \text{Eq. 2.14}$$

with X , S , N and P the concentrations of biomass, glycerol, ammonia and EPS in the bioreactor respectively, $D = F/V$ the dilution rate ($D = 0 \text{ h}^{-1}$ in the batch phase), F the inlet feed rate in the fed-batch phase, V the culture volume and subscript index 'o' denoting concentration in the inlet feed stream.

Kinetic Parameters Estimation

Kinetic parameters estimation was performed using an in-house developed program for MATLAB (Mathworks, Inc). Parameter estimation was performed in the least squares sense using the Levenberg-Marquardt algorithm. Model differential equations were integrated using a 4th/5th order Runge-Kutta solver. The final residuals and Jacobian matrix served to calculate an approximation to the Hessian matrix assuming that the final solution is a local optimum. The Hessian matrix enabled to calculate the parameters covariance matrix and parameters 95% confidence intervals. See Dias et al. (2005) for more details.

2.3.2. Culture Broth Characterisation

Microscopic Observations

Culture broth samples collected throughout *Enterobacter* A47 cultivation run were observed with an Olympus BX51 microscope in phase contrast mode. The EPS was also visualized by its negative staining with China ink, using a technique based on the work of Hahn et al. (2004). Briefly, broth samples were spread out in a slide and stained with a drop of China ink (Pelikan). The microscopic observation was performed in phase contrast, with low light intensity.

Rheological Studies

Culture broth samples were loaded in the cone and plate geometry (diameter 4 cm, angle 2°) of a controlled stress rheometer (ARG2, TA Instruments Inc., New Castle, DE, USA) and the shearing geometry covered with paraffin oil in order to prevent water loss. The samples were equilibrated at 30 °C for 10 min. A strain sweep was performed at 1Hz in order to determine the linear viscoelastic region. Frequency sweeps with 0.1 strain amplitude were then performed to measure the frequency dependence of the storage (G') and loss (G'') moduli at 30 °C. Flow curves were determined using a steady-state flow ramp (torque was imposed using a logarithmic ramp) in the range of shear rate from around 1 to 700 s^{-1} . The shear rate was measured point by point with consecutive 60 s steps of constant shear rate. The viscosity was recorded for each point to obtain the flow curves. Frequency sweeps were carried out at a controlled stress of 1Pa (shown by stress sweeps to give values within the linear viscoelastic region) in order to measure the dynamic moduli G' and G'' .

2.3.3. FucoPol Characterisation

Sugar and Acyl Groups Composition

Extracellular polysaccharide samples (2 – 3 mg) were dissolved in 5 mL deionised water and hydrolysed with 0.1 mL trifluoroacetic acid (TFA 99%), at 120 °C, for 2 h. The hydrolysate was used for the identification and quantification of the sugar monomers and acyl groups present in the purified EPS.

The acid hydrolysate was used for the identification and quantification of the constituent monosaccharides by High Performance Liquid Chromatography (HPLC), using a CarboPac PA10 column (Dionex), equipped with an amperometric detector (Dionex). The analysis was performed at 30 °C, with sodium hydroxide (NaOH 4 mM) as eluent, at a flow rate of 0.9 mL min⁻¹. Galactose (Fluka 99%), glucose (Fluka), mannose (Fluka 99%), rhamnose (Fluka 99%), glucosamine hydrochloride (Sigma 99%), fucose (Sigma 98%) and glucuronic acid (Sigma 99%) solutions (30 – 8 ppm) were used as standards.

The hydrolysate was also used for the identification and quantification of the acyl groups substituents. The analysis was performed by HPLC, with an IonPac ICE-AS1 9x250 mm column (Dionex), coupled to a Photodiode Array PDA ICS series (Dionex), using sulphuric acid (H₂SO₄ 0.01 N) as eluent, at 30°C, with a flow rate of 0.6 mL min⁻¹. The detection was performed at 210 nm. Pyruvate (Alfa Aesar 98 %), succinate (Merck 99.5%) and acetate (Sigma-Aldrich 99.8%) solutions were used as standards in concentrations ranging from 1 to 100 ppm.

Proteins and salts were also measured, since they can be present as remnants of the cultivation broth. For the determination of the EPS protein content, 5.5 ml samples of 4.5 g L⁻¹ aqueous solutions were mixed with 1 ml 20% NaOH and placed at 100 °C for 5 min. After cooling on ice, each sample was mixed with 170 µl of CuSO₄.5H₂O (Merck) (25% v v⁻¹) and centrifuged at 3500 × g for 5 min. The optical density was measured at 560 nm (Spectrophotometer Helios Alpha, Thermo Spectronic, UK). Albumin (Merck) solutions (0.5–3.0 g L⁻¹) were used as protein standards.

The total inorganic content of the biopolymer was evaluated by subjecting it to pyrolysis at a temperature of 550°C for 48 hours.

Fourier Transform Infra Red (FT – IR) Spectroscopy

The infrared spectra of the polymers were acquired with a Nicolet Nexus spectrophotometer interfaced with a Continuum microscope, using a MCT-A detector cooled by liquid nitrogen. All the spectra presented were obtained in transmission mode, using a *Thermo* diamond anvil compression cell. The spectra were obtained, in a 100 μm x 100 μm area, with a resolution of 4 cm^{-1} (8 cm^{-1} in the exopolysaccharide analysis) and 128 scans. They are shown here as acquired, without corrections or any further manipulations, except for the removal of the CO_2 absorption at approximately 2300-2400 cm^{-1} .

Molecular Weight

Number and weight average molecular weights (M_n and M_w , respectively), as well as the polydispersity index ($\text{PD} = M_w/M_n$) were obtained by size exclusion chromatography (SEC) in a low temperature Waters Co. apparatus, equipped with a Waters Ultrahydrogel Linear column and a differential refractive index detector (Waters 2410). A Tris-HCL 0.1M (pH 8) solution at 30 °C was used as eluent, and the polymer concentration was less than 0.1% wt, thus ensuring the pumping of essentially non aggregated polysaccharides in coil conformation by a Waters 510 Solvent Delivery System. The values of M_w and M_n were calculated using a relative calibration curve generated with monodisperse pullulan standards (Shodex, Showa Denko, Japan).

Intrinsic Viscosity

The intrinsic viscosity of the purified polymer was determined by double extrapolation to zero concentration of the Huggins and Kraemer equations, respectively (Rao, 1999):

$$\frac{\eta_{sp}}{C} = [\eta] + k_H [\eta]^2 C \quad \text{Eq. 2.15}$$

$$\frac{\ln(\eta_{rel})}{C} = [\eta] + k_k [\eta]^2 C \quad \text{Eq. 2.16}$$

where $[\eta]$, η_{sp} and η_{rel} are the intrinsic, specific and relative viscosities, respectively; k_H and k_k are the Huggins and Kraemer coefficients, and C is the polymer concentration. An automatic viscosity measuring unit AVS 450 (Schott-Gerate, Germany), with an Ubbelohde capillary viscometer (Ref. 53013/lc, Schott-Gerate, Germany) was used to measure the viscosity of dilute solutions at 25°C, with a relative viscosity in the range between 1.2 and 2.0 in order to ensure a good accuracy in the extrapolations to zero concentration. A volume of 16 mL of each diluted solution was used to fill the viscometer. Elution time of each solution was taken as an average of three concordant readings. Relative viscosities (η_{rel}) were calculated by dividing the average flow time of each biopolymer solution by that of the solvent (water or NaCl solution).

2.4. Results and Discussion

2.4.1. Identification and Characterisation of the Microorganism

The microorganism isolated from a contaminated glycerol aqueous solution was characterized about its morphological, physiological and genetic characterisation of the strain, such characterisation was performed by the Deutsche Sammlung von Mikroorganismen und Zellkulturen (DSMZ), Germany, according to the Standard Methods. The strain was named *Enterobacter* A47 and a Patent deposit was made at DSMZ, under the Budapest Treaty, with accession number 23139. These studies were financed by a Portuguese company named 73100, which is also the owner of the patent WO 2011/073874 A2 (Reis et al., 2011).

Morphological Characterisation

The bacterium *Enterobacter* A47 is a short rod with a length of 0.7 – 0.8 μm and a width of 1.2 – 2.5 μm . It is a Gram negative motile bacterium.

Biochemical Profile

The cellular fatty acid pattern of *Enterobacter* A47 is characterized by high levels of the acids 16:0 (28.3%), sum in feature 3 (16:1 ω 7c/15 iso 2OH) (23.9%) and 18:1 ω 7c (22.8%). The acids 12:0 (3.3%), 14:0 (7.8%), 17:0 (0.2%), 17:0 cyclo (4.0%), 18:0 (0.3%) and sum in feature 2 (14:0 3OH/16:1 ISO I) (6.4%) were also detected. This fatty acid pattern is typical of members of the family *Enterobacteriaceae* (Kampfer et al., 2005). By comparison with TSBA50 library, *Citrobacter koseri*, *Enterobacter cloacae* and *Salmonella choleraesuis* were identified with identification scores > 0.90.

The biochemical and physiological characteristics of *Enterobacter* A47 are presented in Table 2.1. Biochemically and physiologically, the strain was most similar to *Enterobacter* species *E. pyrinus*, *E. hormaechei* and *E. asburiae*. Shared features included: positive results in tests for gas production from glucose, catalase activity, urease activity, citrate utilization and acid production from mannose, maltose, xylose, sucrose, trehalose, arabinose and glycerol; negative results in tests for indole production, DNase activity and gelatin liquefaction. However, phenotypically, *Enterobacter* A47 can be differentiated from the type strains of those related species by several tests (Table 2.1). In contrast with *E. hormaechei* and *E. asburiae*, *Enterobacter* A47 was negative for the methyl red and ornithine decarboxylase activity tests. Another distinguishing result was the production of acid from adonitol, which was positive for *Enterobacter* A47 and negative for all the related species. Other species distinctive characteristics were: *E. asburiae* negative results for acetoin production (Voges-Proskauer test), malonate utilization and acid production from rhamnose; *E. hormaechei* positive results for acid production from dulcitol; and *E. pyrinus* positive results for acid production from inositol and production of H₂S.

Table 2.1 Biochemical and physiological characteristics of *Enterobacter* A47 in comparison with related species type strains *Enterobacter pyrinus* KCTC 2520^T, *E. hormaechei* ATCC 49162^T and *E. asburiae* ATCC 35953^T

Test	<i>Enterobacter</i> A47	<i>E. pyrinus</i> KCTC 2520 ^T	<i>E.</i> <i>hormaechei</i> ATCC 49162 ^T	<i>E. asburiae</i> ATCC 35953 ^T
Catalase	+	+	+	+
Gas from glucose	+	+	+	+
Indole production	-	-	-	-
Methyl red	-	N.D.	+	+
Voges-Proskauer	+	+	+	-
Citrate (Simmons)	+	+	+	+
H ₂ S production	-	+	-	-
Urea hydrolysis	+	+	+	+
Gelatin hydrolysis	-	-	-	-
DNA hydrolysis	-	-	-	-
Arginine dihydrolase	+	N.D.	+	+
Lysine decarboxylase	-	N.D.	-	-
Ornithine decarboxylase	-	N.D.	+	+
ONPG	+	N.D.	+	+
Malonate utilization	+	+	+	-
Acid production from:				
Mannose	+	+	+	+
Maltose	+	+	+	+
Xylose	+	+	+	+
Sucrose	+	+	+	+
Trehalose	+	+	+	+
Arabinose	+	+	+	+
Rhamnose	+	+	+	-
Adonitol	+	-	-	-
Dulcitol	-	-	+	-
Inositol	-	+	-	-
Glycerol	+	+	+	+
Reference	This study	Chung et al., 1993	O'Hara et al., 1989	Brenner et al., 1986

“+” and “-” represent positive and negative results, respectively, to the test.

N.D. – data not available.

16S rDNA Gene Sequence

The complete 16S rDNA gene sequence (1523 bp) was determined and compared with representative sequences of members of the family *Enterobacteriaceae* (Table 2.2). The phylogenetic tree (Figure 2.2) was constructed using the neighbor-joining method. The

species most closely related to *Enterobacter* A47 was *Enterobacter pyrinus*. However, the data was not clear since the strain showed similarity of 98.3% with *E. pyrinus* DSM 12410^T and 96.2% with *E. pyrinus* KCTC 2520^T, which is the strain given as reference in the List of Prokaryotic Names with Standing in Nomenclature. *Enterobacter* A47 showed high similarities of 99.0% and 98.9% (binary values) with the bacteria *E. hormaechei* and *E. asburiae* respectively. The highest similarity found was 99.4% (binary value) with a not yet validated strain, *Enterobacter hormaechei* subsp *steigerwaltii* (Hoffman et al., 2005).

Table 2.2 16S rDNA gene sequence of the bacterium *Enterobacter* A47 (DSM 23139)

1	TGATCCTGGC	TCAGATTGAA	CGCTGGCGGC	AGGCCTAACA	CATGCAAGTC	GAACGGTAAC
61	AGGAAGCAGC	TTGCTGCTTC	GCTGACGAGT	GGCGGACGGG	TGAGTAATGT	CTGGGAAACT
121	GCCTGATGGA	GGGGGATAAC	TACTGGAAAC	GGTAGCTAAT	ACCGCATAAY	GTCGCAAGAC
181	CAAAGAGGGG	GACCTTCGGG	CCTCTTGCCA	TCGGATGTGC	CCAGATGGGA	TTAGCTAGTA
241	GGTGGGGTAA	CGGCTCACCT	AGGCGACGAT	CCCTAGCTGG	TCTGAGAGGA	TGACCAGCCA
301	CACTGGAACT	GAGACACGGT	CCAGACTCCT	ACGGGAGGCA	GCAGTGGGGA	ATATTGCACA
361	ATGGGCGCAA	GCCTGATGTCA	GCCATGCCGC	GTGTATGAAG	AAGGCCTTCG	GGTTGTAAAG
421	TACTTTCAGC	GGGGAGGAAG	GCGATAAGGT	TAATAACCT	GTCGATTGAC	GTTACCCGCA
481	GAAGAAGCAC	CGGCTAACTC	CGTGCCAGCA	GCCGCGGTAA	TACGGAGGGT	GCAAGCGTTA
541	ATCGGAATTA	CTGGGCGTAA	AGCGCACGCA	GGCGGTCTGT	CAAGTCGGAT	GTGAAATCCC
601	CGGGCTCAAC	CTGGGAACTG	CATTCGAAAC	TGGCAGGCTA	GACTCTTGTA	GAGGGGGGTA
661	GAATTCCAGG	TGTAGCGGTG	AAATGCGTAG	AGATCTGGAG	GAATACCGGT	GGCGAAGGCG
721	GCCCCCTGGA	CAAAGACTGA	CGCTCAGGTG	CGAAAGCGTG	GGGAGCAAAC	AGGATTAGAT
781	ACCCTGGTAG	TCCACGCCGT	AAACGATGTC	GACTTGGAGG	TTGTGCCCTT	GAGGCGTGCC
841	TTCCGGAGCT	AACGCGTTAA	GTCGACCGCC	TGGGGAGTAC	GGCCGCAAGG	TAAAACTCA
901	AATGAATTGA	CGGGGGCCCG	CACAAGCGGT	GGAGCATGTG	GTTTAATTCG	ATGCAACCGC
961	AAGAACCTTA	CCTACTCTTG	ACATCCAGAG	AACTTCCAG	AGAGGATTG	GTGCCTTCGG
1021	GAACTCTGAG	ACAGGTGCTG	CATGGCTGTC	GTCAGCTCGT	GTTGTGAAAT	GTTGGGTAA
1081	GTCCCACAAC	GAGCGCAACC	CTTATCCTTT	GTTGCCAGCG	GTGAGCCGG	GAACTCAAAG
1141	GAGACTGCCA	GTGATAAACT	GGAGGAAGGT	GGGGATGACG	TCAAGTCATC	ATGGCCCTTA
1201	CGAGTAGGGC	TACACACGTG	CTACAATGGC	GCATACAAAG	AGAAGCGACC	TCGCGAGAGC
1261	AAGCGGACCT	CATAAAGTGC	GTCGTAGTCC	GGATTGGAGT	CTGCAACTCG	ACTCCATGAA
1321	GTCGGAATCG	CTAGTAATCG	TGGATCAGAA	TGCCACGGTG	AATACGTTCC	CGGGCCTTGT
1381	ACACACCGCC	CGTCACACCA	TGGGAGTGGG	TCGCAAAGA	AGTAGGTAGC	TTAACCTTCG
1441	GGAGGGCGCT	TACCACTTTG	TGATTCATGA	CTGGGGTGAA	GTCGTAACAA	GGTAACCGTA
1501	GGGAACCTGC	GGGCTGGATC	AAC			

The criterion to identify a given microorganism within a known species, defined as having a similarity of at least >90% or, ideally, >99.5%, with the type strain for that species (Janda and Abbott, 2007) was not met. On the basis of these results, *Enterobacter* A47 might represent a new species within the genus *Enterobacter* or a subspecies or species of *E. pyrinus*, *E. hormaechei* or *E. asburiae*.

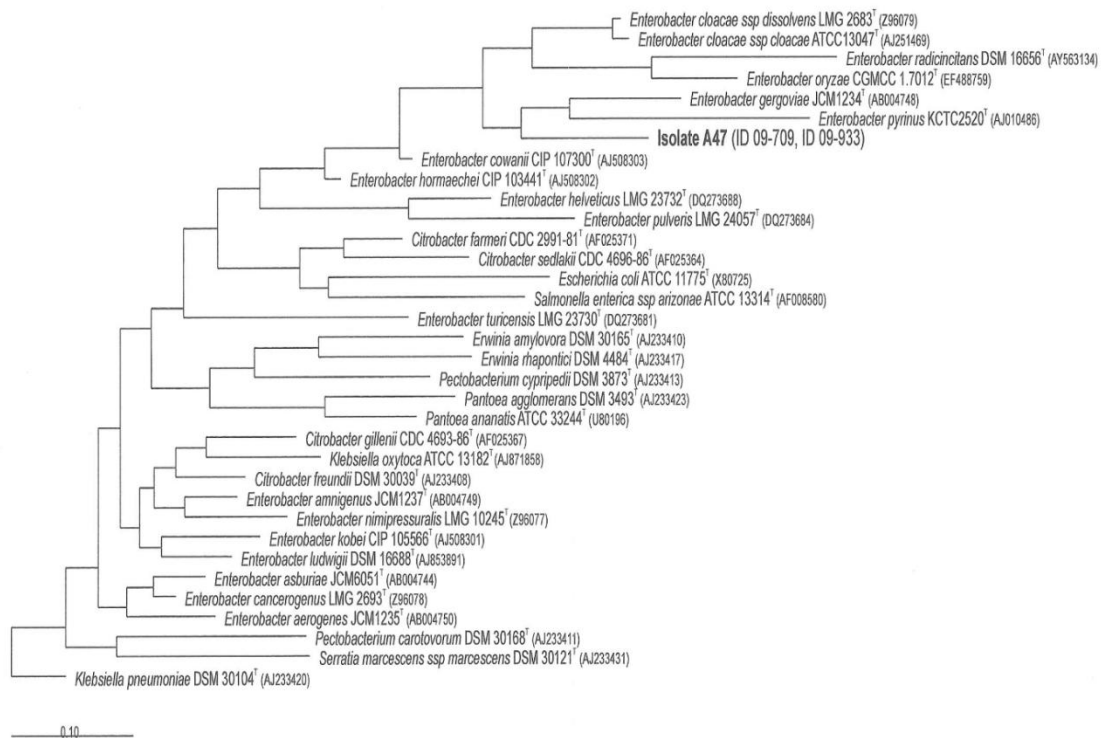


Figure 2.2 Phylogenetic analysis based on 16S rRNA gene sequences available from European Molecular Biology Laboratory (EMBL), Ribosomal Database Program (RDP) and DSMZ databases (accession numbers are given in brackets). The scale bar below the dendrograms indicates 1 nucleotide substitutions per 100 nucleotides.

2.4.2. FucoPol Production Process

Typical Enterobacter A47 Cultivation

A typical cultivation run of *Enterobacter A47* for exopolysaccharide production is presented in Figure 2.3 a, in which the profiles of cell growth on glycerol byproduct and EPS production are shown over time. The cultivation run was performed with a C:N ratio of 14:1 (w/w), corresponding of initial glycerol and nitrogen concentrations of 25 and 0.7 g L⁻¹, respectively.

Enterobacter A47 grew exponentially, attaining maximum biomass concentrations of 5.80 g L⁻¹ within less than 1 day. At that time, the fed-batch phase was initiated, during which cell growth was suppressed by imposing nitrogen limiting conditions (<0.1 g NH₄⁺ L⁻¹). Ammonium concentration was thereafter kept at a residual value (below the detection limit), even though the feeding solution containing 0.9 g NH₄⁺ L⁻¹ was fed to the bioreactor at a constant flow rate (2.5 mL h⁻¹ L⁻¹), while the dissolved oxygen concentration was controlled at 10% by the automatic variation of the stirring rate between 300 – 800 rpm. During this phase, cell dry weight (CDW) steadily decreased, which may be related to a loss of cell viability caused by the nitrogen and oxygen limiting conditions imposed in the bioreactor. Since bacterial cells were not multiplying at this stage, the volume withdraw from the bioreactor for sampling, concomitant with the continuous introduction of feeding medium and solutions for pH control, led to a net reduction of the CDW. Accompanying cell growth, glycerol concentration in the culture broth decreased from the initial 25 to 5 g L⁻¹ by the time that the fed-batch phase was initiated (Figure 2.3 a). From that time on, glycerol concentration was maintained below 2 g L⁻¹, even though it was being continuously fed to the bioreactor with a solution containing 200 g L⁻¹ of glycerol.

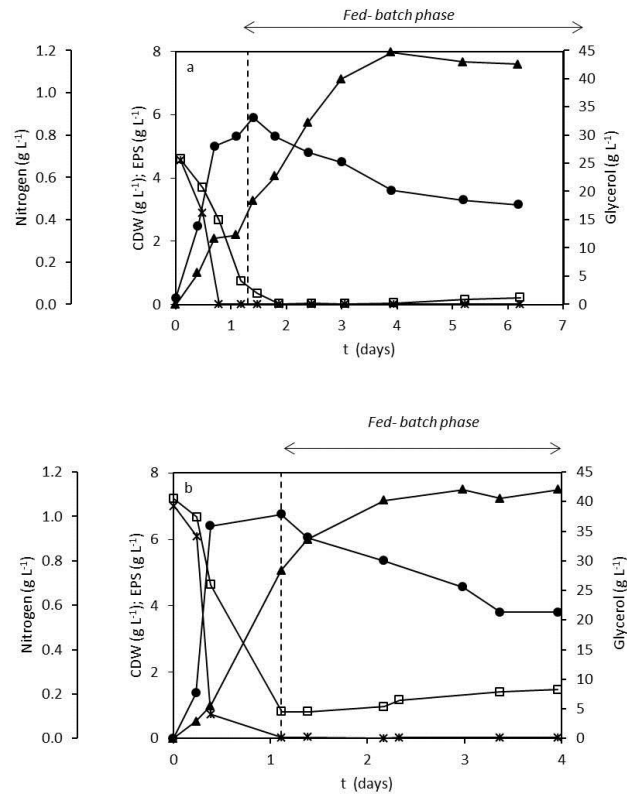


Figure 2.3 Time course of the cultivation of *Enterobacter* A47 on glycerol byproduct: (□) glycerol, (×) ammonium, (●) CDW and (▲) EPS. (a) Initial glycerol and nitrogen concentration of 25 and 0.7 g L⁻¹, respectively; (b) Initial glycerol and nitrogen concentration of 40 and 1.1 g L⁻¹, respectively.

FucoPol synthesis was initiated during the batch phase (~7 h), concomitantly with cell growth, reaching a concentration of 2.09 g L⁻¹ when the fed-batch phase was initiated. However, increased production was observed during the stationary growth phase (Figure 2.3 a), and an EPS concentration of 7.97 g L⁻¹ was attained at day 4. Although the run took 7 days, after day 4 EPS production maintained practically constant. Considering the time frame of increased EPS production (1 to 4 days), a volumetric productivity (r_P) of 2.04 gEPS L⁻¹ d⁻¹ and a specific productivity (q_P) of 0.36 gEPS gCDW⁻¹d⁻¹ were achieved. The net yield of EPS in glycerol ($Y_{P/S}$) was 0.17 g g⁻¹, a lower value than the 0.45 g g⁻¹ achieved by Zhang and Chen (2010) for xanthan production in a glucose/xylose mixtures, Müller et al. (2007) also achieved higher $Y_{P/S}$ for the alginate production optimization (within 0.28 -0.41 g g⁻¹) using glucose as carbon source.

The productivity values achieved are in the range of those presented for xanthan gum by Rottava et al. (2009) (1.46–2.4 gEPS L⁻¹ d⁻¹) and by Zhang and Chen (2010) (0.96 – 10.56 gEPS L⁻¹ d⁻¹), but are higher than the ones obtained for bacterial alginate (0.43–1.53

gEPS L⁻¹ d⁻¹) (Peña et al., 2000) and the EPS produced by *Enterobacter cloacae* WD7 (1.68 gEPS L⁻¹ d⁻¹) (Prasertsan et al., 2008), using glucose or sucrose as substrates.

FucoPol production was also carried out in a 2 L bioreactor fed with higher initial glycerol byproduct and nitrogen, namely, 40 and 1.1 g L⁻¹, respectively, keeping the same initial C:N ratio of 14:1 (w/w). All the other conditions were maintained unchanged. After a short adaptation period (~7.5 h) *Enterobacter* A47 entered an exponential growth phase that ended also within 1 day (as in the cultivation run above mentioned), when the ammonium concentration became limiting (under 0.1 g NH₄⁺L⁻¹), being the fed-batch phase initiated at that time.

Figure 2.3 b shows concentration profiles of biomass, EPS, glycerol and ammonium during the cultivation period. The culture attained a maximum cell dry weight of 6.68 g L⁻¹, at the end of batch phase (~1 day), which was higher than in the prior cultivation run due to the higher initial nitrogen concentration available. Subsequently, a decrease of the cell dry weight (CDW) was also observed (Figure 2.3 a and b). During the batch phase, the glycerol concentration decreased from the initial 40 g L⁻¹ to 5 g L⁻¹ simultaneously with cell growth (Figure 2.3 b). In the fed-batch operation glycerol was kept between 4 – 10 g L⁻¹, a concentration slightly higher than in the previous assay.

Under those conditions, *Enterobacter* A47 initiated EPS production a little earlier (~6 h) and at the end of the batch phase the EPS production was similar (2.69 g L⁻¹) to that obtained in the previous assay. The maximum EPS concentration (7.50 g L⁻¹) was attained at around third day. This value is similar to the one obtained in the prior cultivation run (7.97 g L⁻¹), but in a longer cultivation time. Hence, r_P was slightly higher (2.51 gEPS L⁻¹ d⁻¹), owing to the shorter production time frame (~3 days). Concerning q_P (0.37 gEPS gCDW⁻¹ d⁻¹), as well as the net yield of biomass and EPS on glycerol were similar to the former cultivation run.

Results demonstrated that a typical *Enterobacter* A47 cultivation run may be performed with glycerol and nitrogen concentrations within 25 – 40 g L⁻¹ and 0.7 – 1.1 g L⁻¹, respectively, keeping the C:N ratio at 14:1 (w/w). However, with higher initial glycerol and nitrogen concentrations the productivities achieved were higher.

Kinetics Modelling

A kinetic characterisation of the cultivation run presented in Figure 2.2 b was obtained by fitting the model Equations. (2.6) - (2.14) (see section 2.2.1) to the experimental data obtained in the 4 days cultivation run. Overall modelling results are shown in Figure 2.4 and Table 2.3. The glycerol half saturation constant (K_S) cannot be accurately estimated due to the lack of measured data at very low glycerol concentrations. An arbitrarily low value was used instead, $K_S = 9.21 \times 10^{-5} \text{ g L}^{-1}$ (Lin, 1979). All other parameters were estimated according to the previously described method.

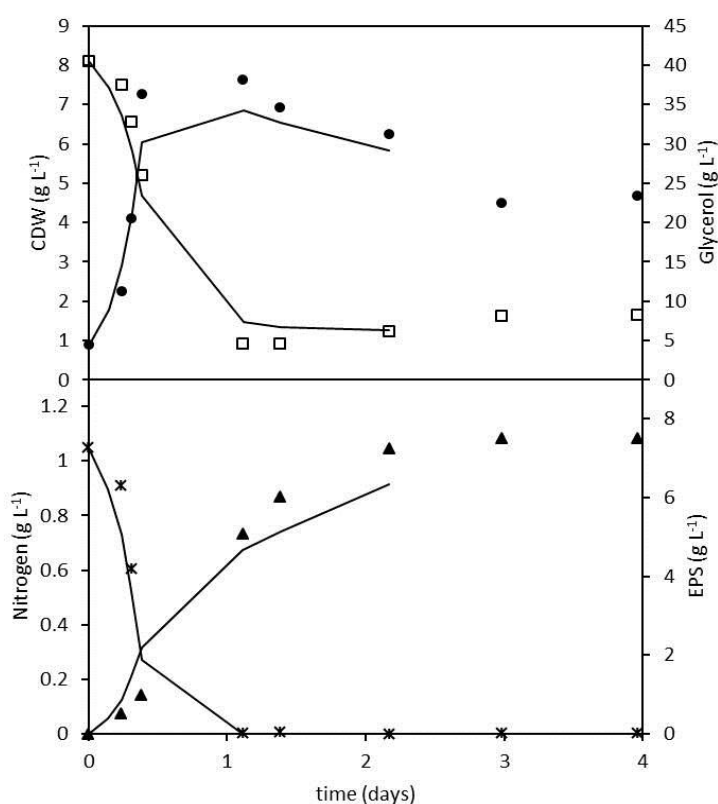


Figure 2.4 Experimental (symbols) and modelling results (continuous lines) showing the (\square) glycerol, (\times) ammonia, (\bullet) biomass and (\blacktriangle) EPS kinetics with time. The mean square errors were 0.194 g L^{-1} , 4.09 g L^{-1} , 0.020 g L^{-1} and 0.181 g L^{-1} for biomass, glycerol, ammonia and EPS respectively.

It can be observed that model predictions and experimental data are in good agreement. Also, parameter estimates show narrow confidence intervals, strengthening their statistical confidence.

The analysis of kinetic parameter values showed that the maximum cell growth rate was rather high ($\mu_{max} = 0.36 \pm 0.02 \text{ h}^{-1}$). The yield $Y_{X/S} = 0.49 \text{ g g}^{-1}$ was also high denoting a

robust and efficient cell growth process. EPS synthesis seemed to be partially growth associated ($\alpha = 0.12 \pm 0.09 \text{ g g}^{-1}$ and $\beta = 0.984 \pm 0.216 \text{ gEPS gCDW}^{-1} \text{ d}^{-1}$) although most of the EPS was synthesized after cell growth arrest at a specific synthesis rate of $0.041 \pm 0.009 \text{ gEPS gCDW}^{-1} \text{ h}^{-1}$. Considering only the nitrogen limited fed-batch phase, the volumetric EPS productivity determined by the model was $6.72 \text{ g L}^{-1} \text{ d}^{-1}$ and the yield $Y_{P/S}$ was $0.24 \pm 0.04 \text{ (g g}^{-1}\text{)}$.

Table 2.3 Maximum yields and Michaelis-Menten constant for glycerol uptake

	Values	Value source
$Y_{X/S}$	$0.49 \pm 0.05 \text{ g g}^{-1}$	Estimated
$Y_{P/S}$	$0.24 \pm 0.04 \text{ g g}^{-1}$	Estimated
$Y_{X/N}$	$5.45 \pm 0.36 \text{ g g}^{-1}$	Estimated
K_S	$\sim 0 \text{ g L}^{-1}$	Lin (1976)
K_N	$2.10 \times 10^{-3} \pm 1.68 \times 10^{-4} \text{ g L}^{-1}$	Estimated
μ_{max}	$3.61 \times 10^{-1} \pm 2.00 \times 10^{-2} \text{ h}^{-1}$	Estimated
$Y_{P/X}$	$1.20 \times 10^{-1} \pm 9.00 \times 10^{-2} \text{ g g}^{-1}$	Estimated
q_P	$0.984 \pm 0.216 \text{ g g}^{-1} \text{ h}^{-1}$	Estimated
m_S	0	Fixed
K_d	0	Fixed

2.4.3. Characterisation of the Culture Broth

Morphological Observations

Microscopic observations of culture broth samples performed throughout the cultivation run are presented in Figure 2.5. *Enterobacter* A47 cells are small rods, almost coccoid in shape, at the beginning of the cultivation, being found separately and in pairs.

Throughout the cultivation, most of the cells increased in length and a few short chains started to form (Figure 2.5 a). For the indirect detection of the EPS in culture broth samples, a negative staining technique (China ink) was used, based on the work of Hahn et al. (2004). At microscope observation, under low light intensity, the EPS appears as a light halo or ring around the cells, while the background is stained in black. At the beginning of the cultivation, the broth presented a low cellular density and no EPS was detected. At 1.0 day of cultivation, CDW attained its maximum concentration (Figure 2.3) and *Enterobacter* A47 cells were visualized under the optical microscope (Figure 2.5 a). Although the amount of EPS produced at this time was still too low to be clearly visualized, China ink staining (Figure 2.5 b) already showed some lighter areas surrounding the cells, which may attributed to the presence of the EPS.

Around 3.0 days cultivation, the microscopic observations showed that *Enterobacter* A47 cells were clumped together, forming aggregates (Figure 2.5 c). This cell aggregation behaviour has also been noticed for other microorganisms, such as, for example, the bacterium *Pseudomonas aeruginosa* (Al-Asheh et al., 2002) and the microalga *Rhodospirillum rubrum* (Basaca-Loya et al., 2008). At this cultivation time, EPS production had reached its maximum concentration (Figure 2.3), so it was possible to detect its presence by China ink staining (Figure 2.5 d). The image shows a white halo around cell aggregates, as well as a lighter background than that observed in Figure 2.5 b.

At the end of the cultivation, cell aggregates were reduced both in number and size (Figure 2.5 e). Figure 2.5 f shows an image of a broth sample taken at the end of cultivation stained with China ink. As shown by the white background of the image, the EPS matrix was spread out occupying nearly all the optical field, being the cells embedded in it, in contrast with the image taken at day 3.0 (Figure 2.5 d), where the EPS seems to be somewhat bounded to the cells. This may suggest that, as the EPS was being synthesized (up to day 4.0) it remained loosely attached to the bacterial cells. After that there was no further significant EPS production and the polymer may have become detached from the cells, thus spreading throughout the broth.

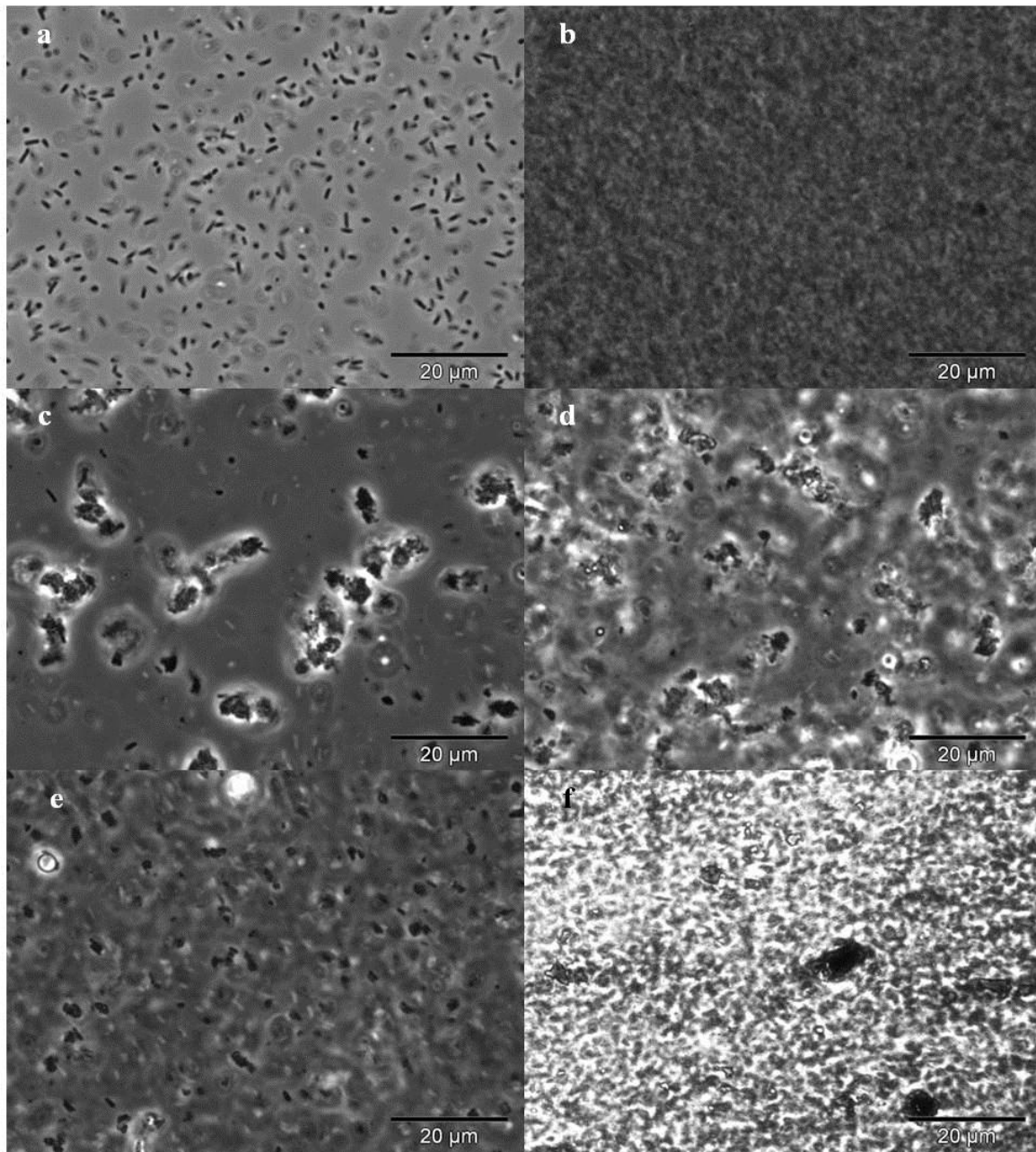


Figure 2.5 Microscopic observations of *Enterobacter* A47 broth samples at different cultivation times: 1.0 day (upper images: A and B), 3.0 days (middle images: C and D) and end of cultivation run (lower images: E and F), observed in phase contrast (left images) and after staining with China ink (right images).

Rheological Studies

Cultivation broth viscosity increases concomitantly with EPS production. In order to improve FucoPol production, it is necessary to keep the highly viscous broth well mixed,

which is problematic, especially at a large scale. In view of this, the study of the rheological properties of microbial culture broths is essential to improve EPS yield and productivity.

Steady-shear behaviour

Figure 2.6 shows the flow curves of *Enterobacter* A47 culture broth samples at different times (from the first day until seventh day) of the cultivation run represented in Figure 2.3 a. For all cases, the apparent viscosity was immediately recovered at low shear rates, after subjecting the samples to shear rate values up to 700 s^{-1} . Until 1.0 day of cultivation, the broth exhibited a Newtonian behaviour (Figure 2.6). Afterwards, it has developed non-Newtonian characteristics acting as a shear-thinning fluid, showing an increase of shear-thinning as the cultivation time proceeded. This viscosity built up is a common feature observed in much microbial cultivation for the production of extracellular polysaccharides and it usually determines the termination of the run due to loss of bulk homogeneity of the culture broth (Freitas et al., 2009b).

The apparent viscosity of the culture broth measured at low shear rates has shown an increase of three orders of magnitude (from 10^{-3} to 10^0 Pa s) (Figure 2.6). The rise in the broth viscosity and the increasingly non-Newtonian behaviour of the culture broth was mostly due to the accumulation of EPS in the aqueous medium. Bacterial cells had a negligible contribution to the changes in the broth rheological properties, since those changes occurred after maximum CDW was reached (day 1). In fact, the flow behaviour at the beginning of the experiment (day 0.2), for a very low cell concentration, was identical to that of the culture broth sample with the highest CDW at day 1.0 (Figure 2.6).

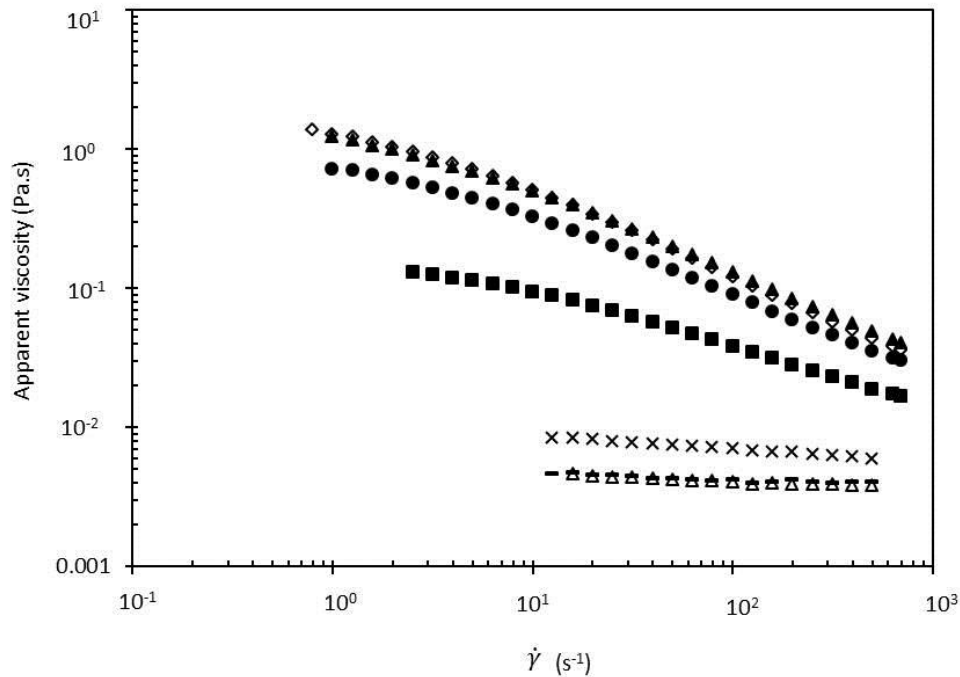


Figure 2.6 Flow curves for culture broth samples at different cultivation times: (Δ) 0 days, (-) 1.0 days, (\times) 2.0 days, (\blacksquare) 4.0 days, (\bullet) 5.0 days, (\diamond) 6.0 days and (\blacktriangle) 7.0 days. The measurements were made at 30 °C.

In each case, the relationship between the shear stress (τ , Pa) and the shear rate ($\dot{\gamma}$, s^{-1}) for the different broth samples could be fitted using the Power law or Ostwald-de-Waele model (Equation 2.17), which is commonly employed, namely by Sanchez et al, (2002) and Candia & Deckwer (1999):

$$\tau = k\dot{\gamma}^n \quad \text{Eq. 2.17}$$

where k is the consistency index ($Pa\ s^n$) and n is the power law index. The latter indicates the degree of non-Newtonian behaviour. For $n = 1$, the fluid is Newtonian, while for $n < 1$ it is considered shear-thinning. Both these parameters have changed throughout the cultivation time (Table 2.4). The power law index decreases as the consistency index increases throughout the cultivation run. In fact, at the beginning (up to 1.0 day) n was around 1, thus confirming the Newtonian behaviour of the broth at that time. Afterwards, n gradually decreased to a value of 0.4, showing the shear-thinning behaviour that is characteristic of most high molecular weight polymers in aqueous media, and observed in some bioreactor

culture broths as well, like those of *Pseudomonas aeruginosa* (Al-Asheh et al., 2002), *Leuconostoc mesenteroides* (Landon et al., 1993), *Xanthomonas campestris* (Candia & Deckwer, 1999) and *Beta vulgaris* (Sanchez et al., 2002). However, in the literature a few systems also referred cultivation broths which behaves differently, such as in the cultivation of *Bacillus cereus*, having a dilatant fluid behaviour with an initial yield stress (Al-Asheh et al., 2002).

Table 2.4 Power Law parameters for *Enterobacter* A47 broth samples taken at different cultivation times

Cultivation time (days)	EPS (g L ⁻¹) ^a	η (Pa s) ^b	Power law model ^c	
			K (Pa s ⁿ)	N
0.0	0.0	0.0047	0.004 ± 0.0005	0.984 ± 0.0190
1.0	3.66 ± 0.02	0.0052	0.006 ± 0.0002	0.948 ± 0.0069
2.0	7.73 ± 1.46	0.0147	0.026 ± 0.0013	0.814 ± 0.0083
4.0	12.24 ± 1.01	0.0814	0.263 ± 0.0105	0.577 ± 0.0067
5.0	12.77 ± 0.60	0.2590	1.174 ± 0.0610	0.439 ± 0.0093
6.0	12.64 ± 0.24	0.3910	2.033 ± 0.1231	0.383 ± 0.0105
7.0	13.28 ± 0.25	0.3939	1.947 ± 0.1097	0.407 ± 0.0099

^a EPS extracted with acetone; ^b At a shear rate of 15.85 s⁻¹, the associated error was ≤0.5%; the relative deviation errors - $RE = \sum_{i=1}^n (|X_{exp,i} - X_{cal,i}|/X_{exp,i})/n$ where ^c 0.0091 ≤ RE ≤ 0.1038.

The consistency index increased over the cultivation time, which is related to the increase of broth viscosity. The increase of the consistency index up to 4.0 days of cultivation may be attributed to the increase in EPS concentration (Figure 2.3; Table 2.4). On the other hand, its further increase between days 4.0 and 7.0 cannot be related only to EPS concentration, since it remained nearly constant. Such increase can be related with changes in the substituent's content and composition, which usually have great impact on the polymer's properties, such as solubility and rheology (Rinaudo, 2004). EPS anionic character is influenced by its content in pyruvyl and succinyl and glucuronic acid (Freitas et al., 2009). Hence, the raise of the broth viscosity and the consistency index after day 4 should be

essentially related to the formation of new interactions between individual EPS molecules and the other components of the complex media that is the cultivation broth, added by the slightly higher negative groups content. Another factor that probably has contributed to the increase of broth viscosity observed during the last days of the cultivation was the death of some microbial cells. As the cells lose their viability, they release their intracellular components, which might have an influence upon the broth viscosity. These hypotheses are in agreement with the results shown in Figure 2.7 a and b, where it is presented the steady-state and oscillatory data of the culture broth at day 7.0, and of an aqueous solution in deionised water of the purified EPS recovered at day 7.0, both samples having an identical polymer concentration (0.81 wt%, calculated subtracting the inorganic content).

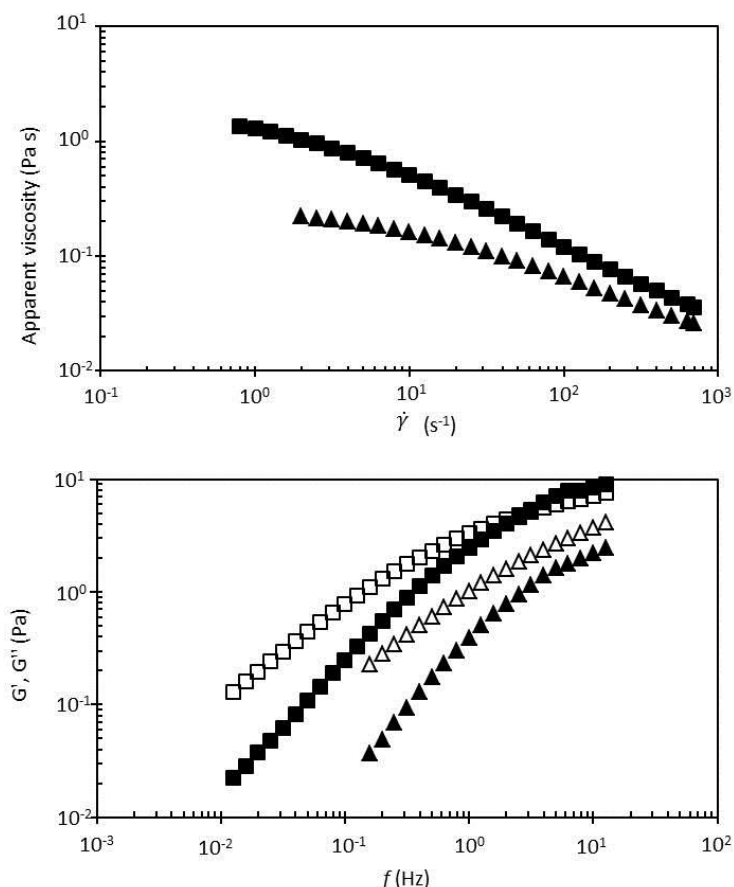


Figure 2.7 Steady-state (A) and oscillatory data (B) of the culture broth at day 7.0 (■), and of an aqueous solution in deionised water of the purified EPS taken at day 7.0 (▲), both samples having the same effective polymer concentration (0.81 wt%). G' (full symbols), G'' (open symbols).

As can be seen, the viscosity of the purified EPS sample is lower, meaning that, the ions and other components of the broth are acting as viscosity enhancers in the presence of EPS molecules. In addition, the mechanical spectrum of the purified EPS sample shows a higher loss modulus (G'') for all frequencies studied, in contrast with the data of the broth sample, for which the storage modulus (G') becomes higher at high frequencies (Figure 2.7).

The flow curves obtained for broth samples taken at 4.0, 5.2, 6.2 and 7.0 days of cultivation could be fitted by Equation (2.18), which is based on the Cross model normally used to describe all stages of the flow curves:

$$\eta_a = \frac{\eta_0}{1+(\tau\dot{\gamma})^m} \quad \text{Eq. 2.18}$$

where $\dot{\gamma}$ is the shear rate (s^{-1}), η_a is the apparent viscosity (Pa s), η_0 is the zero-shear rate viscosity (of the first Newtonian plateau) (Pa s), τ is a time constant (s) and m is a dimensionless constant, which may be related to the exponent of the power law (n) by $m = 1 - n$. Equation (2.18) is obtained from the Cross equation (Cross, 1965) assuming a negligible viscosity of the second Newtonian plateau when compared to η_a and η_0 , which is valid in this work since the second Newtonian plateau was never approached.

Eq. (2.18) fitted quite well the flow curves, and the parameter values obtained are presented in Table 2.5. The values of the exponent m are consistent with those obtained for n , the exponent of the power law. It is also observed an increase of the time constant τ as the viscosity of the culture broth becomes higher, meaning that more time is needed to form new polymer chain entanglements as they are disrupted by the shear stress imposed. As a consequence, the shear rate corresponding to the transition from Newtonian to shear-thinning behaviour moves to lower values as the concentration increases (Figure 2.6).

Table 2.5 Cross model parameters for *Enterobacter* A47 broth samples taken at different cultivation times

Cultivation time (days)	Cross model ^a		
	η_0	τ (s)	m
0.2	-	-	-
0.9	-	-	-
2.0	-	-	-
4.0	0.198 ± 0.010	0.122 ± 0.024	0.563 ± 0.021
5.2	1.980 ± 0.045	0.352 ± 0.046	0.677 ± 0.019
6.2	2.060 ± 0.049	0.492 ± 0.030	0.709 ± 0.009
7.0	2.070 ± 0.066	0.583 ± 0.057	0.659 ± 0.011

^aThe relative deviation error - $RE = \sum_{i=1}^n (|X_{exp,i} - X_{cal,i}|/X_{exp,i})/n$ where $0.0114 \leq RE \leq 0.0192$.

Oscillatory measurements and their correlation to steady-shear data

Figure 2.8 shows the angular frequency dependencies of storage (G') and loss (G'') moduli of the broth samples taken at days 4.0, 5.2, 6.2 and 7.0. At low frequencies (terminal zone), values of G'' were much higher than those of G' . This indicates that a liquid-like behavior predominated for all samples. However, at higher frequencies and for 5.2, 6.2 and 7.0 days broth samples, a cross-over was detected beyond which the elastic contribution predominated. This “cross-over frequency” (where $G' = G''$) moved to lower frequency values when the concentration increased (Figure 2.8 b–d), as a consequence of increasing relaxation times.

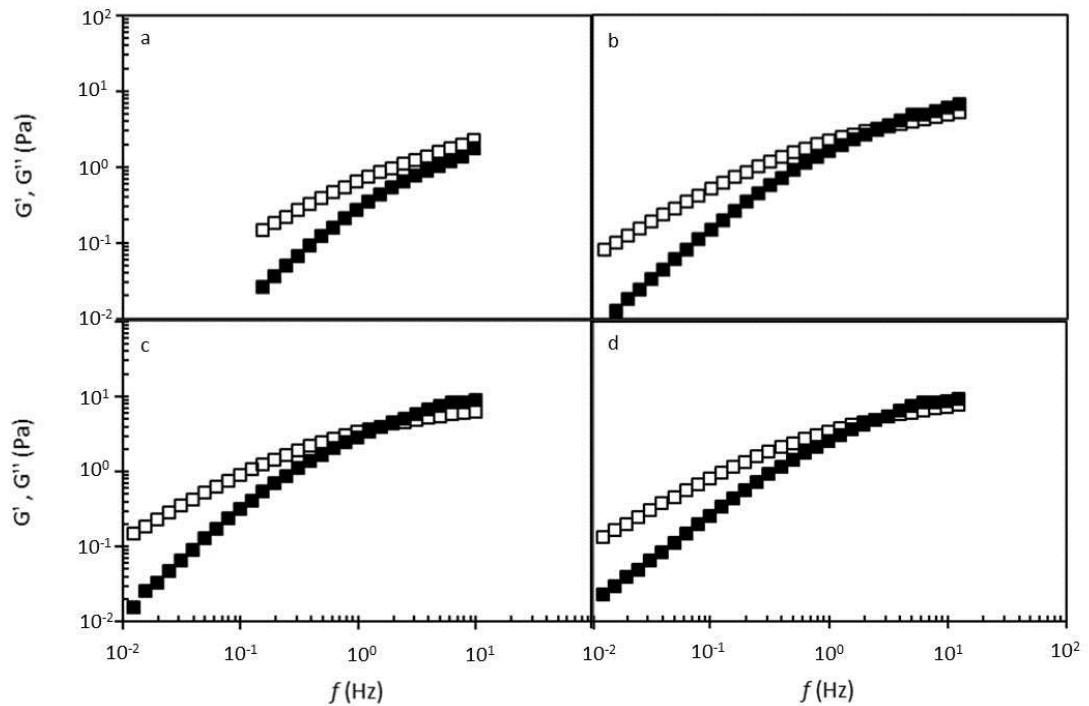


Figure 2.8 Storage (■) and loss modulus (□) for broth samples taken at different cultivation times: (a) 4.0 days; (b) 5.0 days; (c) 6.0 days and (d) 7.0 days.

In the measurement of the viscosity and viscoelasticity of simple polymeric solutions, the angular frequency dependence of complex viscosity is well superimposed on the shear rate dependence of the apparent viscosity, known as the Cox–Merz model. In this study, the correlation between apparent and complex viscosity was determined using *Enterobacter* A47 broth from different cultivation times. The plots of complex viscosity against angular frequency were completely superimposed to the curve of apparent viscosity against shear rate for all samples. Figure 2.9 presents the results obtained for broth samples at 4 and 7 days. This fact means that, although the culture broth is a complex system composed, not only by a high molecular weight polysaccharide, but also by other components, such as salts, glycerol and cells, it still possesses simple rheological properties. As the cultivation process proceeded, similar types of molecular rearrangements were taking place in the two flow patterns for the applied shear rate and frequency ranges (Xu et al., 2009).

The dynamic viscosity is also presented in Figure 2.9, and behaves as in many polysaccharide systems: approaching the zero-shear rate viscosity at low shear rates and diverging from the complex and apparent viscosities as the angular frequency increases. This

fact may be attributed to different molecular motions present in the dynamic and steady conditions at high frequency and shear rate (Ferry, 1980).

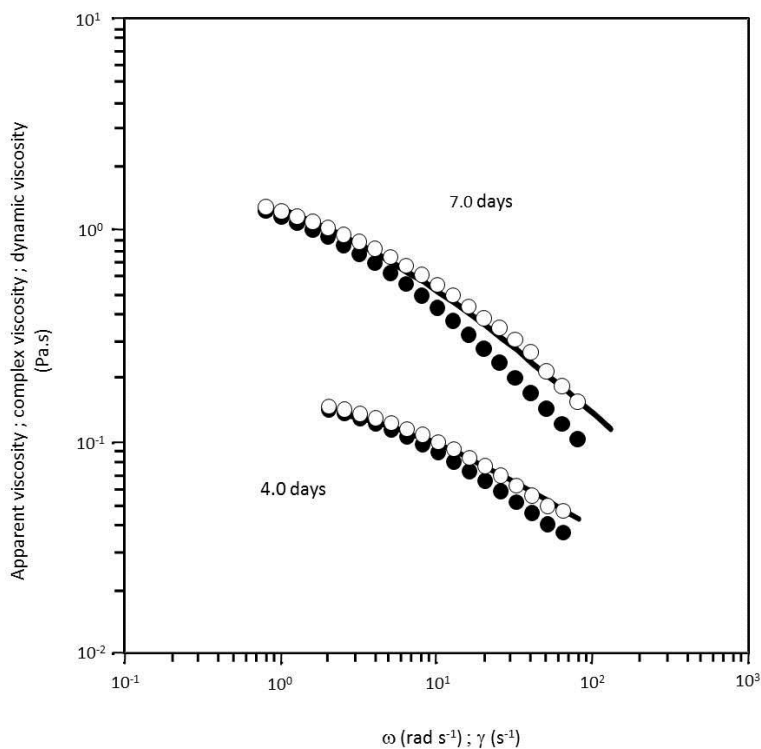


Figure 2.9 Cox–Merz plots for the broth samples isolated at days 4.0 and 7.0: (-) apparent viscosity; (○) complex viscosity and (●) dynamic viscosity.

2.4.4. FucoPol Characterisation

Sugar and Acyl Groups Composition

The glycosyl composition analysis of the purified EPS produced by *Enterobacter* A47 from glycerol byproduct revealed that it was a heteropolysaccharide mainly composed of neutral sugars: fucose (32 – 36 %mol), galactose (25 – 26 %mol) and glucose (28 – 34 %mol). Glucuronic acid, an acidic sugar, was also detected, accounting for 9 – 10 %mol of the polymer's sugar content. Different acyl groups substituents, namely, pyruvyl (13 – 14 wt. %), acetyl (3 – 5 wt.%) and succinyl (3 wt.%) were also detected. Identical EPS composition was obtained for both cultivations of Figure 2.3.

The evolution of EPS neutral sugar composition it was followed across a typical cultivation run, between days 1 and 4. As expected, the relative proportion of the neutral sugar monomers has suffered some changes throughout the assay (Figure 2.10 a). Around day 1 of cultivation, glucose was the main sugar monomer of the EPS with a content of 83 %mol. Galactose and fucose were present in much lower amounts (8 and 9 %mol, respectively). Between days 1 and 2, the neutral sugar monomers composition has suffered changes, namely, a reduction of the glucose content from 83 to 70 %mol, simultaneously with an increase of the content in galactose and fucose (from 8 to 19 %mol and from 9 to 11 %mol, respectively) (Figure 2.10 a). From that time on, the neutral sugar monomer composition of the EPS has changed significantly, being the final EPS (4 days) composed of fucose (32 %mol), galactose (25 %mol) and glucose (34 %mol). Longer cultivations (up to 7 days) showed that the composition of the EPS did not suffer any further changes of its sugar monomer composition.

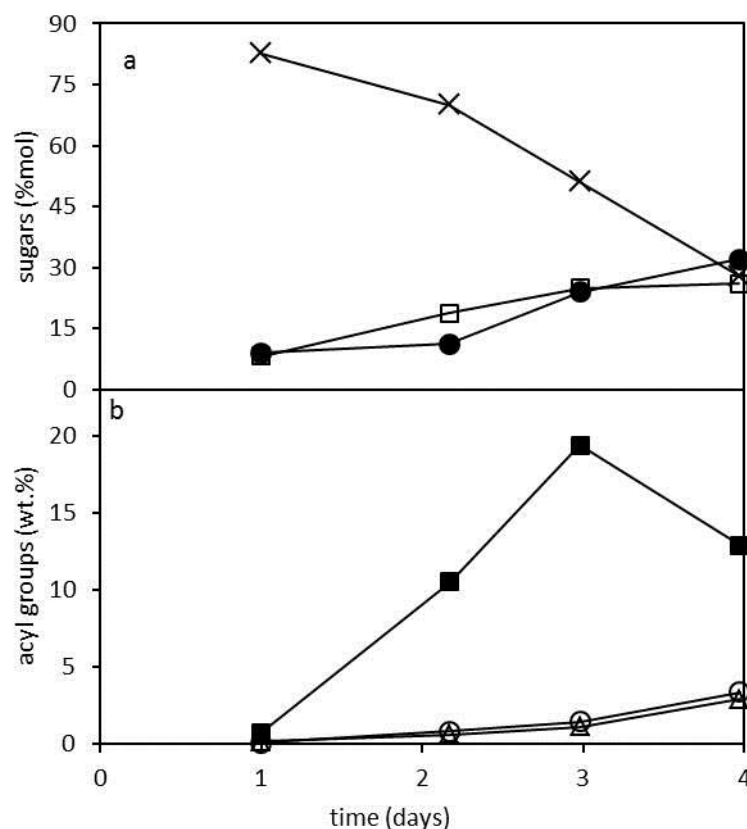


Figure 2.10 Profile of the FucoPol neutral sugar composition ((×) glucose; (□) galactose; (●) fucose) (A) and acyl groups ((■) succinyl; (○) pyruvyl and (△) acetyl) (B) along the cultivation run.

The observed changes in the polymer's sugar composition may reflect bacterial metabolism changes occurring throughout the run. EPS synthesis by bacteria needs energy-rich form monosaccharides as precursors, namely nucleoside diphosphate sugars (NDP-sugars), which are derived from phosphorylated sugars (Figure 2.11) (Sutherland, 1982; Freitas et al., 2011). All sugar nucleotides share a common precursor, which is glucose-6-P. The shortest pathway is the synthesis of UDP-glucose (Figure 2.11). Therefore, maybe the polymer is enriched in glucose at the beginning of the cultivation because the enzymes needed for the synthesis of the other sugar nucleotides (GDP-fucose, UDP-galactose, UDP-glucuronic acid) were still not available. The pathways leading to such sugar nucleotides require several enzymes and longer pathways for their synthesis (Kumar et al., 2007; Freitas et al., 2011).

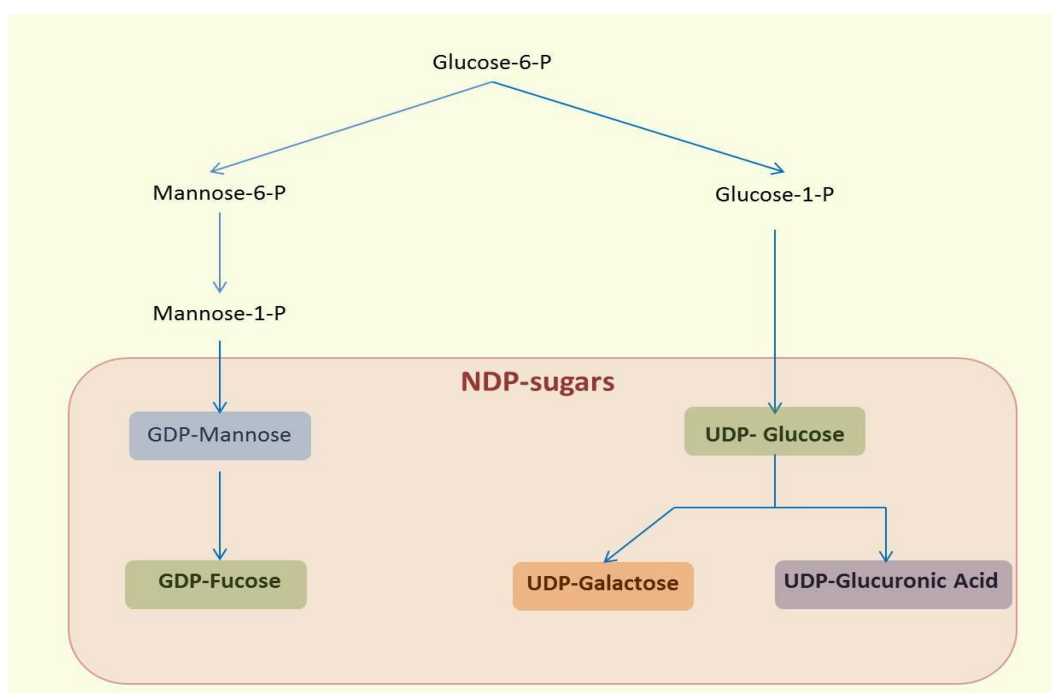


Figure 2.11 Resumed diagram of nucleotide biosynthetic pathway involved in bacterial EPS synthesis by Gram-negative bacteria. NDP, nucleoside diphosphate; UDP, uridine diphosphate; GDP, guanosine diphosphate (adapted from Freitas et al., 2011).

The evolution of acyl groups (Figure 2.10 b) substituents were also evaluated throughout the cultivation run (Figure 2.9 b). The total content in acyl groups increased from 0.7 wt.% at day 1 to 19.2 wt.% at day 4. The identified acyl groups in the acid hydrolysate were acetyl, pyruvyl and succinyl. Succinyl had the most significant increase throughout the

run, attaining its maximum content (19.4 wt.%) by the third day. Afterwards, it has decreased to 12.9 wt.% at day 4 (Figure 2.10 b). Acetyl and pyruvyl contents gradually increased throughout the entire run, reaching final contents of 2.9 wt.% and 3.4 wt.%, respectively. Further extending the cultivation to 7 days (data not shown) resulted in some additional changes in the polymer's content in succinyl, pyruvyl and acetyl (1.1 wt.%, 3.9 wt.% and 6.8 wt.%, respectively).

These differences verified in the acyl groups concentration from day 4 to day 7 may be one of the causes of the culture broth increase viscosity, as previous stated the succinyl content had a pronounced decrease, while acetyl and pyruvyl content increased. Casas et al. (2000) reported a similar behaviour for xanthan production, i.e. an increase of viscosity with the increase of acetyl and pyruvyl contents.

Proteins and Salts Contents

For the extraction of the EPS from the cultivation broth, two procedures have been tested and the resulting polymers were characterized in terms of their content in contaminants. The acetone contained considerable amounts of contaminants, namely, proteins (7.6-15.9 wt%) and inorganic residues (32.5%), remnants of the culture broth that co-precipitated with the polysaccharide. Thus, with the objective of obtaining a refined polymer, the EPS was extracted by dialysis of the cell-free supernatant with a 10000 MWCO membrane. This procedure allowed for the elimination of additional contaminants, whose content was considerably reduced. In fact, no inorganic residues were detected in the polymer. A fraction of the protein content still remained in the dialyzed polymer (<5 wt%), suggesting that such proteins were high molecular weight molecules.

Fourier Transform Infrared Spectroscopy

FucoPol's FT-IR spectrum is presented in Figure 2.12 along with the spectra of several other commercial polysaccharides for comparison. The polysaccharides analyzed were: Fucogel, which is a bacterial fucose-containing EPS, composed by fucose, galactose and galacturonic acid; alginate, which is an algae polysaccharide, composed by mannuronic and

guluronic acids, and acetate; and guar gum (a neutral plant polysaccharide composed of galactose and mannose).

The broad and intense band around 3400 cm^{-1} , common to all polysaccharides, represents O-H stretching of hydroxyls and bound water (Synytsya et al., 2003), which overlaps in part with the C-H stretching peak of CH_2 groups appearing at 2940 cm^{-1} . The well-defined envelope found between $1200\text{-}900\text{ cm}^{-1}$ represents skeletal C-O and C-C vibration bands of glycosidic bonds and pyranoid ring (Synytsya et al., 2003).

The band at 1720 cm^{-1} observed in the FucoPol and Fucogel spectra, but not identified in guar gum nor Alginate, may be attributed to the C=O stretching of carbonyls in acyl groups (Alvarez-Mancenido et al., 2008). Similarly, the band at 1250 cm^{-1} may also be attributed to the C-O-C vibration of acyls (Synytsya et al., 2003). The two strong bands around 1607 and 1405 cm^{-1} in alginate spectrum (Figure 2.12 c) can be attributed to the asymmetric and symmetric stretching of carboxylates, respectively (Synytsya et al., 2003). Such bands are also observed in the Fucogel and FucoPol spectra (Figure 2.12 a and b), which can be related with the presence of galacturonic and glucuronic acids in each polymer, respectively. Those bands are not seen in guar gum (Figure 2.12 d), since this polysaccharide is a neutral polymer. Even though the fucose-containing EPS and Fucogel spectra are quite similar, there is a distinctive band at 1564 cm^{-1} observed for the fucose-containing EPS (Figure 2.12 a) that may be attributed to the C=O anti-symmetric stretching vibrations of succinate (Krishnan et al., 2007). The identification of bands corresponding to acid groups in the FucoPol's spectrum is consistent with the presence of acyl groups, which account for 11 to 20 wt.% of the polymer.

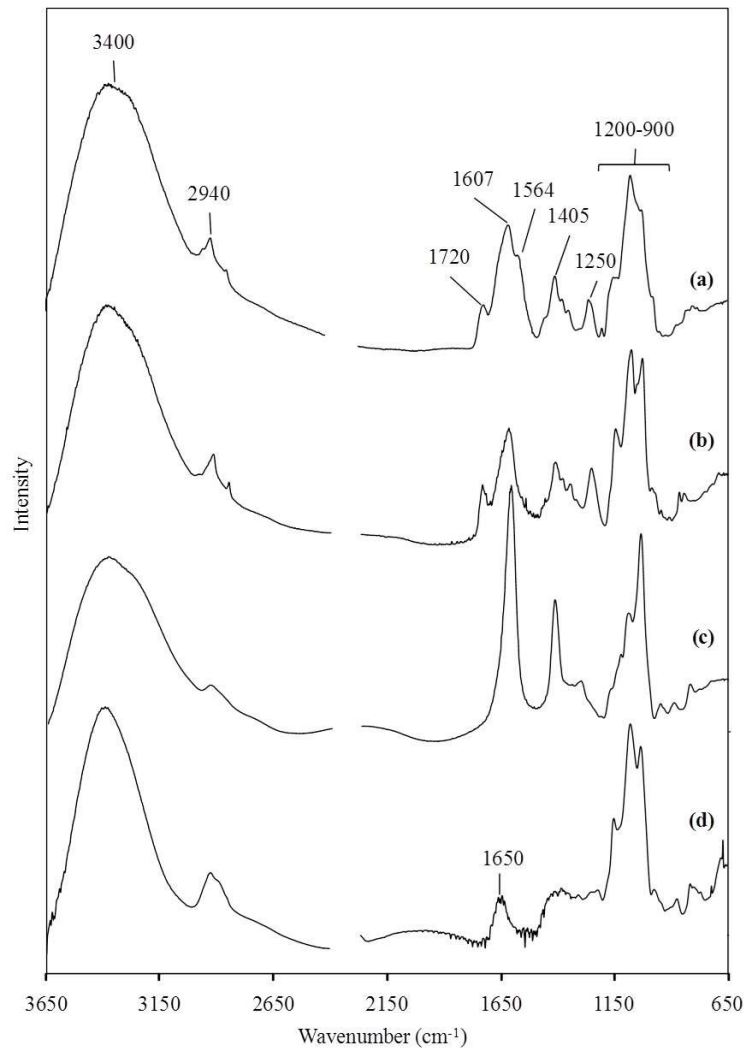


Figure 2.12 Comparative FT-IR spectra of polysaccharides: (a) FucoPol, (b) Fucogel, (c) alginate and (d) guar gum.

FucoPol Average Molecular Weight

Molecular weight (Mw) and polydispersity (PD) are important parameters that will determine the suitability of a given polymer for specific application. The PD reflects the degree of heterogeneity of the polymer's chain lengths.

FucoPol's weight average Mw was estimated by size exclusion chromatography (SEC). As shown in Figure 2.13 a, both the EPS Mw and the polymer's PD changed during the cultivation run. The Mw increased across the cultivation run (from 8×10^5 to 5×10^6), on the other hand the PD increase from 1.2 to 2.2 and after decreases again to 1.2.

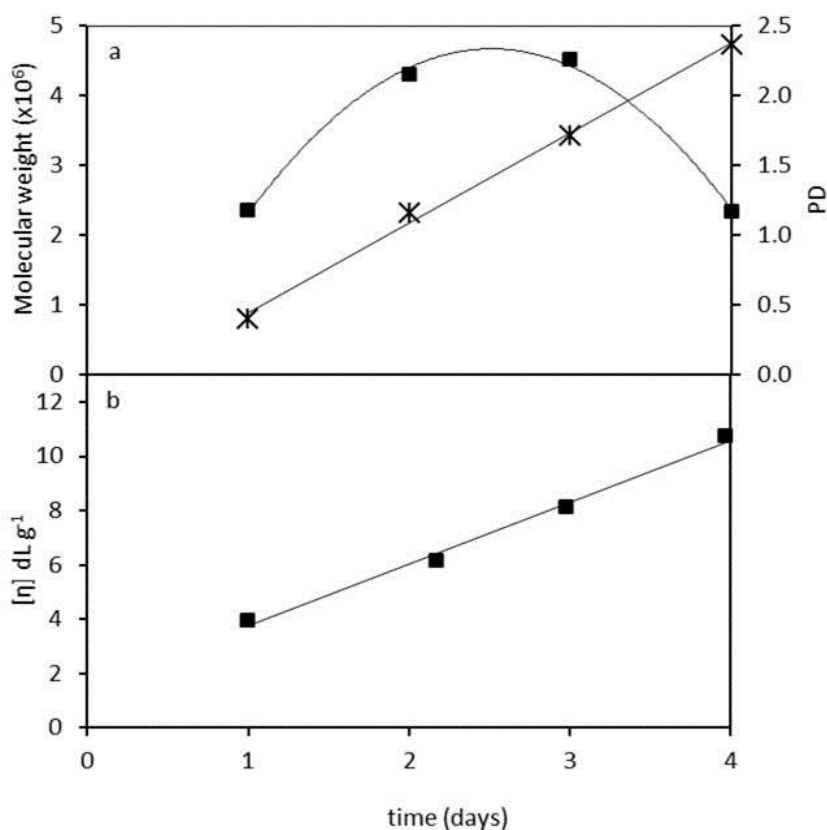


Figure 2.13 (a) Evolution of FucoPol's average molecular weight (X) and polydispersity (■) along the cultivation run. (b) Variation of the intrinsic viscosity over time.

The bimodal shape of the chromatograms (Figure 2.14) seems to suggest that the culture might have synthesized at least two distinct EPS, with different sugar composition and average Mw, and either of them predominated at different cultivation stages. At the beginning (day 1) of the cultivation, the lower Mw EPS seems to have prevailed (Figure 2.14). Considering that the polymer recovered from the broth at that time was mainly composed of glucose (83 %mol), this EPS might be a glucose homopolymer. The lower polymer content in fucose and galactose (9 and 8 %mol, respectively) may possibly be attributed to the higher Mw peak (Figure 2.14). The value of PD, calculated considering a whole peak, only for comparison purposes, was 1.2 (Figure 2.13 a).

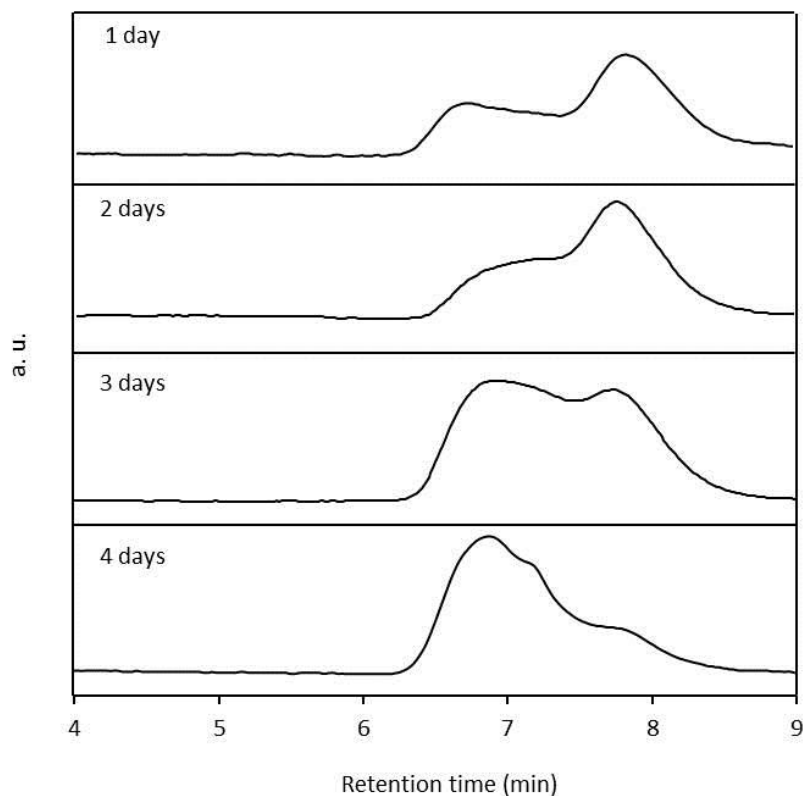


Figure 2.14 Mw chromatogram profiles for different cultivation times.

Concomitant with the reduction of the content in glucose (about 10 %mol) and the increase of the fucose and galactose contents (about 13 %mol each), between days 1 and 2, there was an increase on the polymer's Mw from 8.0×10^5 to 2.0×10^6 (Figure 2.13 a). Moreover, there was also an increase of the intensity of the peak corresponding to the higher Mw fraction of the polymer and a reduction of the lower Mw peak (Figure 2.14) that was observed until the end of the run. Hence, apparently the high Mw EPS became predominant. Although its content was lower, glucose was still a major sugar component of the polymer at that time, suggesting that the high Mw EPS might be composed of fucose, galactose and glucose.

The higher heterogeneity of the polymer between days 2 – 3 is also evidenced by the higher PD value obtained (2.2) during that period (Figure 2.13 a). At day 4 the EPS had a value Mw of 5.0×10^6 , and it was rather homogenous, as shown by the low PD of 1.2. The reduction of the PD is evidenced by the narrower chromatogram shape and the loss of the great bimodal character seen in Figure 2.14. The polymer obtained by the seventh day had a similar Mw 5.8×10^6 and PD (1.3).

These results are in accordance with the increase of the culture broth viscosity, indicating that besides the influence of the EPS composition on this characteristic, it is also deeply influenced by the raise of the EPS polymerization degree.

The Mw of some commercial polysaccharides was also measured under the same conditions. FucoPol showed to have a similar Mw to Fucogel (Solabia) (3.1×10^6) and commercial xanthan (5.0×10^6). Alginate, citrus pectin and CMC (carboxymethylcellulose) presented lower molecular weight values (4.3×10^5 , 2.2×10^5 and 5.1×10^5 , respectively).

FucoPol's Mw was higher than the value reported by Salah et al. (2010) for xanthan produced (8.0×10^4) by *Xanthomonas campestris* NRRL B-1459 using palm date juice byproduct as carbon source and similar (1.1×10^6) to the one reported by Reyes et al. (2003) for alginate produced by *Azotobacter vinelandii* in a modified Burk's medium.

Intrinsic Viscosity

The intrinsic viscosity ($[\eta]$) is a characteristic property of a single macromolecule in a given solvent and is a measure of the hydrodynamic volume occupied by the polymer itself. It depends on the polymer's molecular mass, chain rigidity and type of solvent.

The polymer's intrinsic viscosity was also evaluated between days 1 and 4 of the cultivation run (Figure 2.13 b). At the end of the run, FucoPol presented an intrinsic viscosity around 10.72 dL g^{-1} . This value is in agreement with the ones reported for several commercial typical commercial polysaccharides, such as xanthan and guar gum, $5\text{--}50 \text{ dL g}^{-1}$ (Arvidson et al., 2006). The intrinsic viscosity of Fucogel (16.7 dL g^{-1}) was also reported to be within this range (Guetta et al., 2003).

The Huggins constant ($k_H = 0.57$) of the EPS seems to indicate the presence of aggregates, since for flexible macromolecules in a good solvent k_H is generally around 0.3. Fucogel has a similar Huggins constant ($k_H = 0.55$), indicating some similarity between both fucose-containing polysaccharides in terms of aggregation.

The EPS intrinsic viscosity and the molecular weight had presented a similar trend, namely, as a linear increase along the cultivation run (Figure 2.13 a and b). This linearity is correlated, since the $[\eta]$ is a measure of the molecule's hydrodynamic volume and,

consequently, we may expect an increase of $[\eta]$ with the increase of its molecular weight (Bae et al., 2008). In fact, the average molecular weight of the polymer formed increased from 8.0×10^5 to 5.0×10^6 , which is concomitant with the increase of the intrinsic viscosity (Figure 2.6 a and b), between days 1 and 4.

Between the third and fourth day, the composition in neutral sugars barely varied, as well as EPS concentration. However, the same was not observed with the acyl groups. Their composition had a considerably variation, with a great decrease in succinyl and an increase in pyruvyl and acetyl content. This fact can affect the intrinsic viscosity, since the presence of these non-sacharide ionizable components, namely pyruvyl and succinyl, can affect the interactions between EPS molecules and within the same molecule (García-Ochoa et al., 2000). In other words, the presence of acyl groups affects the hydrodynamic volume, through molecule-molecule, molecule-solvent and intramolecular interactions, which may also be the source of the increase of $[\eta]$.

2.5. Conclusions

FucoPol's producing bacteria was identified as *Enterobacter* A47 by biochemical and physiological identification and by 16S rRNA gene sequence determination. Tests revealed that *Enterobacter* A47 could be a new species among the genus *Enterobacter* or a subspecies or species of *E. pyrinus*, *E. absuriae* or *E. homoarchei*.

FucoPol's bioprocess was composed of a batch phase where *Enterobacter* A47 grew exponentially and a fed-batch phase where the EPS production was more pronounced. Thus, EPS synthesis seems to be partially growth associated, as suggested by the experimental results and confirmed by the mathematical model.

The initial C:N ratio was kept at 14 :1 (w/w), however two distinctive initial glycerol and nitrogen concentrations were used, 25 – 40 and 0.7 – 1.1 g L⁻¹, respectively. Such difference in initial glycerol and nitrogen concentrations tested did not significantly affect *Enterobacter* A47 performance. Maximum FucoPol concentration of 7.50 – 7.97 g L⁻¹ was

achieved within 3 – 4 days of cultivation, corresponding to volumetric rates of 2.04 and 2.51 g L⁻¹ d⁻¹.

Along the cultivation run, the morphology of the culture broth changed, revealing the formation of cell aggregates surrounded by the EPS at the beginning of the cultivation run, while, at the end, aggregates were reduced both in number and size, and an EPS matrix with the cell embedded in it was observed. On the other hand, the culture broth flow behaviour also changed, from Newtonian in the beginning, to shear-thinning as the EPS was produced. It has been shown that the viscosity of *Enterobacter* A47 culture broth was not only dependent on EPS concentration, molecular weight and chemical composition, as the broth viscosity continued to increase when polymer production ceased, and when there was not a significant variation of the EPS molecular weight and chemical composition. The increase of broth viscosity in the end of the cultivation run should be essentially related to the formation of new interactions between individual EPS molecules and the other components of the broth. Nevertheless, changes in culture broth viscosity reflected the progress of the cultivation and, hence, rheological data can be used, in some extent, for monitoring the EPS production process.

The relative proportion of sugar monomers, as well as the content and composition of the acyl groups substituents of Fucopol have changed considerably throughout the cultivation run, reaching a stable composition at the end of the experiments. FucoPol was composed of fucose (32 – 36 %mol), galactose (25 – 26 %mol), glucose (28 – 34 %mol), glucuronic acid (9 – 10 %mol) and acyl groups substituents (succinyl, pyruyl and acetyl). FT-IR spectrum of the EPS was in accordance with the composition analysis.

FucoPol's average molecular weight was 5.0×10^6 at 4 days of cultivation run and 5.8×10^6 at 7th day. Mw and intrinsic viscosity of the EPS have increased linearly along the run and these two properties are closely related. The changes of polymer's physical-chemical characteristics could be correlated to the viscosity built up observed in the broth during the assay. *Enterobacter* A47 seems to be able to synthesize two distinct EPS, with different sugar composition and average Mw, as suggested by the bimodal shape of the SEC chromatograms.

Chapter 3

Optimization of FucoPol Production Study of the Interactive Effect of Temperature and pH using Multivariate Statistical Analysis

The results presented in this chapter were published in a peer reviewed paper.

Torres, C.A.V., Antunes, S., Ricardo, A.R., Grandfils, C., Alves, V.D., Freitas, F., Reis, M.A.M., 2012. Study of the interactive effect of temperature and pH on exopolysaccharide production by *Enterobacter* A47 using multivariate statistical analysis. *Bioresource Technology* 119, 148-156.

3.1. Summary

Enterobacter A47 synthesizes FucoPol, a fucose-containing EPS, using glycerol byproduct at 30 °C and pH 6.8. It has a Mw $\sim 5.0 \times 10^6$ and a fucose content within 32 – 36 %mol. In order to evaluate the impact of temperature (15.6 to 44.1 °C) and pH (5.6 to 8.4) on cellular growth and EPS production, in the current chapter a RSM (Response Surface Methodology) was used and a central composite rotatable design was applied. The effect of such conditions on polymer composition and average molecular weight was also assessed.

Maximum EPS production ($> 7.00 \text{ g L}^{-1}$) was obtained for temperature and pH within 25 – 35 °C and 6.0 – 8.0, respectively. Under these conditions, the polymers contained over 30 %mol fucose. Glucose, galactose, and glucuronic acid contents were about 28, 25, and 10 %mol, respectively, and the total acyl groups content was about 20 wt.%. The average molecular weight (Mw) was around 4.0×10^6 . Outside the optimal temperature and pH ranges, fucose, galactose and glucuronic acid, and the total acyl group contents were reduced, while the glucose content increased, new monomers (rhamnose and glucosamine) were detected, and the Mw increased to $\geq 1.10 \times 10^7$.

This study revealed the ability of *Enterobacter* A47 to synthesize different heteropolysaccharides as a function of pH and temperature, a feature that can be exploited to obtain tailored polymer composition. Moreover, the production of high fucose content EPS was stable for wide pH and temperature ranges, which is important for the envisaged industrial development of the bioprocess.

3.2. Introduction

Despite their valuable properties, only a reduced number of bacterial EPS has reached industrial development and is currently commercially available (e.g. xanthan, gellan gum, hyaluronic acid) (Freitas et al., 2011). The main limitation of bacterial production of polysaccharides is their high production costs. One of the strategies to turn such processes more cost effective is the improvement of product yield and productivity, which can be achieved by optimization of the fermentation conditions (e.g. pH, temperature, carbon and nitrogen source concentration) (Freitas et al., 2011). Similarly to other microbial bioprocesses, nutritional and environmental conditions strongly affect EPS synthesis (Kumar et al., 2007). Temperature and pH, which considerably influence the activity of bacterial enzymes (Kanari et al., 2002), are important environmental factors controlling both microbial growth and metabolite synthesis (Toledo et al., 2008).

To improve bioreactor operational conditions, several optimization tools have been developed. Response surface methodology (RSM) is a recognized method for optimization of diverse areas of biotechnology. This approach is composed by statistical design of experiments, mathematical modelling and coefficient estimation, along with response prediction and model accuracy testing (Ratnam et al., 2003). The most common model used in RSM for bioprocesses optimisation is the second order polynomial (Banik et al., 2007; Jiang, 2010; Majumder et al., 2009; Sousa et al., 2010).

In chapter 2, the production of FucoPol, a new fucose-containing EPS, by the bacterium *Enterobacter A47* (DSM 23139), using glycerol byproduct from the biodiesel industry as the sole carbon source was described. The standard process was performed with controlled temperature and pH at 30 °C and 6.8, respectively. In the current chapter, the interactive effect of temperature (15.6 to 44.1 °C) and pH (5.6 to 8.4) on *Enterobacter A47* cellular growth and EPS production were evaluated. The impact of such conditions on polymer composition and average molecular weight was also evaluated. RSM was used and a central composite rotatable design

was applied, where the standard conditions previously described in Chapter 2 were set as the central point conditions.

3.3. Material and Methods

3.3.1. FucoPol Production

Microorganism and Media

Enterobacter A47 was grown as described in section 2.2.1. – Chapter 2.

Bioreactor Operation

All experiments were carried out in 2 L bioreactors and operated as described in section 2.3.1. – Chapter 2. For this set of experiments runs were performed with an initial glycerol and nitrogen concentration of 40 and 1.1 g L⁻¹, respectively. The bioreactor was operated with controlled temperature and pH, which were in the range of 15.9 - 44.1 °C and 5.6 - 8.4, respectively, for the different runs performed, according to the experimental design (see section 3.3.3).

Analytical Techniques

Were used the same analytical techniques described in section 2.3.1. – Chapter 2.

3.3.2. FucoPol Characterisation

Sugar and Acyl Groups

The sugar and acyl groups composition was analysed as described in section 2.3.3. – Chapter 2.

Molecular Weight

In this chapter EPS average molecular weight (M_w) and polydispersity were determined by SEC-MALLS (Size Exclusion Chromatography - Multi-Angle Laser Light Scattering). EPS solutions (0.2 g/dL) were dissolved first by dispersion the powder in Tris-HCl 0.1M; NaCl (0.2 M), pH 8.1 buffer. These aqueous dispersions were warmed for 1 hour at 80°C in a water bath under lateral agitation (50 rpm). Dissolution of the polymer was future continued for 36 hours under rolling agitation at room temperature The polymer solutions were filtrated on polysulfone filter (0.45 μm ; 23 mm Whatman Puradisc 25AS) before their injection on the SEC-MALS system. The molecular weight distribution of EPS was analysed by Size Exclusion Chromatography coupled with Multiple Angle Light Scattering (SEC-MALS) adopting a SEC mobile phase made of Tris-HCl 0.1M; NaCl (0.2 M), pH 8.1 buffer. The latter combines in series respectively: a HPLC pump (Hewlett Packard quaternary 1050), an autoinjector (Hitachi-Merck, Lachrom L7200, model: 1405 – 040); an analytical SEC linear columns (PL aquagel-OH mixed 8 μm , 30 x 7.5 mm) protected by a guard column (Polymer Laboratory; 50 x 7.5 mm, part n° 1149-1840). The SEC columns were equilibrated for 24 hours before running the analysis at a flow rate of 0.7 ml min⁻¹ at room temperature. The analysis was performed by injection of 100 μL volume of EPS solution (0.2 g dL⁻¹). Each analysis was conducted in duplicate.

Signals from MALS (Wyatt Technology Corporation Dawn Model mounted with an Uniphase Argon laser (488 nm; 10 mW; K5 cell Flow cell) and RI signals (Optilab DSP, Wyatt Technology Corporation 488.0 nm, P10 cell thermostated at 30°C) were recorded in parallel and treated with Astra (V 4.73.04) in order to follow the purity and molecular mass distribution

of the polysaccharide. A dn/dc of 0.190 mL g^{-1} has been adopted to calculate the Mw of the EPS. Quality of the whole MALS installation was verified adopting PEG standards and protein standards (bovine serum albumin and egg albumin).

3.3.3. Experimental Design

Response Surface Methodology

To assess the optimal cultivation conditions for EPS production by *Enterobacter* A47, a statistical approach was applied, namely, response surface methodology (RSM) (Lundstedt et al., 1998). RSM was used to evaluate the impact and the interaction between the experimental variables (X_i): pH and temperature, and the observed responses (Y_i): specific growth rate (μ, h^{-1}); maximum EPS concentration ($\text{EPS}_{\text{max}}, \text{g L}^{-1}$); specific productivity ($Q_p = \Delta \text{EPS} / (\Delta X \times \Delta t)$), $\text{gEPS gCDW}^{-1} \text{d}^{-1}$, determined considering the time range wherein EPS_{max} was achieved for each run); relative molar fractions of each sugar monomer, namely, fucose (Fuc), glucose (Glc), galactose (Gal), glucuronic acid (GlcA), rhamnose (Rha) and glucosamine (GlcN); acyl groups content, namely, pyruvyl (Pyr), succinyl (Succ) and acetyl (Acet), and average molecular weight (Mw).

A central composite rotatable design (CCRD), with two independent variables, was used to study the responses, where X_1 is the temperature ($^{\circ}\text{C}$) and X_2 the pH (Table 3.1). This design was composed of nine experiments, performed randomly: four factorial design points at levels ± 1 ; four experiments of axial level $\alpha = \pm 1.414$; and a central point with three replicas. The system's behaviour was evaluated by fitting the experimental data to the following second order model:

$$Y_p = b_0 + b_1X_1 + b_2X_2 + b_{11}X_1^2 + b_{22}X_2^2 + b_{12}X_1X_2 \quad (3.1)$$

where Y_p corresponds to the predicted responses, X_1, X_2 are the coded values of the independent variables; b_0, b_i, b_j, b_{ij} ($i, j = 1, 2$) are the coefficient estimates, where b_0 is the interception, b_1 and b_2 the linear terms, b_{11} and b_{22} the quadratic terms and b_{12} the interaction term. In order to identify an appropriate reduced quadratic model, the significance of each source of variation was obtained from statistical analysis (ANOVA and Multiple Linear Regression). The statistical analysis was done using the software Statistica, version 6.0 (StatSoft, Inc., Tulsa UK).

Statistical validity

Analysis of variance (ANOVA) and multiple linear regression gave information about the model fitting. The model was considered to be a good predictive tool when accurately described the experimental results assuming that the maximum error of prediction was within the experimental deviation range. Therefore, the model should satisfy the following criteria: a good correlation value ($R^2 > 0.7$, acceptable for biological samples, according to Lundstedt et al. (1998), with statistical meaning (p -value < 0.05 , for a 95% confidence level) and with no lack of fit (p -value > 0.05 , for 95% confidence level), i.e. the model error was in the same range as the pure error. The factors and their interaction were also evaluated by p -value at 95% confidence level. The effect of temperature and pH on the response was given by the statistic and the surface plots analysis.

3.4. Results and Discussion

In Chapter 2, the production of an extracellular fucose-containing polysaccharide – FucoPol – by the bacterium *Enterobacter* A47, using glycerol as the sole carbon source has been described. Bioreactor cultivation runs were performed with pH and temperature controlled at 6.8 ± 0.05 and 30 ± 0.1 °C, respectively. These pH and temperature values are commonly used

for cultivation of *Enterobacter* strains, such as *Enterobacter agglomerans* (Prasertsan et al., 2006), *Enterobacter cloacae* WD7 (Prasertsan et al., 2008) and *Enterobacter* sp. BY-29 (Yokoi et al., 2001). Therefore, those operation conditions were selected as the starting point to assess the impact of temperature and pH on *Enterobacter* A47 growth and EPS synthesis.

3.4.1. Standard Conditions for EPS Production

The typical cultivation profile for *Enterobacter* A47 growth and EPS production, using glycerol as carbon source, with pH and temperature control at 6.8 and 30 °C, respectively, is presented in Figure 2.3 (section 2.3.2 – Chapter 2). In the current work, the conditions of this typical cultivation profile, namely, controlled temperature at 30 °C and pH 7.0, were performed in triplicate and taken as the central point assays on the central composite rotatable design.

3.4.2. Influence of Temperature and pH: Response Analysis

Influence of Temperature and pH on Cellular Growth and EPS synthesis

The results obtained under the different temperature (15.9 – 44.1 °C) and pH (5.6 – 8.4) conditions tested are presented in Table 3.1. Maximum specific productivities (q_p) were achieved at 30 °C, with pH 7.0 (0.53 – 0.56 gEPS gCDW⁻¹ d⁻¹) and pH 8.4 (0.65 gEPS gCDW⁻¹ d⁻¹). The central point conditions also resulted in high specific growth rates (0.30 – 0.32 h⁻¹) and high EPS concentrations (7.23 – 7.79 g L⁻¹). Under the remaining conditions, EPS production was lower, except for run 7 (30 °C; pH=5.6), wherein a similar maximum EPS concentration (7.50 g L⁻¹) was obtained. These conditions also resulted in a high specific growth rate (0.25 h⁻¹). Hence, a lower specific productivity (0.28 gEPS gCDW⁻¹ d⁻¹) was obtained in that run.

Results showed that at 20 °C (runs 1 and 3), for both pH values tested (6.0 and 8.0), the culture grew slowly (specific growth rates of 0.14 and 0.12 h⁻¹, respectively). In contrast, at high

temperatures (40 °C) (runs 2 and 4), cellular growth was favoured for both pH values tested, as shown by the high specific growth rates observed in those runs (0.34 and 0.32 h⁻¹, respectively). The effect of temperature and pH on EPS synthesis was even more pronounced (Table 3.1), since in runs 1, 2 and 4, EPS production was between 0.82 and 2.59 g L⁻¹, corresponding to specific productivities below 0.13 gEPS gCDW⁻¹ d⁻¹.

With respect to the temperature extremes tested (15.9 °C and 44.1 °C), only 44.1 °C impacted cellular growth (0.17 g L⁻¹). EPS production at 15.9 °C was extremely affected, as the final EPS concentration was only 1.12 g L⁻¹. Therefore, the temperature had a stronger impact on EPS production than on cell growth.

It was observed that growth and EPS production were also influenced by pH. The decrease from pH 7.0 to pH 5.6 (run 7), did not affect EPS production and only a slight reduction of the specific growth rate was observed, whereas at pH 8.4 (run 8) significant reductions in both specific growth rate and EPS synthesis (0.12 h⁻¹ and 2.67 g L⁻¹, respectively) were observed.

These results suggest that *Enterobacter* A47 growth was not significantly affected by temperature within the range 15.9 – 40.0 °C, while EPS synthesis reached a maximum value around 30 °C, within a pH range of 5.6 – 7.0. For the lower and higher values of temperature tested, EPS production was negatively affected regardless of pH.

Composition of the EPS Synthesized by Enterobacter A47

The composition of the EPS obtained under the different experimental conditions is provided in Table 3.1. The typical polymer composition was obtained for the EPS produced under the central point conditions (30°C, pH=7.0), namely, 36 – 37 %mol fucose, 25 – 26 %mol galactose, 27 – 28 %mol glucose and 10 – 11 glucuronic acid.

The results obtained in this study seem to indicate that lower temperatures (15.9 – 20 °C; runs 3 and 5) led to a slight reduction in fucose and galactose monomers (26 – 30 %mol and 21 – 22 %mol, respectively), when compared to the central point (Table 3.1). Concomitantly,

there was an increase in glucose (to 36 %mol) and the inclusion of new monomers, rhamnose and glucosamine, in minor amounts (< 2 %mol).

Lowering the pH from 7.0 to 6.0 and 5.6 (runs 1, 2 and 7) had a much more pronounced effect on the composition of the EPS since fucose and galactose contents were reduced to 9 - 13%mol and 13 - 20 %mol, respectively, while glucose became the main sugar component (48 – 59 %mol) (Table 3.1). Additionally, there was also an increase in the rhamnose content to 6 – 9 %mol.

The combination of high temperatures (40 – 44.1 °C) and high pH (8.0 – 8.4) (runs 4, 6 and 8) led to the synthesis of EPS without fucose and higher contents in rhamnose and glucosamine. For the highest pH value tested (8.4; run 8) a rhamnose-rich EPS (29 %mol rhamnose content) was produced, simultaneously with an increase in glucosamine content to 11 %mol (Table 3.1).

Temperature and pH also had an impact on the EPS acyl groups content and composition (Table 3.1). The highest content in acyl groups (17 – 24 wt% of the polymer's dry weight) was obtained under the central point conditions (30 °C; pH 7.0), where pyruvyl, succinyl and acetyl accounted for 9 – 13 wt% , 2 – 3 wt% and 5 – 8 wt% of the polymer's dry mass, respectively. All the other tested conditions led to a reduction of the acyl groups content of the EPS (Table 3.1).

Table 3.1 Central composite rotatable design (CCRD) with two independent variable, X_1 (Temperature, T) and X_2 (pH), and the observed responses studied, Y_i (μ , specific growth rate; EPS max, maximum EPS concentration; q_p , specific productivity; Fuc, fucose, Gal, galactose; Glc, glucose; Rha, rhamnose; GlcN, glucosamine; Pyr, pyruvyl; Succ; succinyl; Acet, acetyl; Mw, average molecular weight)

Run number	T (°C)	pH	μ (h^{-1})	EPS max ($g L^{-1}$)	q_p ($gEPS dCDW^{-1} d^{-1}$)	Sugar Composition							Acyl groups composition (wt.%)					Mw				
						Fuc			Glc			GlcN			Pyr				Succ		Acet	
						Y_4	Y_5	Y_6	Y_7	Y_8	Y_9	Y_{10}	Y_{11}	Y_{12}	Y_{13}							
1	20.0	6.0	0.14	0.82	0.06	11	20	48	9	9	2	2	0	2	0	2	1.10 $\times 10^7$					
2	40.0	6.0	0.34	2.59	0.13	9	16	59	6	8	2	2	1	2	1	2	1.42 $\times 10^7$					
3	20.0	8.0	0.12	4.18	0.18	30	22	36	11	1	0	7	3	5	5	2.60 $\times 10^6$						
4	40.0	8.0	0.32	1.62	0.12	0	24	54	8	10	4	0	0	1	1	1.32 $\times 10^7$						
5	15.9	7.0	0.08	1.12	0.09	26	21	36	12	2	2	3	2	3	2	3	6.28 $\times 10^6$					
6	44.1	7.0	0.00	0.23	0.41	0	21	61	10	2	5	0	3	1	1	1.46 $\times 10^7$						
7	30.0	5.6	0.25	7.50	0.28	13	13	58	8	6	2	3	0	4	4	9.76 $\times 10^6$						
8	30.0	8.4	0.12	2.67	0.65	0	12	37	11	29	11	1	0	3	3	8.45 $\times 10^6$						
9	30.0	7.0	0.32	8.85	0.52	36	26	28	10	0	0	9	2	7	7	4.31 $\times 10^6$						
10	30.0	7.0	0.30	7.23	0.64	36	25	28	11	0	0	10	2	5	5	4.19 $\times 10^6$						
11	30.0	7.0	0.32	7.30	0.56	37	26	27	10	0	0	13	3	8	8	4.61 $\times 10^6$						

Average Molecular Weight of the EPS Synthesized by Enterobacter A47

The mean molecular weight and related polydispersity are critical macromolecular parameters which can drastically affect several functionalities of the final materials, in particular viscosity behaviour, diffusion properties or mechanical properties. For all the conditions tested, the EPS obtained had high Mw ($\geq 2.6 \times 10^6$), similar to the values reported for xanthan (5.0×10^6) and guar gums (2.6×10^6) (section 2.4.4 – Chapter 2). The highest Mw values were obtained for the EPS synthesized at 20 °C and pH 6.0, (1.10×10^7) and for temperatures ≥ 40 °C ($1.32 - 1.46 \times 10^7$) (Table 3.1). It should be stressed that the polymer recovery after SEC analysis, estimated on a mean dn/dc of 0.190 mL/g, has been found typically low, i.e. ranging from 10 to 41%. This observation is not really surprising due to the fact that most of these biopolymers have given colloid dispersions instead of true solutions whatever the duration of dissolution (15 – 36 hours). Most of the SEC profiles of the polysaccharides have also demonstrated heterogeneities with the presence of a bimodal population detected by MALS and RI detectors.

3.4.3 RSM Modelling

Although the one-to-one factor analysis enabled to evaluate the effect of temperature or pH on the different responses, it was not possible to identify the interaction between the two variables. In view of this, response surface methodology (RSM) was used to evaluate their combined effect. This statistical model was also used to define the working region to produce the highest EPS yield, as well as to determine conditions for production of an EPS with a targeted composition.

RSM (ANOVA and MLR) analysis used for the several responses is summarized in Table 3.2. For the whole set of responses, the second order developed model showed a good fitting ($R^2 > 0.90$), except for maximum EPS concentration (Y_2), rhamnose content (Y_8) and acetyl content (Y_{12}) responses, which, nevertheless, had an acceptable R^2 (> 0.80), according to Lundstedt et al. (1998). The ANOVA p -values showed that the second order model had

significance ($p < 0.05$) for all thirteen responses, except for the rhamnose content (Y_8). Even though, for certain responses (EPS_{max} , q_p , rhamnose content and Mw) there was evidence of lack of fit ($p < 0.05$), meaning that the model prediction error was above the error of the replicas. However, in these specific cases, the lack of fit could be explained by the pure error (calculated with the replicates of the central point), which was close to zero, thus giving an artificial sense of a model with lack of fit.

Table 3.2 Model and lack of fit p -values (significance levels) and R^2 values for the analysis of variance (ANOVA) for the responses of the central composite design

	Model	Lack of Fit	R^2
	p -value	p -value	
μ (Y_1)	0.007	0.067	0.959
EPS_{max} (Y_2)	0.027	0.024	0.873
q_p (Y_3)	0.010	0.022	0.952
Fuc (Y_4)	0.000	0.076	0.996
Gal (Y_5)	0.005	0.117	0.965
Glc (Y_6)	0.000	0.110	0.997
GlcA (Y_7)	0.028	0.265	0.917
Rha (Y_8)	0.140	0.000	0.801
GlcN (Y_9)	0.003	(---)	0.971
Pyr (Y_{10})	0.010	0.679	0.918
Succ (Y_{11})	0.017	0.629	0.936
Acet (Y_{12})	0.023	0.862	0.882
Mw (Y_{13})	0.002	0.018	0.960

μ – Specific growth rate (h^{-1}); EPS_{max} – Exopolysaccharide maximum concentration ($g L^{-1}$); q_p – Specific productivity ($gEPS gCDW^{-1} d^{-1}$); Fuc – Fucose content (%mol); Gal – Galactose content (%mol); Glc – Glucose content (%mol); GlcA – Glucuronic Acid content (%mol); Rha – Rhamnose content (%mol); GlcN – Glucosamine content (%mol); Pyr – Pyruvyl content (wt.%); Succ – Succinyl content (wt.%); Acet – Acetyl content (wt.%); Mw – Molecular weight.

Optimal Temperature and pH Ranges for Growth and EPS Synthesis

Multiple linear regression (MLR) gave information about the linear, quadratic and interaction effect of temperature and pH on the different responses (Table 3.3). The specific cell growth rate was affected mostly by the linear temperature and the quadratic terms of pH ($p <$

0.05) (Table 3.3). Such quadratic effect is represented by the parabola format on the 3D surface plot (Figure 3.1 a). The model predicted that *Enterobacter* A47 achieved higher cell growth rates within temperatures and pH ranges of 30–40 °C and 6.0–8.0, respectively.

Concerning EPS concentration and specific productivity models, the quadratic term of temperature (TxT) had an impact, which is also represented by the 3D surface plot with a parabola format (Figure 3.1 b and c), in which a nil EPS production and, consequently, a nil specific EPS productivity are predicted for extremes of temperature (below 20 °C or above 40 °C) and pH (below 6.0 or above 7.0). The model allowed estimating the conditions for maximal EPS production by the bacterium ($>7.00 \text{ g L}^{-1}$), which were: temperature and pH within the ranges 25–35 °C and 6.0–8.0, respectively. The highest production was obtained at 30 °C and pH 7.0 (Figure 3.1 b). Within those ranges, the specific EPS productivity, which is influenced by biomass concentration, was also maximal ($>0.50 \text{ gEPS gCDW}^{-1} \text{ d}^{-1}$) (Figure 3.1 c).

According to Lawson and Sutherland (1978), the optimum pH range for growth and EPS synthesis was 6.0–7.5 for most known polysaccharide-producing strains. pH and temperature optima of 7.0 and 30 °C, respectively, were reported for growth and EPS synthesis by *E. cloacae* WD7 (Prasertsan et al., 2008) and *E. agglomerans* WD50 (Prasertsan et al., 2006). However, the maximum EPS production achieved by those strains was much lower (2.71 and 0.83 g L^{-1} , respectively) than that obtained in the current work for *Enterobacter* A47. The optimal conditions for the production of gellan and xanthan were similar, namely, pH = 6.5–7.0 and T = 25–30 °C (Bajaj et al., 2006; Kalogiannis et al., 2003; Kanari et al., 2002).

Table 3.3 Constants and coefficients of polynomial models and *p*-values for both linear and quadratic effects and interaction of temperature and pH for the several responses (Y_n)

Effect	Linear			Quadratic		Interaction
	Constant	T (X_1)	pH (X_2)	TxT (X_1^2)	pH*pH (X_2^2)	TxpH (X_1X_2)
μ (Y_1)	0.313	0.107	-0.028	-0.032	-0.060	0.000
<i>p</i> - value	0.000	0.002	0.066	0.122	0.012	1.000
EPS _{max} (Y_2)	-108.200	2.855	21.468	-0.035	-1.341	-0.108
<i>p</i> - value	0.000	0.653	0.352	0.003	0.093	0.212
q _p (Y_3)	-3.033	0.033	0.670	-0.002	-0.062	0.012
<i>p</i> - value	0.000	0.011	0.007	0.006	0.126	0.068
Fuc (Y_4)	-875.786	10.637	219.588	-0.110	-14.248	-0.700
<i>p</i> - value	0.000	0.004	0.622	0.003	0.001	0.032
Gal (Y_5)	-163.658	0.146	50.639	-0.020	-3.729	0.150
<i>p</i> - value	0.000	0.584	0.006	0.017	0.004	0.066
Glc (Y_6)	686.264	-6.857	-156.379	0.107	10.377	0.175
<i>p</i> - value	0.000	0.000	0.001	0.000	0.000	0.204
GlcA (Y_7)	-29.893	0.314	9.876	-0.008	-0.631	0.000
<i>p</i> - value	0.000	0.008	0.021	0.119	0.145	1.000
Rha (Y_8)	266.172	-2.658	-64.530	0.017	4.033	0.250
<i>p</i> - value	0.989	0.352	0.670	0.224	0.046	0.137
GlcN (Y_9)	64.320	-1.574	-11.889	0.016	0.622	0.100
<i>p</i> - value	0.987	0.003	0.424	0.001	0.058	0.011
Pyr (Y_{10})	-263.372	3.6806	63.0981	-0.0432732	-4.13021	-0.175
<i>p</i> - value	0.000	0.079	0.970	0.002	0.003	0.110
Succ (Y_{11})	-83.2638	0.992581	20.1341	0.00160421	-1.11169	-0.15282
<i>p</i> - value	0.001	0.416	0.950	0.513	0.008	0.010
Acet (Y_{12})	-115.663	2.05393	26.44	-0.0239905	-1.66888	-0.1
<i>p</i> - value	0.000	0.085	0.858	0.004	0.018	0.137
Mw (Y_{13})	$1.959*10^8$	- $2.885*10^6$	⁻⁴ $230*10^7$	$3.164*10^4$	$2.520*10^6$	$1.868*10^5$
<i>p</i> - value	0.002	0.001	0.024	0.002	0.005	0.031

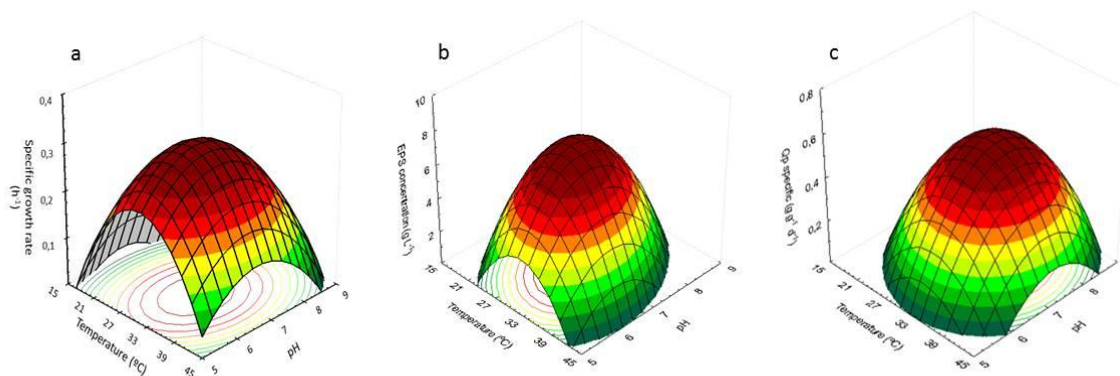


Figure 3.1 Response surface of specific growth rate (a); EPS concentration (b) and specific productivity (c) as a function of temperature and pH.

Influence of Temperature and pH on EPS Composition

Linear, quadratic and interaction terms of temperature and pH, had diverse effects on the different sugar monomer components of the EPS synthesized by *Enterobacter* A47 (Table 3.3; Figure 3.2). For fucose and glucose contents of the EPS, most of the linear and quadratic terms had a great impact ($p < 0.05$), although with different signs. A contrasting behaviour was expected for fucose and glucose contents within the ranges $20 < T < 35$ °C and $6.5 < \text{pH} < 7.5$, namely, maximal fucose content concomitant with the lowest glucose content (Figures 3.2 a and c). In contrast, the EPS galactose content was not influenced by temperature (Figure 3.2 b). The production of polymer enriched in galactose was greatly favoured by the mid-range pH (6.5 – 7.5), regardless of the temperature. A similar profile was observed for glucuronic acid, in which a linear relation between temperature and glucuronic acid content was observed (Figure 3.2 d). In this model, only the linear terms had impact ($p < 0.05$), with a maximum for pH between 6.5 – 8.0, and temperature under 30 °C.

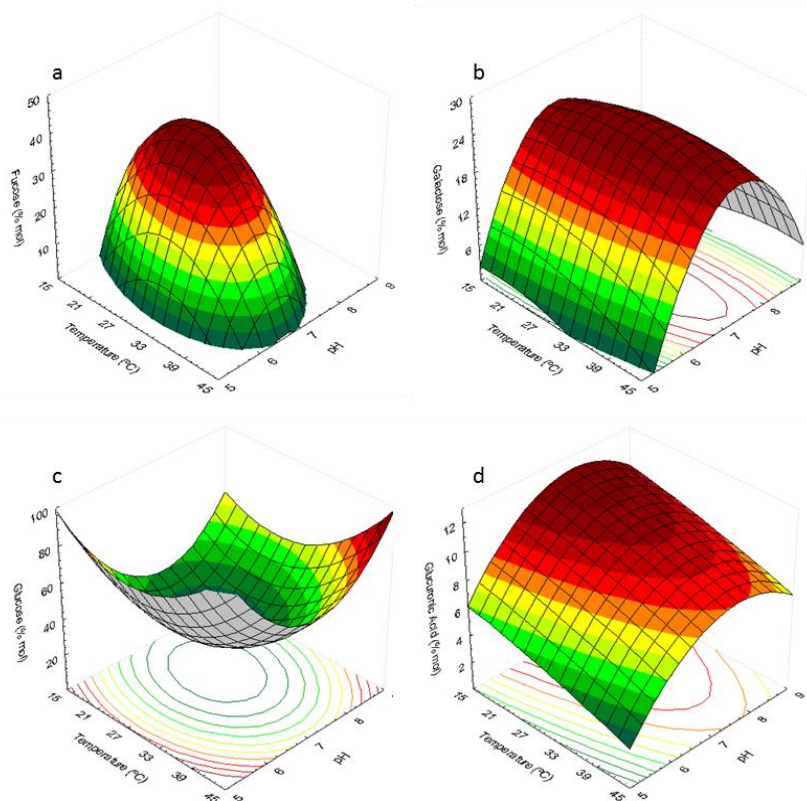


Figure 3.2 Response surface of fucose (a); galactose (b) glucose (c); glucuronic acid (d); rhamnose (e) and glucosamine (f) as a function of temperature and pH.

Within the estimated optimal conditions for EPS production (temperature and pH within 25 and 35 °C and 6.0 - 8.0, respectively), the polymers synthesized had the highest content in fucose (36.33 ± 0.58 %mol), galactose (25.67 ± 0.58 %mol) and glucuronic acid (10.33 ± 0.58 %mol), with the lowest content in glucose (36.33 ± 0.58 %mol). Outside these ranges, fucose, galactose and glucuronic acid contents were reduced and glucose content was increased (Figure 3.2). Moreover, new monomers, namely, rhamnose and glucosamine residues, were included in the synthesized polymers. Glucosamine content was favoured at higher pH and temperatures. Since for this aminosugar the interaction term had significance, the model predicted a range for which the polymer had nil glucosamine content: $21 < T < 35$ °C and $5.8 < \text{pH} < 6.4$. According to the model, rhamnose content, though low for most conditions, was independent of the temperature. In the rhamnose content model, only the pH quadratic term had significance ($p < 0.05$), which was supported by the higher contents obtained in the experiment operated at high pH (8.4).

Cultivation of *Enterobacter* A47 at different pH and temperature values revealed the versatility of this culture to produce different heteropolysaccharides with the same carbon source. This feature can be exploited to obtain a tailored sugar EPS composition, as a function of reactor operating conditions. This behaviour, presented by *Enterobacter* A47, has been reported for some EPS-producing strains, such as *Rhizobium* and *Pseudomonas* (Rehm, 2010). However, it is not a common behaviour amongst bacterial EPS producers. In fact, for most EPS, the basic carbohydrate monomer composition does not change significantly with growth conditions (Rehm, 2010).

The acyl group content and composition were affected by temperature and pH (Table 3.3). The total acyl groups content was higher for pH between 6.0 and 8.0 and temperatures between 25 and 35 °C (Figure 3.3). The content for pyruvyl, acetyl and succinyl, was influenced by temperature and pH. The pH and temperature ranges that gave rise to a maximal pyruvyl content were $6.5 < \text{pH} < 7.0$ and $25 < T < 30$ °C, respectively. A similar behaviour was obtained for acetyl, with a maximum acetyl content at $20 < T < 35$ °C and $6.0 < \text{pH} < 8.0$. Since only the quadratic pH and the interaction between temperature and pH model parameters seemed to have effect ($p < 0.05$) for succinyl content, the highest succinyl content was obtained between pH 6.5 and 8.5, for temperatures above 35 °C and below 25 °C.

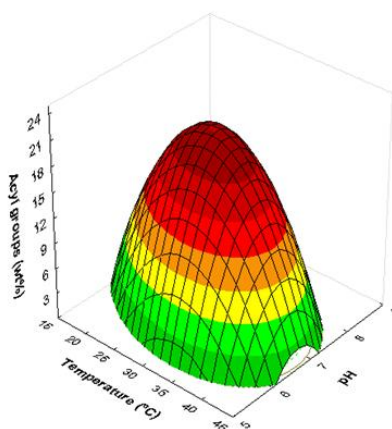


Figure 3.3 Response surface of acyl groups total content (% wt.) as a function of temperature and pH.

The content in substituent groups can vary extensively, thus changing polymer properties (Rehm, 2010). Xanthan is a good example of such variability. The content in acetyl and pyruvyl groups highly influence xanthan solution properties, i.e. xanthan with low acetyl and pyruvyl contents will have lower viscosity than xanthan with higher acetyl content (Casas et al., 2000). In xanthan production, temperature of cultivation also influences the polymer's acyl groups content (acetyl and pyruvyl). Xanthan acetyl content is usually greater at lower temperatures (25 – 28 °C) (Casas et al., 2000). García-Ochoa et al. (2000) reported that higher pyruvyl content in xanthan was obtained within 27 – 31 °C.

Influence of Temperature and pH on the EPS Average Molecular Weight

The different terms (linear, quadratic and interaction) of temperature and pH affected the polymer's average molecular weight ($p < 0.05$; Table 3.3). Results from MLR were corroborated by the data shown in Figure 3.4, where it is observed that polymers with higher Mw were obtained for temperatures above 40 °C, and also for pH below 5.5. Within the optimal ranges of temperature (25 – 35 °C) and pH (6.0 – 8.0) for EPS production, the biopolymers synthesized had an average Mw around 4.37×10^6 . Outside those ranges, the polymer's Mw was increased (Figure 3.4).

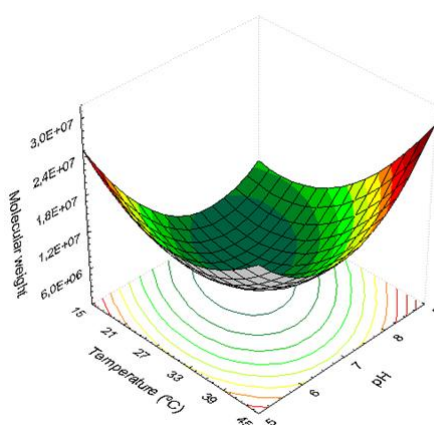


Figure 3.4 Response surface of molecular weight as a function of temperature and pH.

García-Ochoa et al. (2000) have reported that xanthan's Mw was directly related to the temperature of cultivation, being reduced as the temperature was increased between 24 and 34 °C. In contrast with xanthan production, in this work, the EPS Mw was practically unchanged within such a temperature range. Moreover, for higher and lower temperatures the Mw of the EPS produced by *Enterobacter* A47 increased. Such differing behaviour is probably related to the different composition of the biopolymers obtained in this study.

3.5. Conclusions

Enterobacter A47 was able to grow and synthesize EPS under most of the experimental conditions assessed. However, FucoPol production and the macromolecular characteristics were considerably affected by temperature and pH.

The synthesis of high fucose content EPS was stable for wide temperature (25-35 °C) and pH (6.0 – 8.0) ranges, which make the bioprocess robust. Outside those ranges, the polymer's fucose content decrease, while glucose content increased. Moreover, new sugar monomers were identified in the synthesized EPS, namely rhamnose and glucosamine. All the EPS obtained were high Mw polymers ($10^6 - 10^7$). The EPS with the highest fucose content presented Mw around 4.0×10^6 , whereas polymers with higher glucose content had higher Mw values ($\geq 1.0 \times 10^7$).

The main focus of this work is the rich-fucose polysaccharides due to their high market demand. However, the ability showed by the bacterium to synthesize EPS with different composition, only modifying the cultivation conditions, is very interesting. In view of this, such capability confers to the bioprocess a great versatility, enabling to achieve different polymers, which can be used in different applications.

Chapter 4

Optimization of FucoPol Production

Impact of Glycerol and Nitrogen

Concentration

The results presented in this chapter integrate a manuscript being prepared for submission to publication:

Torres, C.A.V., Marques, R., Ferreira, A.R., Antunes, S., Gouveia, A.R., Grandfils, C., Alves, V.D., Freitas, F., Reis, M.A.M. Impact of glycerol and nitrogen concentration on *Enterobacter* A47 growth and exopolysaccharide production.

4.1. Summary

The standard process conditions for EPS production by *Enterobacter A47* include initial glycerol and nitrogen concentrations of 25 – 40 g L⁻¹ and 0.70 – 1.10 g L⁻¹, respectively (Chapter 2). Within such nutrient concentration ranges, the synthesized EPS presents stable physical-chemical properties, namely, sugar and acyl groups' composition, and average molecular weight. Although, commonly carbon (e.g. glycerol) and nitrogen concentration influences the biologic processes. Therefore, the study of their impact on the EPS production by *Enterobacter A47* is important to optimize the process. Hence, two sets of experiments were done. In the first set of experiments, different initial glycerol and nitrogen concentrations at the beginning of the batch phase were tested, while in the second set the nitrogen and glycerol concentration of the feeding solution fed to the bioreactor during the fed-batch phase were changed.

The results of the first set of experiments have shown that EPS synthesis was severely impaired when the initial nitrogen concentration was above 1.10 g L⁻¹, with low polymer production (< 1.80 g L⁻¹) and productivities (~.35 g L⁻¹ d⁻¹). For lower initial nitrogen concentrations and initial glycerol concentrations up to 50 g L⁻¹, high EPS productions (7.50 – 8.85 g L⁻¹) were achieved, with productivities of 2.00 – 2.51 g L⁻¹ d⁻¹.

Increasing the nitrogen concentration in the feeding solution (9 g L⁻¹) resulted in identical EPS production (≥ 8.00 g L⁻¹), but the volumetric productivity was increased to 3.97 g L⁻¹ d⁻¹. The highest EPS synthesis (10.18 g L⁻¹) and volumetric productivity (5.52 g L⁻¹ d⁻¹) was reached when the feeding solution had a glycerol nitrogen concentration of 400 g L⁻¹ and 9 g L⁻¹, respectively.

Comparing to the standard runs the EPS produced in the highest productivity run had a higher fucose content (41 %mol), concomitant with lower glucose content (19 %mol). Moreover, the total acyl groups content decreased from 19-22 wt.% to 14 wt.%, noticing a great decrease in the pyruvyl content from 14 wt.% to 4 wt.%. Such polymer was also characterized by a lower average molecular weight (Mw) was (7.20x10⁵) than the EPS obtained in the standard runs (4.31x10⁶).

In the runs wherein EPS productivity was low, the polymers synthesized had a significantly different sugar and acyl groups composition, namely, lower fucose contents (14 – 17 %mol) and higher glucose contents (36 – 39 %mol). Moreover, new sugars monomers (rhamnose and glucosamine) were identified, which accounted for 6 – 16 %mol of the polymer's carbohydrate content. On the other hand, the acyl groups are also very different, in these runs the EPS achieved had no succinyl and the pyruvate content was also much lower (0 – 3 wt.%) than in the EPS achieved within the standard conditions.

4.2. Introduction

For most producing bacteria, exopolysaccharides (EPS) synthesis is stimulated by carbon availability concomitantly with limitation by another nutrient, such as nitrogen, usually requiring a high C:N ratio for high polymer synthesis (Sutherland, 1982; Tait et al.; 1986). As reported for several EPS-producing strains, such as *Aeromonas salmonicida* (Bonet et al., 1993), *Pseudomonas* NCIB11264 (Williams and Wimpenny, 1978), *Rhizobium tropici* (Staudt et al., 2011), *Sphingomonas paucimobilis* (Ashtaputre and Shah, 1995, Bajaj et al., 2007) and *Xanthomonas campestris* (Lo et al., 1997; Garcia-Ochoa et al., 2000; Moshaf et al., 2011), high nitrogen concentrations usually promote cell growth and often reduce EPS production.

The most significant factor restricting the commercial development of many microbial polymers is their high production costs. One of the strategies to overcome such limitation and allow for bacterial polysaccharides to get a higher market penetration is the reduction of their production costs and the improvement of their production yields. This can be done by optimizing fermentation conditions, such as, for example, carbon and/or nitrogen concentrations (Rehm, 2010; Freitas et al., 2011a).

In previous chapters, it was reported that FucoPol is produced by the bacterium *Enterobacter* A47, using glycerol byproduct from the biodiesel industry as the sole

carbon source (Chapter 2). *Enterobacter* A47 cultivation for FucoPol production is typically performed with an initial batch phase, in which most of the cell growth occurs and EPS synthesis is initiated, followed by a fed-batch phase, wherein cell growth is restricted by nitrogen and oxygen limitation, and the glycerol fed to the bioreactor is used for EPS production. The standard initial glycerol and nitrogen concentrations were within 25 - 40 and 0.70 - 1.10 g L⁻¹, respectively (section 2.4.2 – Chapter 2).

In this work, several experiments were performed to evaluate the impact of glycerol and nitrogen concentrations on EPS production by *Enterobacter* A47. Firstly, a set of experiments with different initial glycerol and nitrogen concentrations were tested to assess their influence on bacterial growth and EPS synthesis. Subsequently, a second set of experiments was carried out by changing the glycerol and nitrogen concentrations in the feeding solution supplied to the bioreactor during the fed-batch phase. The impact of the tested conditions on polymer's composition and average molecular weight were also assessed.

4.3. Materials and Methods

4.3.1. FucoPol Production

Microorganism and Media

Enterobacter A47 was cultivated as described in section 2.2.1. – Chapter 2.

Bioreactor Operation

All experiments were carried out in 2 L bioreactors and operated as described in section 2.3.1. – Chapter 2. That is, all the cultivation runs had an initial batch phase,

followed by a fed-batch phase, wherein a glycerol feeding solution was fed to the bioreactor.

In this study, two sets of experiments were performed. In the first set of experiments, the impact of different initial glycerol and nitrogen concentrations was studied in three different runs (Table 4.1), while in the second the impact of glycerol and nitrogen was evaluated during the fed-batch phase, by changing their concentrations in the feeding solution (Table 4.1).

Analytical Techniques

The analytical techniques used are described in sections 2.3.1. and 2.3.2. – Chapter 2.

4.4. Results and Discussion

As mentioned in section 2.4.2 – Chapter 2 – EPS production by *Enterobacter A47* is a partly growth associated cultivation, starting with a batch phase, wherein most of the cell growth occurs and EPS synthesis is initiated, followed by a fed-batch phase, during which cell growth is restricted by nitrogen depletion and polymer synthesis proceeds. In the standard bioprocess operation (Table 4.1), the initial glycerol and nitrogen concentrations were in the range of 25 – 40 g L⁻¹ and 0.70 – 1.10 g L⁻¹, respectively. After nitrogen depletion (within less than 24 hours), a feeding solution with about 200 g L⁻¹ glycerol and 0.9 g L⁻¹ nitrogen was supplied at a constant rate (fed-batch phase) (Chapter 2). Under those conditions, an EPS production of 7.50 – 7.97 g L⁻¹ was achieved within around 3 – 4 days, corresponding to a global volumetric productivity (r_p) of 2.04 – 2.51 g L⁻¹ d⁻¹ (standard runs – Table 4.1).

Concomitant with EPS production, there is usually a significant increase of the culture broth viscosity that leads to a loss of bulk homogeneity and dictates the end of

the cultivation run (see section 2.4.3. – Chapter 2). Usually, under the standard bioprocess operation, the culture broth viscosity increases about three orders of magnitude, from around 1.9 mPa s to over 2000 mPa s.

As it was already mentioned in the Chapter 2, increasing the initial glycerol and nitrogen concentrations (from 25 and 0.70 g L⁻¹ to 40 and 1.10 g L⁻¹, respectively) had no significant impact on *Enterobacter* A47 performance, i.e. the EPS production and volumetric productivity were similar. Thus, aiming to better understand whether other range of concentrations of those nutrients may affect *Enterobacter* A47 growth and EPS synthesis, three tests with different initial glycerol and nitrogen concentrations were performed (Table 4.1).

4.4.1. Effect of Initial Glycerol and Nitrogen Concentrations

In the batch phase, different initial glycerol and nitrogen concentrations were tested (49 – 83 and 0.98 – 1.39 g L⁻¹, respectively – Table 4.1 – runs 1-3), while the conditions of the fed-batch phase were kept similar to the standard runs (200 g L⁻¹ glycerol and 0.9 g L⁻¹ nitrogen). Figure 4.1 describes *Enterobacter* A47 growth, EPS synthesis and nutrient profiles for runs 1 to 3.

In run 1, in which the initial glycerol and nitrogen concentrations (83 and 1.34 g L⁻¹, respectively) were higher than the ones used in standard runs 1 and 2, resulted in a higher biomass production (7.30 g L⁻¹) (Table 4.1). Although this result was expected due to the higher initial nitrogen concentration used, the maximum specific cell growth rate (μ_{\max}) was lower (0.20 h⁻¹) than in standard experiments (0.27 – 0.29 h⁻¹). These results may evidence inhibition caused by the high glycerol concentration used. Furthermore, polymer production was significantly decreased to 1.08 g L⁻¹.

In order to avoid inhibition by substrate, in run 2 the initial glycerol concentration was decreased (from 83 to 49 g L⁻¹) and the nitrogen concentration was kept similar (1.39 g L⁻¹) to run 1. The maximum biomass achieved was similar (7.50 g L⁻¹) to run 1,

which is in accordance with the ammonia concentration used. The maximum specific cell growth rate (0.26 h^{-1}) was identical to the values obtained for the standard runs 1 and 2. However, EPS production (1.80 g L^{-1}) and productivity ($0.34 \text{ g L}^{-1} \text{ d}^{-1}$) were still lower than in standard runs ($7.50 - 7.97 \text{ g L}^{-1}$ and 2.04 and $2.51 \text{ g L}^{-1} \text{ d}^{-1}$, respectively) (Table 4.1). Given that the difference between run 2 and the standard runs is the nitrogen concentration, it is likely that the low EPS production achieved in runs 2 it was caused by the higher initial nitrogen concentration used which may have led to a shift in the metabolism of *Enterobacter* A47: shift from polymer production to growth.

Such behaviour, i.e. higher biomass production concomitant with lower EPS synthesis as a result of higher initial nitrogen concentration had been reported by several authors for other EPS synthesizing bacteria, such as *Aeromonas salmonicida* (Bonet et al., 1993), *Sphingomonas paucimobilis* –GS1 (Ashtaputre and Shah, 1995), and *Xanthomonas campestris* (Sutherland, 1982; Lo et al., 1997; García-Ochoa et al., 2000). The effect of nitrogen concentration on carbon flux to growth or polymer production was reported by Linton, (1991) and Bajaj et al., (2007).

In run 3 (Figure 4.1 c), the initial glycerol concentration was kept similar (52 g L^{-1}) to run 2 and the initial nitrogen concentration was decreased to 0.98 g L^{-1} . As a result, maximum biomass production was lower (6.41 g L^{-1}) than in run 2, but similar to the one achieved in standard run 2 (6.75 g L^{-1}), where a similar ammonia concentration was used. The specific cell growth rate was identical (0.29 h^{-1}) to the standard runs (Table 4.1). The final EPS production (8.85 g L^{-1}), the global volumetric productivity ($2.00 \text{ g L}^{-1} \text{ d}^{-1}$) and the global net yield of product on glycerol ($Y_{P/S} = 0.23 \text{ g g}^{-1}$) were within the values obtained for the standard runs.

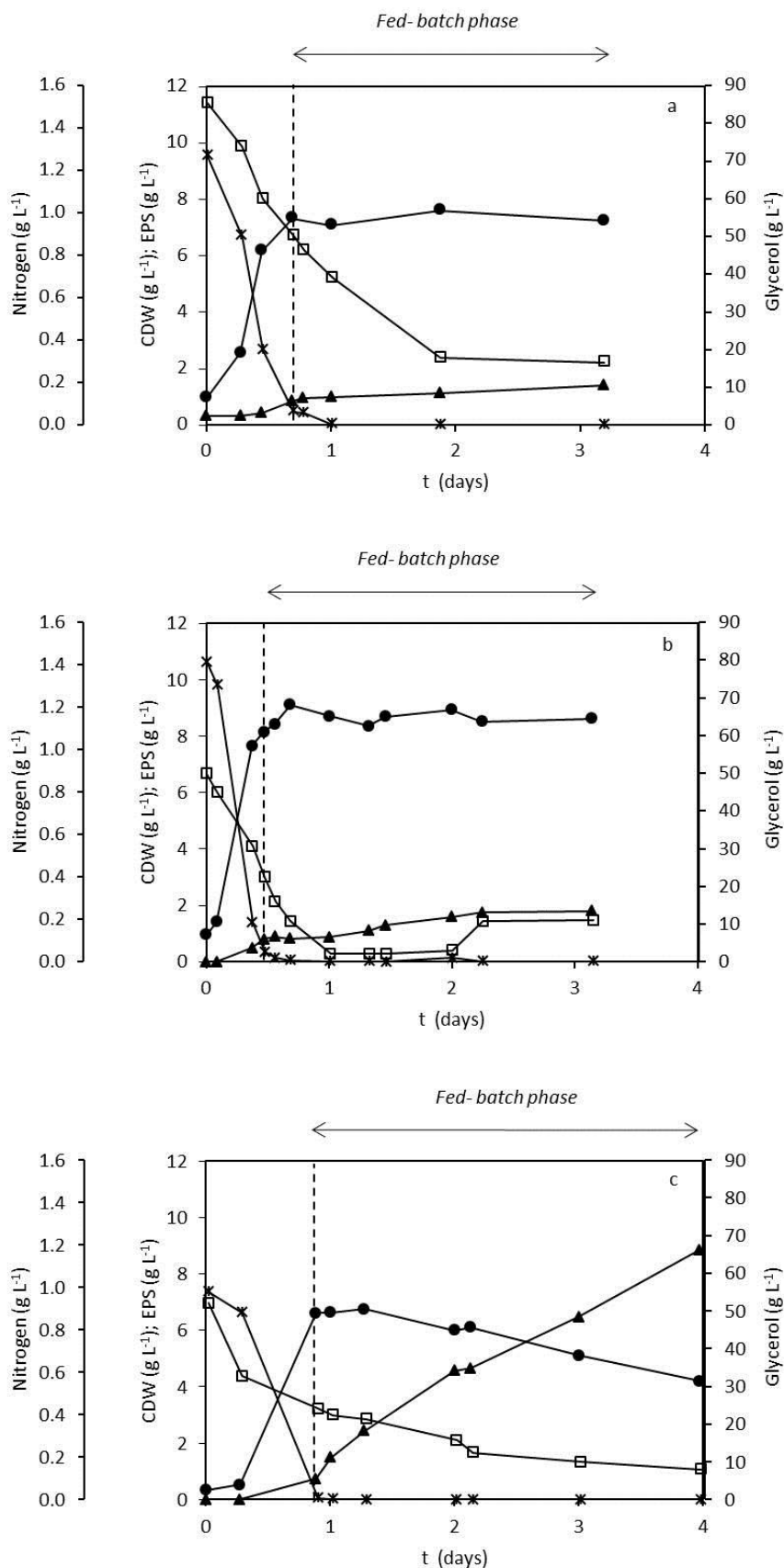


Figure 4.1 Impact of the initial glycerol and nitrogen concentrations on cell growth and EPS production across the different cultivation runs (a) Run 1; (b) Run 2 and (c) Run 3. Profile of cultivation runs: (▲) EPS (g L⁻¹); (●) CDW (g L⁻¹); (*) N-NH₄⁺ (g L⁻¹); (□) glycerol (g L⁻¹).

The impact of nitrogen on EPS and biomass production is highlighted in Figure 4.2. The initial nitrogen concentration had a significant impact on EPS production, as well as in cell growth; biomass increases proportionally with the nitrogen concentration, while above 1.05 gN L⁻¹ EPS production declines steeply. Moreover, results show that an initial glycerol concentration within 25 and 50 g L⁻¹, combined with an initial nitrogen concentration of 0.68 - 1.05 gN L⁻¹, are the best conditions for EPS production.

Concomitant with EPS synthesis, in run 3 there was also a significant increase of the broth's viscosity (up to 1800 mPa s, measured at 0.3 s⁻¹), similarly to the standard runs 1 and 2. This viscosity built up was not observed in run 1 and 2, wherein very low EPS production was reached (1.08 g L⁻¹).

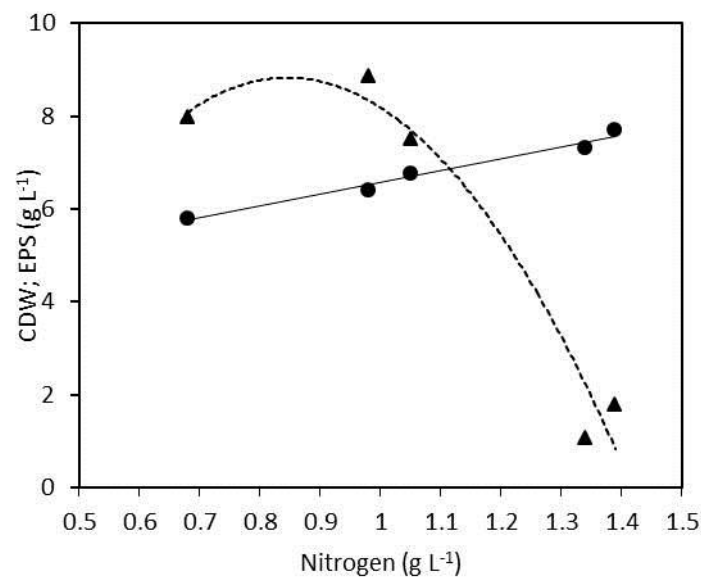


Figure 4.2 Impact of nitrogen concentration on biomass (●) and EPS production (▲), for all the 5 runs (Str 1 and 2 and runs 1 to 3).

Table 4.1 Kinetic parameters during batch and fed batch phase, as well as global values for the standard cultivation runs (section 2.4.2 – Chapter 2) and for runs 1 – 6

Runs	Batch phase						Fed-batch phase						Global							
	Glycerol (g L ⁻¹)	N-NH ₄ ⁺ (g L ⁻¹)	CDW _b (g L ⁻¹)	μ (h ⁻¹)	EPS (g L ⁻¹)	Y _{X/S} (gg ⁻¹)	Y _{P/S} (gg ⁻¹)	Glycerol (g L ⁻¹)	N-NH ₄ ⁺ (g L ⁻¹)	CDW _f (g L ⁻¹)	μ (h ⁻¹)	EPS (g L ⁻¹)	Y _{X/S} (gg ⁻¹)	Y _{P/S} (gg ⁻¹)	r _p (g L ⁻¹ d ⁻¹)	r _p (g L ⁻¹ d ⁻¹)	Y _{P/S} (gg ⁻¹)	q _p (gEPSgCDW ⁻¹ d ⁻¹)		
Std1 ¹	26	0.68	5.60	0.27	2.09	0.32	0.12	207	0.85	5.80	0.01	7.97	0.03	0.20	1.89	0.33	0.24	0.17	2.04	0.35
Std2 ¹	41	1.05	6.57	0.29	2.69	0.20	0.15	210	0.91	6.75	0.01	7.50	0.05	0.16	1.60	0.24	0.18	0.14	2.51	0.37
1	83	1.34	7.15	0.20	0.43	0.17	0.01	203	0.86	7.30	0.01	1.08	0.07	0.01	0.22	0.03	0.21	0.03	0.34	0.05
2	49	1.39	7.50	0.26	0.90	0.26	0.02	206	0.88	7.70	0.01	1.80	0.08	0.01	0.34	0.04	0.17	0.01	0.35	0.05
3	52	0.98	6.27	0.29	1.48	0.30	0.06	209	0.92	6.41	0.00	8.85	0.01	0.21	2.48	0.39	0.23	0.20	2.00	0.31
4	36	0.69	5.40	0.25	2.20	0.20	0.04	206	0.00	5.40	0.00	8.75	0.00	0.17	2.87	0.53	0.20	0.17	2.86	0.53
5	35	0.72	5.46	0.27	1.40	0.23	0.02	211	9.20	9.18	0.13	8.80	0.47	0.25	4.72	0.51	0.27	0.24	3.97	0.43
6	34	0.66	5.87	0.27	0.25	0.20	0.01	405	8.70	10.66	0.06	10.18	0.32	0.54	7.42	0.70	0.27	0.31	5.52	0.52

¹ Chapter 2 – section 2.4.2; Std1 – Standard; N, nitrogen concentration (g L⁻¹); μ (Specific growth rates, h⁻¹); CDW_b, maximum cell dry weight at the end of the batch phase (g L⁻¹); CDW_f, maximum cell dry weight on the fed-batch phase (g L⁻¹); Y_{X/S} (net yield of biomass on glycerol, g g⁻¹); Y_{P/S} (net yield of EPS on glycerol, g g⁻¹); r_p (volumetric productivity, g L⁻¹ d⁻¹) and q_p (specific productivity, gEPS gCDW⁻¹ d⁻¹); N, initial nitrogen concentration (g L⁻¹).

4.4.2. Effect of Nitrogen Concentration in the Feeding Solution

In the typical FucoPol bioprocess, the greater increase in EPS production occurs during fed-batch phase, under nitrogen limiting condition. However, the impact of this concentration on polymer production was never evaluated. Hence, two tests were performed in which the nitrogen concentration of the feeding solution was below the values of the standard runs (i.e. no nitrogen - run 4) and above (nitrogen concentration of 9 g L^{-1} - run 5), while keeping the glycerol concentration similarly to the standard assays (Table 4.1). The batch phase was operated within the best conditions reported above: initial nitrogen concentration around 0.70 g L^{-1} and, hence, the results obtained in batch phase were similar to those achieved under those conditions (in previous runs). Analysis of the fed-batch phase with no nitrogen supplied (run 4) showed an EPS production of 8.75 g L^{-1} , achieved within ~ 3 days (Figure 4.3 a), resulting in a global volumetric productivity of $2.86 \text{ g L}^{-1} \text{ d}^{-1}$. These values, as well as the global net yield of EPS on glycerol ($Y_{P/S} = 0.20 \text{ g g}^{-1}$) were within the ones obtained in the standard runs 1 and 2. These results suggest that absence of nitrogen during the fed-batch phase did not affect EPS synthesis by *Enterobacter A47*.

On the other hand, increasing ten times the nitrogen concentration in the feeding solution (9 g L^{-1} - run5) relatively to the standard runs led to a higher biomass concentration (9.18 g L^{-1}) and yield of biomass on glycerol ($Y_{X/S} = 0.47 \text{ g g}^{-1}$). A final EPS production of 8.80 g L^{-1} was reached, which was within the values achieved for previous runs (Standard 1 and 2 and runs 3 and 4) (Figure 4.3 b). However, a higher global volumetric productivity ($3.97 \text{ g L}^{-1} \text{ d}^{-1}$) was obtained within 2.20 days.

It can be concluded that the availability of nitrogen during fed-batch has a significant impact on the EPS productivity, probably due to the higher biomass achieved, which led to a faster EPS production. Although, more cells did not result in higher EPS production probably due to a limitation in glycerol, resulting in a lower specific productivity ($0.43 \text{ gEPS gCDW}^{-1} \text{ d}^{-1}$) comparing to run 4 ($0.53 \text{ gEPS gCDW}^{-1} \text{ d}^{-1}$).

In run 5, in spite of the high nitrogen concentration in the bulk, the residual glycerol concentration was very low ($< 0.5 \text{ g L}^{-1}$), which could have restricted growth and

polymer production. In order to assess if the glycerol was the limiting factor for the capacity of the culture to produce the EPS, in run 6 the glycerol concentration in the feeding solution was increased by 2 fold (400 g L^{-1}), while maintaining the nitrogen concentration tested in run 5 (9 g L^{-1} – Table 4.1). This strategy enabled a complete consumption of the nitrogen source and glycerol availability throughout the assay (Figure 4.3 c). Under these conditions a maximum biomass concentration of 10.66 g L^{-1} at 1.24 days was achieved. Furthermore, EPS production was 10.18 g L^{-1} obtained in 1.84 days, corresponding to a volumetric production rate (r_p) of $5.52 \text{ g L}^{-1} \text{ d}^{-1}$, and the $Y_{p/s}$ was 0.31 g g^{-1} . These were the highest values obtained so far with this strain.

In run 6 the culture broth viscosity increased from 1.21 to 13000 mPa s, measured at 0.3 s^{-1} , in 1.84 days, leading to the run termination due to the poor mixing. In run 4 the culture broth viscosity increased from 1.08 to 371 mPa s (at 1.5 s^{-1}) achieved at the end of 3.06 days, while in run 5 the viscosity in 2.20 days increased from achieved and 1.78 to 302 mPa s (at 1.5 s^{-1}), which is concomitant with the polymer production.

The present work has shown that increasing the glycerol and nitrogen in the feeding solution from 200 to 400 g L^{-1} and 0.9 to 9.0 g L^{-1} respectively, significantly improved EPS synthesis. This was probably due to the extended period of growth, provided by the higher glycerol and nitrogen availability (Figure 4.3 b and c). Several authors reported that EPS producing bacteria needs a high C:N ratio to promote EPS synthesis (Sutherland, 1990; Garcia-Ochoa et al., 2000; Liu et al., 2011; Staudt et al., 2011). Such behaviour may be related with the fact that cells are more viable, which in turn may lead to a higher production of sugar nucleotide precursors involved in EPS synthesis. Moreover, as suggested by Sutherland (2001), a longer growth period leads to increased isoprenoid carrier content in the cell membrane, which results in higher rates of EPS synthesis. This isoprenoid lipid carrier is important in the EPS synthesis, since it is one of the cell wall components, which is involved in EPS polymerization and secretion across the cell membrane (Sutherland, 1990; Freitas et al., 2011a).

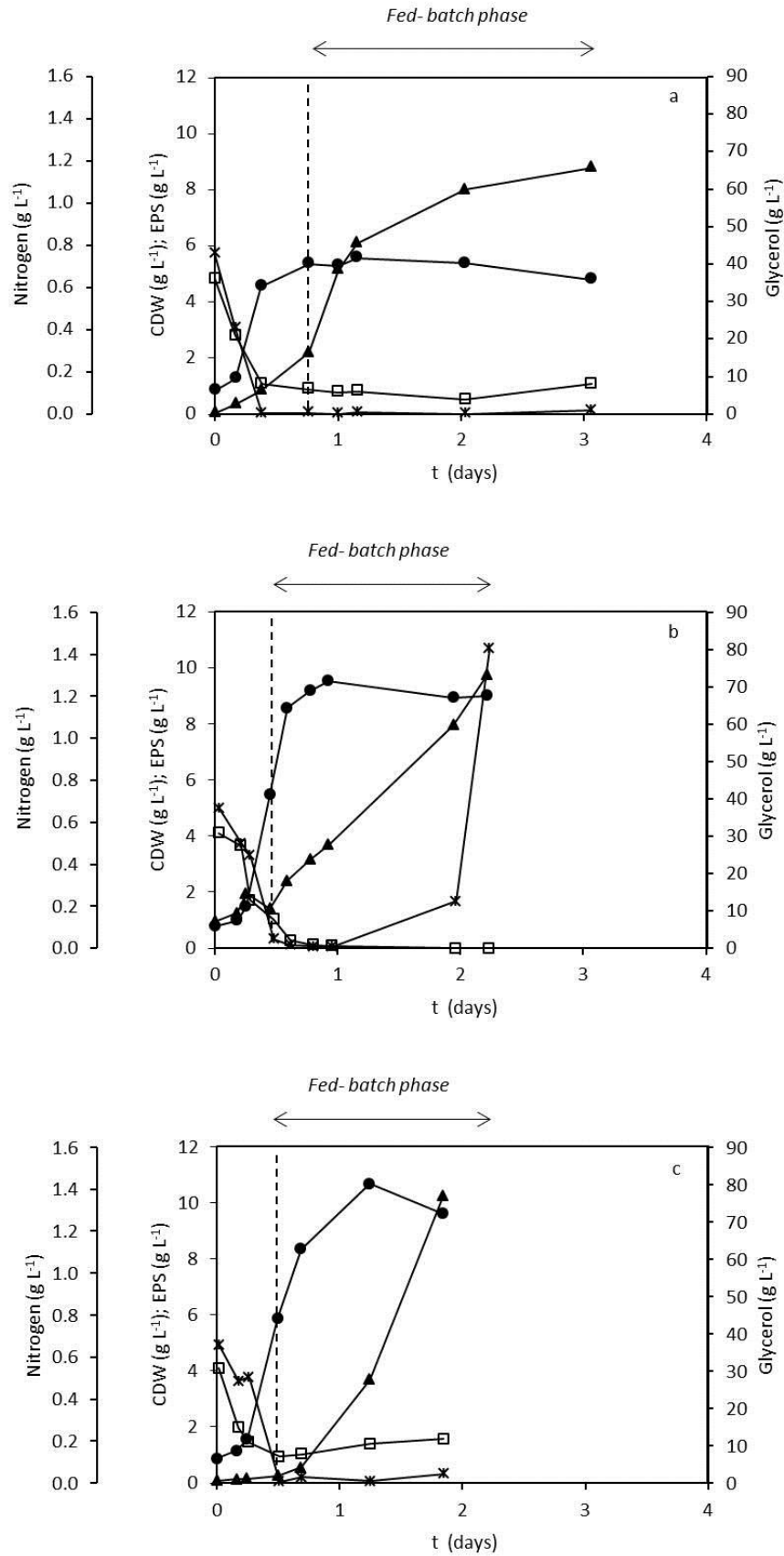


Figure 4.3 Impact of glycerol and nitrogen concentrations in the feeding solution. Time course of the cultivation runs: (a) Run 4, (b) Run 5 and (c) Run 6 ((▲) EPS (g L^{-1}); (●) CDW (g L^{-1}); (*) N-NH_4^+ (g L^{-1}); (□) glycerol (g L^{-1})).

4.4.3. EPS Physical-chemical Characterization

EPS composition

The sugar components of the EPS obtained in the standard runs were fucose (32 – 36 %mol), galactose (25 – 26 %mol), glucose (28 – 34 %mol) and glucuronic acid (9 – 10 %mol) (see section 2.4.4 – Chapter 2). Additionally, FucoPol typically contains acetyl (3 – 5 wt.%), pyruvyl (13 – 14 wt.%) and succinyl (~3 wt.%) as non-sugar components. As shown in Table 4.2, the different glycerol and nitrogen concentrations used in this study have affected the polymers' sugar and acyl groups composition.

The runs 1 and 2, wherein polysaccharide production was very reduced, presented an EPS with a lower fucose content (14 – 17 %mol) than in the standard runs (32 – 36 %mol), while glucose content increased from 28 – 34 %mol to 36 – 39 %mol. Besides, other sugar monomers (rhamnose, mannose and glucosamine), not previously present in the EPS of the standard runs, were found in contents within 6 – 16 %. As explained in section 2.4.4 (Chapter 2), the higher content in glucose and lower in fucose may be related with the fact that all sugar nucleotides share a common precursor, which is glucose-6-P. The shortest pathway for the synthesis of sugar nucleotides is the synthesis of UDP-glucose, which is the precursor of glucose monomers to be incorporated into the EPS. On the other hand, the synthesis of the other sugar nucleotides (GDP-fucose, UDP-galactose, UDP-glucuronic acid) requires several enzymes and longer pathways for their synthesis (Kumar et al., 2007; Freitas et al., 2011). Therefore, it can be hypothesized that, in those runs, the polymers were enriched in glucose because the enzymes needed for the synthesis of the other sugar nucleotides were not available.

Furthermore, in runs 1 and 2 the total acyl groups content also varied. A great decrease was observed (3 – 7 wt.%) relatively to the standard runs (19 – 22 wt.%). Succinyl was absent of the EPS obtained in both runs and the content in pyruvyl was significantly reduced in run 2 (3 wt%) or also absent (run 1).

On the other hand, the EPS produced in run 3 presented an EPS sugar and acyl groups composition similar to the EPS composition of the standard runs (Table 4.2).

The polymers achieved in runs 4 and 6 also presented a different sugar and acyl groups composition comparing to the typical FucoPol polymer (standard runs). There was an increase of fucose content to 40 – 41 %mol and a reduction of glucose content to 18 – 19 %mol. Moreover, the acyl groups content was also reduced (14 wt.%), being the main differences the reduction of pyruvyl content to 4 wt% and the increase of succinyl to 6 wt% (Table 4.2).

The EPS synthesized in run 5 was also characterized by a different sugar and acyl groups composition: the content in fucose was lower (25 %mol) and the content in galactose was higher (33 %mol) than in the standard runs. The acyl groups content was also lower (8 wt %), presenting low pyruvyl and succinyl contents (3 and 1 wt.%) (Table 4.2). This difference in the EPS composition may be related with the limitation in glycerol observed during the fed-batch phase, in contrast with the other runs, in which glycerol was never limited.

The lower content in acyl groups detected in the EPS produced in runs 1, 2 and 5, as well as 4 and 6 was possibly associated to the higher biomass contents achieved. Since the precursors of the acyl groups were also involved in pathways of bacterial growth, such as phosphoenolpyruvate and acetyl-CoA (Sutherland 1982; Tait et al., 1986), the precursors probably were not available in quantities to permit complete acylation of the polysaccharides.

It should be noted that for the EPS with higher fucose content as well as higher acyl groups content the cultivation broth presented a high viscosity (224 – 13000 mPa s). In turn, for runs 1 and 2, which had a lower fucose and acyl groups content the broth viscosity was much lower (4 – 19 mPa s). Such behaviour can be related with what is reported by Rinaudo (2004) that the composition and the content in acyl groups substituents can affect the polymer rheology. For example, for xanthan production Casas et al. (2000) reported that high degree of acetylation produced solutions with higher viscosity.

Table 4.2 Physical-chemical EPS characterization: sugar composition (%mol); acyl groups content (wt.%) and average molecular weight

Runs	Sugar composition (%mol)					Acyl groups content (wt.%)				Molecular weight
	Fucose	Galactose	Glucose	Glucuronic Acid	Other	Pyruvyl	Succinyl	Acetyl		
Std1 1	32	25	34	9	0	14	3	5	5.80×10^6	
Std1 2	36	26	28	10	0	13	3	3	4.19×10^6	
1	14	19	39	13	16	0	0	3	2.71×10^6	
2	17	27	36	14	6	3	0	4	6.65×10^6	
3	37	26	27	10	0	13	3	8	4.31×10^6	
4	40	25	18	17	0	4	6	4	7.20×10^5	
5	25	33	29	12	0	3	1	4	9.40×10^5	
6	41	28	19	12	0	4	6	4	7.20×10^5	

EPS average molecular weight

Molecular weight (Mw) also influences the polymers' solution properties, determining their potential to be used in specific applications (Tosh et al., 2004). In this work, all the obtained polymers had high Mw values within 7.20×10^5 – 6.65×10^6 (Table 4.2). FucoPol typically has a Mw within 4.19×10^6 – 5.80×10^6 (Table 4.2). On the other hand, the polymers with higher fucose (40 – 41 %mol) and lower glucose contents (18 – 19 %mol) (runs 4 and 6) were characterized by lower Mw (7.20×10^5). In contrast, the polymers with lower fucose and higher glucose contents (runs 1 and 2), presented Mw similar to the standard runs (2.71×10^6 – 6.65×10^6).

There is no evidence of a direct effect of glycerol and nitrogen concentrations on the polymers Mw, withal the lower Mw, observed in run 4, 5, and 6. It might be related to the shorter cultivation times of the runs (73, 53 and 44 h, respectively) comparing to the standard runs (96 h), since as it was already reported for the EPS synthesized by *Enterobacter* A47, Mw usually increases throughout the cultivation runs (see section 2.4.4 – Chapter 2). Sutherland (1982) and García-Ochoa et al. (2000) has also reported a similar behaviour to xanthan production by *Xanthomonas campestris*.

4.5. Conclusions

Enterobacter A47 was able to grow and produce EPS for all the initial glycerol and nitrogen concentrations evaluated. However, the impact of the initial nitrogen concentration was more evident during batch phase, both in growth and in EPS synthesis. For initial nitrogen concentrations above 1.05 g L^{-1} EPS synthesis decreased dramatically. Furthermore, the EPS synthesis was similar for initial glycerol and nitrogen concentrations within the range of 25 – 50 and 0.68 – 1.05 g L^{-1} , respectively.

During the fed-batch phase, nitrogen concentrations in the feeding solution within 0 and 9 g L^{-1} did not affect *Enterobacter* A47 EPS synthesis, with EPS production higher than 8.00 g L^{-1} . Increasing the glycerol concentration in the feeding solution from

200 to 400 g L⁻¹ and using a nitrogen concentration of 9 g L⁻¹ resulted in the highest EPS synthesis and highest volumetric productivity.

Furthermore, the macromolecular characteristics of the polymers produced under the different conditions tested were also affected. The highest productivity run yielded the EPS with the highest fucose content.

Enterobacter A47 has shown to be able to synthesize fucose-containing EPS within different nitrogen and glycerol concentrations. Moreover, the observed increase in fucose content is remarkable due to the possible different applications, as already mentioned in chapter 2.

Chapter 5

FucoPol

Properties in aqueous solutions

Some of the results presented in this chapter were already published in a peer reviewed paper, while others will be published in a paper which is being prepared.

Cruz, M., Freitas, F., Torres, C.A.V., Reis, M.A.M., Alves, V.D., 2011. Influence of temperature on the rheological behavior of a new fucose-containing bacterial exopolysaccharide. *International Journal of Biological Macromolecules*, 48, 695-699.

Torres, C.A.V., Ferreira, A. R., Sousa, I., Reis, M.A.M., Freitas, F., Alves, V.D. FucoPol Rheological Studies. (In preparation).

5.1. Summary

Taking into account that FucoPol is a novel polysaccharide produced by glycerol from the biodiesel industry with a high Mw, it is essential to study its solution properties, in order to better understand its potential applications.

The effect of pH (3.5 – 10.5) and ionic strength (0.05 – 0.75 M NaCl) on FucoPol intrinsic viscosity and steady shear flow was assessed using a central composite rotatable design of experiments and response surface methodology. FucoPol intrinsic viscosity ($\sim 8.00 \text{ dL g}^{-1}$) and shear behaviour has shown to be stable under a wide range of pH and ionic strength (3.5– 8.0 and 0.05 – 0.50 M NaCl, respectively). The influence of temperature on steady shear and oscillatory data was also evaluated in the temperature range from 15 to 65 °C. For all of the conditions tested, FucoPol formed high viscosity solutions with a shear-thinning behaviour. Therefore, the application of FucoPol as thickening agent is foreseen in aqueous solutions with variations of pH, ionic strength as well as temperature. Furthermore, the viscous and viscoelastic properties at 25°C were maintained after consecutive heating and cooling cycles, indicating a good thermal stability under temperature fluctuations.

5.2. Introduction

Microbial polysaccharides are especially important in the domain of water soluble polymers, due to their important role as thickening, gelling, emulsifying, hydrating and suspending agents (Rinaudo, 2008). The remarkable variety of physical chemical properties reflect the structural diversity of polysaccharides, such as sugar composition, molecular weight, presence of ionisable groups and association of single polysaccharide chains (Kumar

et al., 2007, Freitas et al., 2011). Understanding polysaccharides' properties in aqueous solutions is critical to forecast their potential industrial applications. These properties can be affected by several parameters, such as pH, salt concentration, temperature, polymer average molecular weight and shear rate (Xu et al., 2009).

The physical properties of microbial polysaccharides are explained in terms of different rheological behaviour. In view of that, it is important to perform viscometry studies in dilute solution conditions, to obtain information about the molecular characteristics, such as intrinsic viscosity (hydrodynamic volume of a single molecule). On the other hand, it is also important to study the concentrated polymer solutions to assess the viscosity behaviour (Newtonian or non-Newtonian) and viscoelastic properties (Freitas et al., 2011). For such evaluation, rheology provides important tools especially useful to monitor and to probe structural changes in the systems. The rheological behaviour of polymer solutions manifests the fundamental structure of the systems (Williams, 2007).

This chapter is focused on the assessment of FucoPol properties in aqueous solutions, which involved the study of the intrinsic viscosity and steady shear behaviour using a design of experiments (central composite rotatable design), with particular interest on studying the influence of pH and ionic strength. In addition, the attention was also driven to evaluate the influence of temperature on the apparent viscosity and on the viscoelastic properties. FucoPol's concentration regimes were also assessed.

These studies are essential to characterize this biopolymer, since most water soluble polysaccharides are mainly used as hydrocolloids, being used in aqueous formulations for a wide range of applications, namely in food, cosmetic or pharmaceutical products or processes.

5.3. Material and Methods

5.3.1. Preparation of FucoPol Aqueous Solutions

FucoPol solutions were prepared by mixing the freeze dried polymer with deionised water or with a NaCl solution with the desired salt concentration, followed by stirring overnight at room temperature.

5.3.2. Rheological Measurements

Intrinsic Viscosity

The intrinsic viscosity $[\eta]$ of FucoPol was assessed under different conditions. The measurements presented in this chapter were performed by double extrapolation of Kraemer and Huggins equations, as described in Chapter 2, section 2.3.3.

- Standard Conditions Studies (0.1 M NaCl; pH ~5.6; T = 25°C)

A 0.1 wt.% FucoPol stock solution was prepared by dissolving the purified biopolymer in 0.1 M NaCl. Dilutions also with 0.1 M NaCl of the stock solution were performed to achieve five lower polymer concentrations (0.06, 0.05, 0.04, 0.03 and 0.02 wt.%). The relative and specific viscosities of these solutions were then assessed by capillary viscometry.

- Study of the Ionic Strength and pH Effect (T = 25°C)

FucoPol solutions with a polymer concentration of 1.0 wt.% were prepared with the desired salt concentration, by using solutions with NaCl concentrations within 0.05 to 0.75 M as solvent, were used as stock solutions. The solutions pH was adjusted to the desired value (within the range 3.5 - 10.5), with the addition of small drops of HCl (15% wt) and/or

NaOH (10% wt) solutions. After that, the solutions were stirred for 2 hours in order to ensure a stable pH value (with pH measured every 30 min). Each stock solution was diluted with the respective NaCl concentration, to the desired concentration, the pH was readjusted, and the specific and relative viscosities were then assessed by capillary viscometry.

Apparent Viscosity and mechanical spectra

The rheology measurements of FucoPol's aqueous solutions (oscillatory and steady-shear tests) were performed by loading directly the different solutions in the cone and plate geometry (diameter 35 mm, angle 2°) of a controlled stress rheometer. The shearing geometry was covered with paraffin oil in order to prevent water loss. The measurements were executed as described in Chapter 2, section 2.3.2. The exception was the rheometer used in the measurements of samples in the standard conditions and in the study of pH and salt effect, which was the controlled stress rheometer Rheostress RS 75, Germany. The oscillatory tests were performed within the linear viscoelastic region, applying a tension chosen after performing stress sweeps at constant frequency ($f = 1$ Hz).

The conditions studied were:

- Studies at Standard Conditions (0.1 M NaCl; pH ~ 5.6; T = 25 °C)

Measurements were performed using solutions with polymer concentrations ranging from 0.2 to 1.2 wt.% in a 0.1 M NaCl solution. The pH was the natural pH of the solutions after polymer dissolution (pH ~ 5.60).

- Study of the Ionic Strength and pH Effect (T = 25 °C)

1.0 wt.% FucoPol aqueous solutions prepared as described in the sub-section Intrinsic viscosity- ionic strength and pH effect were studied.

- Temperature Effect (pH ~ 5.6)

For the temperature effect assessment the polymer was dissolved in deionised water. A solution with an effective polymer concentration of 0.81 wt.% was used.

Both oscillatory and steady-state tests were carried out at different temperatures ranging from 15 to 65 °C. The purified EPS solution was also submitted to temperatures cycles of consecutive heating and cooling steps. After recording the mechanical spectrum and the steady-state data at 25 °C, the sample was heated up to 40 °C at a rate of 3 °C min⁻¹, followed by an oscillatory time sweep (strain=0.2 and $f=1$ Hz) at that temperature for 10 minutes. Afterwards, the sample was cooled down at a rate of -3 °C min⁻¹ to 25 °C, and new oscillatory and steady-state tests were performed at the same conditions. The cycle was repeated by heating the sample up to 55, 70 and 80 °C.

5.3.3. Experimental Design

Response surface methodology (RSM) was applied to evaluate simultaneously the effect of ionic strength (NaCl concentration) and pH, on the observed FucoPol intrinsic viscosity $[\eta]$ (Y_1) and in the zero-shear rate viscosity (first Newtonian plateau) (Y_2) of FucoPol solutions. A central composite rotatable design (CCRD), with two independent variables at five levels was used, where X_1 is the ionic strength (M, NaCl concentration) and X_2 the pH (Table 5.1). The central point was repeated three times, to allow estimating experimental error. All experiments were carried on a randomized order to prevent the effect of unexplained variability due to exogenous factors. A solution with a NaCl concentration of 0.40 M and pH 7.0, was used as the central point. The data analysis was performed as described in Chapter 3 – section 3.3.3.

5.4. Results and Discussion

5.4.1. Intrinsic Viscosity

The intrinsic viscosity represents the hydrodynamic volume of individual polymer molecules, giving information about the molecule's size and shape (Bae et al., 2008). It was calculated by estimating the value of reduced and inherent viscosities of FucoPol solutions approaching zero concentration, according to the Huggins and Kraemer equations (Eqs 2.15 and 2.16 – Chapter 2; section 2.3.3).

Figure 5.1 a presents the variation of the reduced viscosity as a function of FucoPol concentration in a salt free aqueous solution showing a non-linear dependence of these two parameters. As the polymer concentration decreased, there was a decline of the reduced viscosity, and afterwards it increased for polymer concentration values below 0.02 wt.%. This behaviour is usually perceived at low ionic strength aqueous solutions of polyelectrolytes (Mitchell & Ledward, 1985), and is attributed to repulsive forces between intra-chain groups with equal charges, which leads to an increase of the molecules hydrodynamic volume, and consequently, to an increase of the intrinsic viscosity. As the biopolymer concentration increases, inter-chain interactions prevail against the intra-chain repulsive forces, becoming dominant at higher concentration values, leading to reduced viscosity-concentration dependence normally observed for uncharged polymers (Walter, 1998).

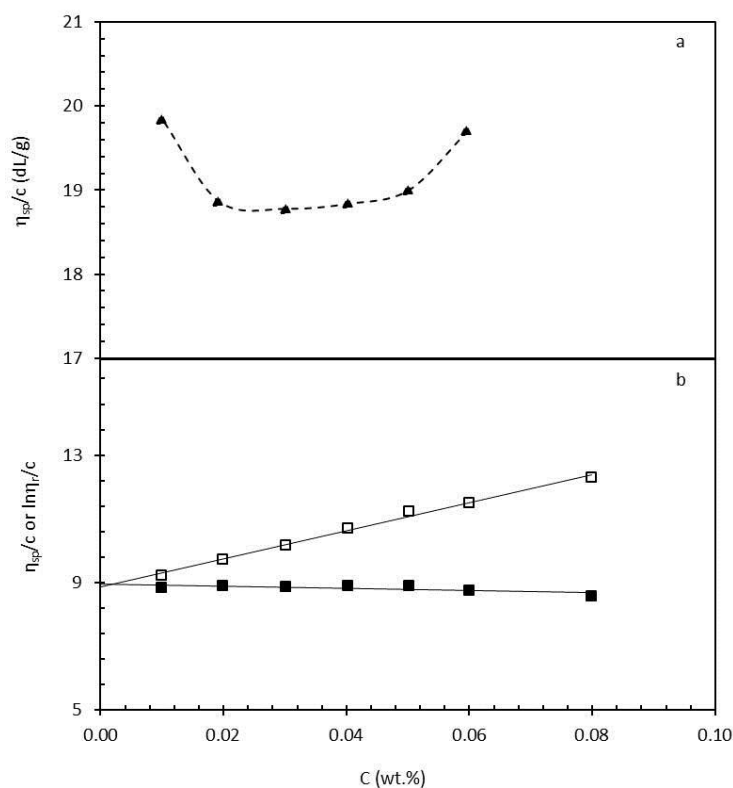


Figure 5.1 (a) Reduced viscosity as a function of FucoPol concentration in salt free solution; (b) determination of the intrinsic viscosity in 0.1 M NaCl using the Huggins (\square) and (\blacksquare) Kraemer equations.

The addition of ions to FucoPol solutions leads to shielding of polysaccharide negative charges and disabling intra-chain repulsions. As a consequence, when the measurements were performed in the presence of salt (0.1M NaCl), linear plots for Huggins and Kraemer extrapolations were obtained (Figure 5.1 b), enabling the determination of the intrinsic viscosity. The value obtained was $8.86 \pm 0.09 \text{ dL g}^{-1}$, which is within the values referred in the literature for typical commercial polysaccharides, namely. guar gum, carrageenan, cellulose and xanthan, $5 - 50 \text{ dL g}^{-1}$, respectively (Arvidson et al., 2006). Fucogel, a commercial fucose-containing bacterial polysaccharide, is referred to have an intrinsic viscosity around 16.7 dL g^{-1} (Guetta et al., 2003).

The Huggins constant (K_H) determined for FucoPol was 0.58 ± 0.04 , which is quite similar to that measured for Fucogel ($K_H = 0.55$, Guetta et al., 2003). According to Morris et

al. (1981), K_H should lie between 0.3 and 0.8, while values of K_H higher than 1.0 are indicative of molecular aggregation.

Ionic Strength and pH effect

To get a better knowledge of the behaviour of FucoPol 's intrinsic viscosity ($[\eta]$) under different aqueous environments, namely, different ionic strength and pH values, a central composite rotatable design with the two independent variables was performed. The inputs and outputs are listed on Table 5.1.

Table 5.1 Central composite rotatable design (CCRD) with two independents variables X_1 (Ionic Strength, IS) and X_2 (pH), and the observed responses studied Y_1 (intrinsic viscosity, $[\eta]$) and Y_2 (zero-shear rate viscosity, η_0)

	Run number	IS NaCl (M)	pH	$[\eta]$ (dL g ⁻¹)	η_0 (Pa s)
		X_1	X_2	Y_1	Y_2
Factorial design	1	0.15	4.50	8.17	0.94
	2	0.65	4.50	7.37	0.88
	3	0.15	9.50	7.38	0.41
	4	0.65	9.50	7.21	0.43
Central point	5	0.40	7.00	8.30	1.20
	6	0.40	7.00	8.28	1.20
	7	0.40	7.00	8.23	1.20
Axial points	8	0.05	7.00	8.54	0.64
	9	0.75	7.00	5.65	0.61
	10	0.40	3.47	8.07	1.07
	11	0.40	10.54	5.51	0.37

For the central point runs (0.40 M NaCl and pH 7.0) the $[\eta]$ achieved was within 8.23 – 8.30 dL g⁻¹, a value similar to the one obtained in standard conditions (8.86±0.09 at 0.1 M NaCl and natural pH). On the other hand, results have also shown that within the wide range of ionic strengths and pH tested, the $[\eta]$ did not have great changes, remaining within 7.21 and 8.54 dL g⁻¹. Only for the higher ionic strength (0.75 M NaCl) and higher pH (10.5)

tested the intrinsic viscosity demonstrated a pronounced decrease to 5.65 and 5.51 dL g⁻¹, respectively.

RSM Modelling of the Ionic Strength and pH Effect on intrinsic viscosity

Statistical analysis was used to evaluate the significance of ionic strength NaCl (M) and pH effect and their interactions on the quadratic model for describing $[\eta]$. An appropriate analysis of variance (ANOVA) of the second order model (Masmoudi et al., 2008) showed a good fit ($R^2 = 0.99$) and a sum of squares (SS) of 10.476, with 10 degrees of freedom (Table 5.2). Despite that, there was evidence of lack-of fit ($p < 0.05$), which means that the error predicted by the model was above the error of the replicas (the same behaviour was seen for the second order model for some of the responses studied in Chapter 3 – section 3.3.1.3).

Table 5.2 Analysis of variance of the second order model for parameter $[\eta]$ (intrinsic viscosity)

Source of variation	$[\eta]$				
	Sum of squares	Df	Mean squared	F - values	P
X_1	5.706	1	5.706	595.128	0.000
X_2	1.999	1	1.999	208.478	0.000
X_1X_1	5.013	1	5.013	522.783	0.000
X_2X_2	3.097	1	3.097	323.038	0.000
X_1X_2	0.666	1	0.666	69.510	0.001
Lack-of-fit	0.055	2	0.027	20.033	0.047
Pure error	0.002	2	0.001		
Total (corr.)	10.476	10	1.164		
R^2	0.994				

The linear (X_1 ; X_2), quadratic (X_1X_1 ; X_2X_2) and the interaction (X_1X_2) effects of ionic strength (NaCl (M) (X_1) and pH (X_2)) on $[\eta]$ is described in Table 5.2. The intrinsic viscosity was affected by all the effects of ionic strength and pH (linear, quadratic and interaction), since $p < 0.05$ for all the effects.

Such correlation between response and independent variables can be illustrated graphically by plotting 3D response surface plots. The quadratic effect is represented by the parabola format on the 3D surface plot (Figure 5.2). It can be observed that the intrinsic viscosity was kept practically unchanged for a wide range of ionic strength and pH (0.05 – 0.50 M NaCl and 3.0 – 8.0, respectively). Withal, it decreases for combinations between ionic strength and pH above 0.50 M NaCl and 8.0, respectively. By the information taken from Figure 4.2, it seems that for ionic strengths above 0.75 M NaCl, the intrinsic viscosity will decrease for any pH tested.

This lowering of $[\eta]$ with the increase of ionic strength is common to other polysaccharides, such as colanic acid, for which the intrinsic viscosity decreases from 47.5 to 22.7 dL g⁻¹ when the ionic strength increases from 0.002 to 0.2 M NaCl (Ren et al., 2003 b).

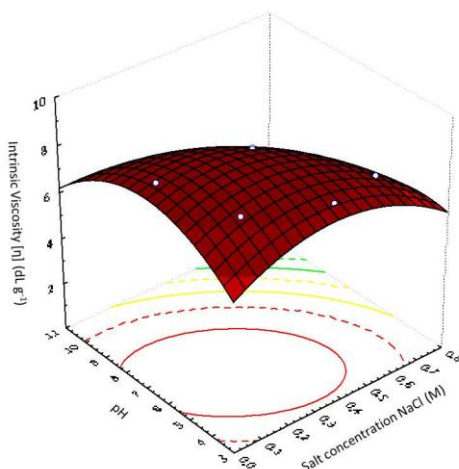


Figure 5.2 Response surface plot of intrinsic viscosity $[\eta]$ as a function of pH and NaCl concentration.

5.4.2. Rheological Properties under Steady and Dynamic Shear

5.4.2.1. Measurements at Standard Conditions (pH~5.6; T = 25°C)

Steady shear measurements

Flow curves of FucoPol aqueous solutions with concentrations ranging from 0.2 to 1.2 wt.% are shown in Figure 5.3. For all the concentrations studied, the apparent viscosity was immediately recovered at low shear rates, after subjecting the samples to shear rate values up to 700 s^{-1} . This may indicate that the sample has not strong internal interactions forming a structured matrix (e.g. gel like) that could be disrupted by the strong stress imposed, and it is able to recover instantly (data not shown).

FucoPol molecules are high molecular weight structures able to establish interactions in solution (e.g. entanglements and hydrogen, electrostatic and hydrophobic bonds). The energy transferred to the sample influences the creation and disruption of such interactions. At low shear rates, the disruption of interactions is balanced by the formation of new ones, resulting in a constant apparent viscosity (Newtonian plateau) (Sittikijyothin et al., 2004). At high shear rates, the disruption of those interactions predominates and the molecules align in the direction of the flow, resulting in the observed decrease of the apparent viscosity (shear-thinning), which is a typical behaviour of macromolecular solutions, reported by several authors (Morris et al., 1981; Ren et al., 2003; Simsek et al., 2009; Chenlo et al., 2011). It is possible to observe the curves approaching a Newtonian plateau at low shear rates, followed by a decrease of apparent viscosity as the shear rate increases. The onset of the Newtonian plateau moves to lower shear rates with increasing polymer concentrations.

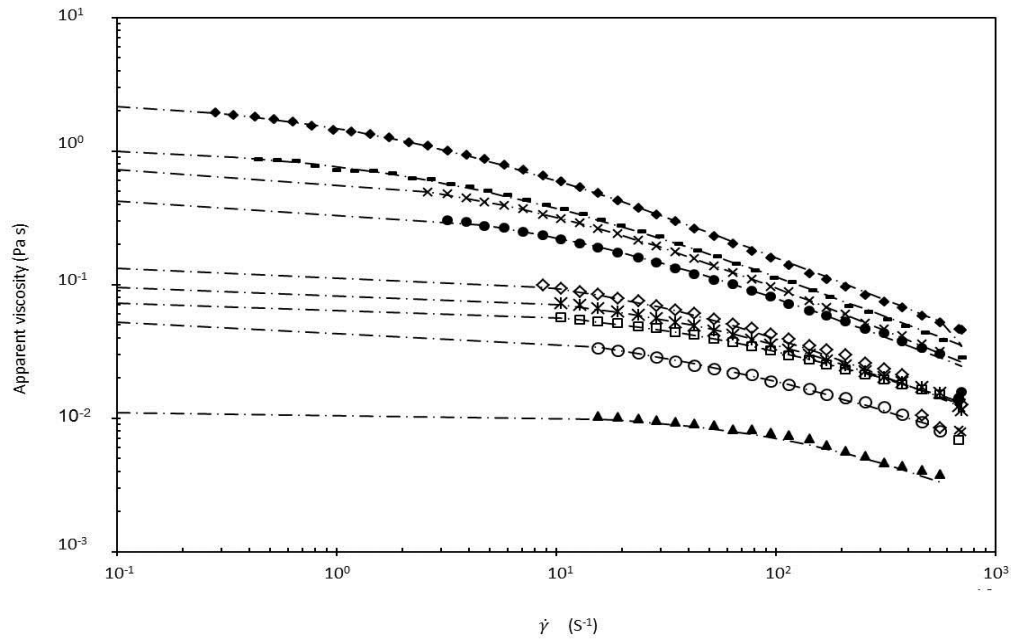


Figure 5.3 Shear rate dependence of viscosity for different concentrations of FucoPol. (\blacktriangle) 0.20 wt.%; (\circ) 0.35 wt.%; (\square) 0.45 wt.%; (\ast) 0.50 wt.%; (\diamond) 0.60 wt.%; (\bullet) 0.80 wt.%; (\times) 0.90 wt.%; (--) 1.0 wt.%; (\blacklozenge) 1.2 wt. %. Lines represented the fitted Cross equation.

Flow curves were fitted by Eq. 5.1, which is based on the Cross model, often used to describe shear thinning-behaviour, assuming η_∞ (the viscosity of the second Newtonian plateau) much lower than η_0 and η , since the second Newtonian plateau was never approached:

$$\eta = \frac{\eta_0}{1+(\tau\dot{\gamma})^m} \quad \text{Eq. 5.1}$$

where $\dot{\gamma}$ is the shear rate (s^{-1}), η is the apparent viscosity (Pa s), η_0 is the zero-shear rate viscosity (of the first Newtonian plateau) (Pa s), τ is a relaxation time (s) and m is a dimensionless constant, which may be related to the exponent of the power law (n) by

$$m = 1 - n \quad \text{Eq. 5.2}$$

The flow curves (Figure 5.3) were fairly well fitted by Eq. 5.1. The parameter values are summarized in Table 5.3.

The time constant (τ) increases with increasing FucoPol concentration. This fact means that more time is needed to form new entanglements in a number high enough to compensate the ones disrupted by the imposed shear stress. Hence, the shear rate at which there is the transition from Newtonian to non-Newtonian behaviour shifts to lower values, and corresponds to the reciprocal of τ .

Table 5.3 Cross model parameters estimated for different FucoPol concentrations

FucoPol (wt.%)	Cross model		
	η_0 (Pa s)	τ (s)	m
0.20	0.011±0.000	0.005±0.000	0.825±0.092
0.35	0.054±0.006	0.028±0.012	0.613±0.058
0.45	0.074±0.002	0.016±0.002	0.634±0.028
0.50	0.096±0.004	0.022±0.004	0.693±0.046
0.60	0.134±0.008	0.033±0.007	0.735±0.066
0.80	0.439±0.038	0.098±0.018	0.677±0.036
0.90	0.759±0.024	0.159±0.018	0.707±0.030
1.00	1.095±0.036	0.282±0.036	0.645±0.024
1.20	2.465±0.066	0.553±0.052	0.666±0.016

Flow curves depicted on Figure 5.3 were overlaid by scaling vertically, dividing by the respective zero shear rate viscosity (η_0), and horizontally, multiplying by the relaxation time (τ), which generated a master curve (Figure 5.4) (Morris, et al., 1981). This procedure was employed successfully for several polysaccharide solutions, such as an EPS produced by *Pseudomonas acidi-propionici* and a galactose-rich EPS produced by *Pseudomonas oleovorans* (Gorret et al., 2003; Hilliou et al., 2009). With the application of the generalized equation:

$$\eta/\eta_0 = \frac{1}{1+(\tau\dot{\gamma})^m} \quad \text{Eq. 5.3}$$

a value $m = 0.681 \pm 0.008$ was obtained. This value is in accordance with the one presented by Morris (1990), $m = 0.76$, for polysaccharides presenting strong interactions between polymer chains, such as hydrogen bonds (Graessley, 1974). The concentration dependence of τ is illustrated in the inset of Figure 5.4. The solid line suggests $\tau \sim c^4$ for concentrations above 0.6 wt.%, with an exponent near the one referred in the literature for polysaccharides exhibiting a strong inter-chain association (Burchard, 2001). Additionally, de Gennes (1979) has estimated a power law behaviour of $\tau \sim c^{2.75}$ for entangled polymer melts. By the contrary, polysaccharides with linear chains revealing non-association presented exponent values of 2.08 (Doi & Edwards, 1986). Therefore, we may infer that, for the concentration range studied, FucoPol presents a rheological behaviour of an entangled solution with high inter-chain association.

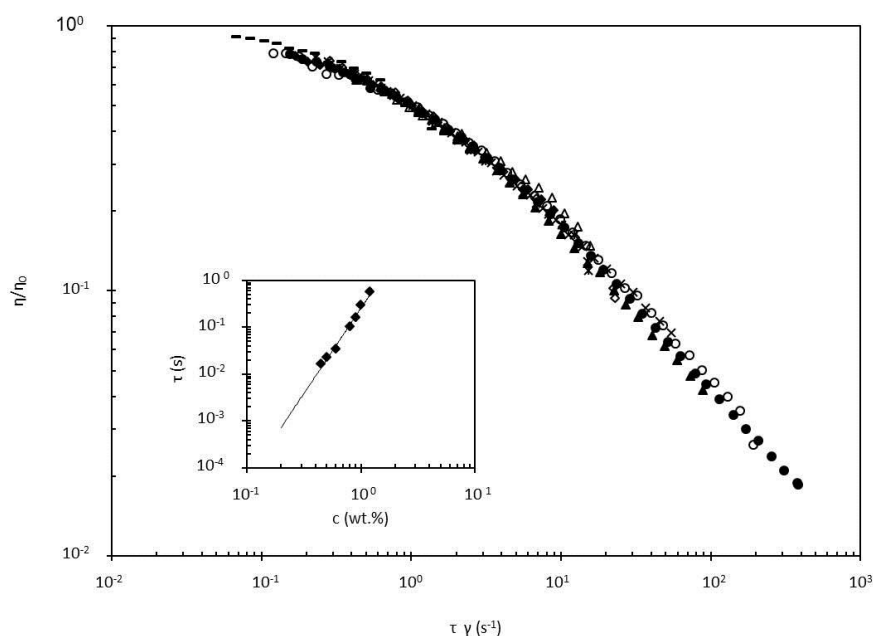


Figure 5.4 Master curve obtained shifting vertically dividing by η_0 , and horizontally multiplying by relaxation time (τ). Inset: τ as a function of FucoPol concentration.

Furthermore, FucoPol 's aqueous solution (1.00 wt.%) was compared to several comercial polysaccharides with the same concentration and solvent (0.1 M NaCl) (Figure 5.5). The flow curve of FucoPol aqueous solution (1.00 wt.%) already mentioned (Figure

5.3), showed a Newtonian plateau at low shear rates, with a zero shear viscosity approaching 1.0 Pa.s, followed by a shear-thinning behaviour, with the apparent viscosity decreasing with the increase of shear rate. This behaviour is similar to the one demonstrated by the guar gum solution. The solution prepared with Fucogel, had also a similar behaviour under the tested conditions, but the apparent viscosity was somewhat higher. Although xanthan solution was much more viscous than FucoPol for low shear rates, for high shear rates its viscosity was similar to Fucogel, guar gum and FucoPol solutions. These non-Newtonian behaviour of polysaccharide solutions makes them interesting to be used in several industries, such as food, textile, pharmaceutical and cosmetic, as stabilizing, suspending or thickening agents.

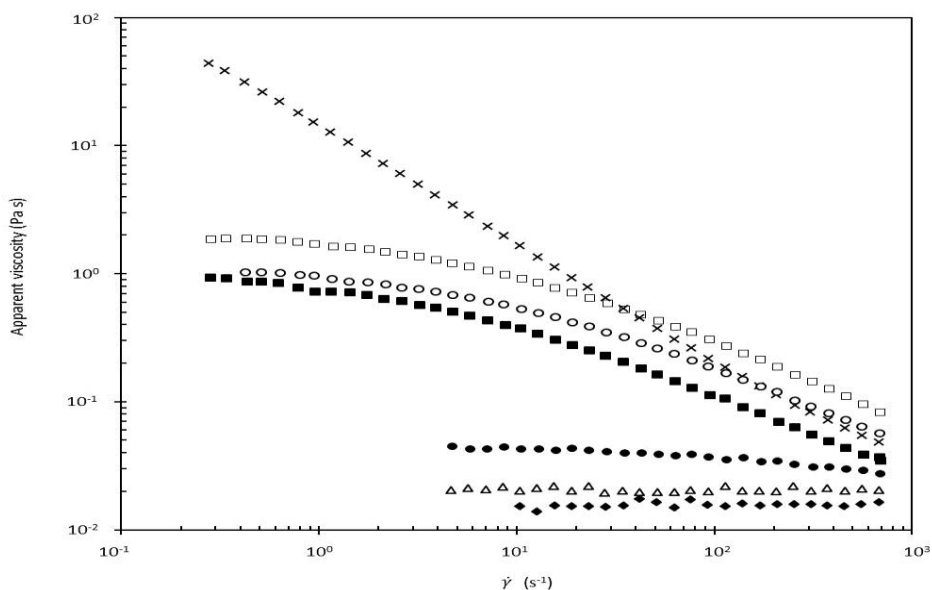


Figure 5.5 Comparative flow curves of polysaccharides (C=1%wt, 0.1M NaCl): (■) FucoPol; (□) Fucogel; (×) xanthan; (○) guar gum; (●) CMC; (▲) pectin and (◆) alginate.

As seen in Figure 5.5, there is a clear differentiation between the behaviour of the higher average molecular weight ($M_w > 10^6$) (FucoPol, xanthan, Fucogel and guar gum) and the lower molecular weight polysaccharides ($M_w \sim 10^5$) (alginate, pectin and CMC), which were considerably less viscous and had an almost Newtonian behaviour.

Dynamic measurements

The mechanical spectra of aqueous solutions with different FucoPol concentrations are presented in Figure 5.6. For all the concentrations tested, FucoPol solutions were predominantly liquid-like, since the loss modulus (G'') is above the storage modulus (G') in the entire frequency range studied, except at higher frequencies, where a cross-over is approached at an angular frequency of about 2.8 Hz for the solutions with 1.0 and 1.2 wt.% (Figure 5.6 c and d). This dependence of the dynamic moduli with the frequency indicates the presence of solutions with entangled polymer chains.

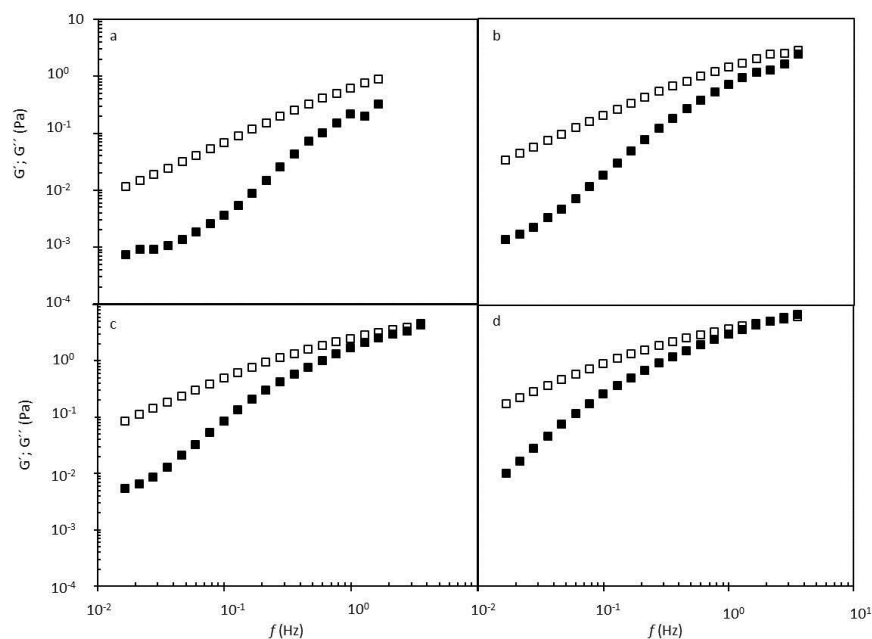


Figure 5.6 Mechanical spectra (G' (■); G'' (□)) of FucoPol aqueous solution at different concentrations in 0.1 M NaCl. (a) 0.6 wt.%; (b) 0.8 wt.%; (c) 1 wt.% and (d) 1.2 wt.%.

Furthermore, the Cox-Merz rule was also applied. This rule is an empirical relationship that predicts that the magnitude of the complex viscosity should be compared with the apparent viscosity at equal values of frequency and shear rate. It is used to establish relationships between steady shear flow and dynamic rheology, and is especially

useful to estimate the complex viscosity for cases in which the oscillatory operating mode is not available. In addition, a qualitative perception of the sample microstructure may be perceived according to its applicability. In general, it is not valid for most particulate dispersions or when there is the formation of large aggregates and gel systems, as reported for several exopolysaccharides, including xanthan, curdlan and *Aeromonas* gum (Rocheffort, 1987; Lo, et al., 2003; Xu et al., 2006).

FucoPol solutions obeyed the Cox-Merz rule. The results obtained for 1% FucoPol solution (Figure 5.7) show a good superposition of the angular frequency dependence of complex viscosity (η^*) with the shear-rate dependence of apparent viscosity (η). These facts suggest samples with a viscous behaviour constituted by entangled polymer chains without gel-like interactions. This behaviour was also referred for other polymers, namely the fucose containing polymer colanic acid (Ren et al., 2003 b).

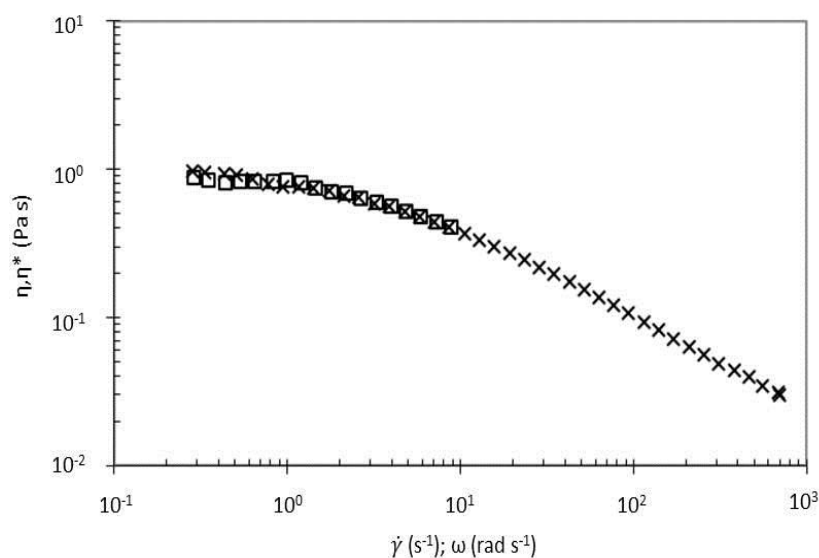


Figure 5.7 Apparent viscosity and complex viscosity (FucoPol solution 1.0 wt.%) as a function of the shear rate and angular frequency, respectively.

5.4.2.2. Effect of Ionic Strength and pH (1 wt.% FucoPol; T = 25°C)

Steady shear measurements

The stock solutions used to assess the effect of ionic strength and pH on intrinsic viscosity were also used to study the influence of those parameters on the steady shear behaviour, applying a central composite design as well. The inputs and outputs are listed on Table 5.1. Figure 5.8 presents the flow curves of the FucoPol aqueous solutions with different ionic strength and pH values. The results show that all solutions present a shear thinning behaviour with an apparent viscosity at the lowest shear rates studied varying between 0.1 and 1 Pa s.

The flow curves were also properly fitted by Eq. 5.1 (based on the Cross model) (Figure 5.8). The zero-shear viscosity (η_0) values calculated are summarized in Table 5.1.

For the central point runs (0.40 M NaCl and pH 7.0) η_0 achieved the highest value (1.20 Pa s), which was similar to the one obtained for the 1 wt% FucoPol aqueous solution in standard conditions (1.10 Pa s at 0.1 M NaCl and pH ~5.6). The lowest values were obtained for the solutions with 0.40 M NaCl – pH 10.54, 0.15 M NaCl – pH 9.5 and 0.65 M NaCl – pH 9.5, with zero-shear viscosities of 0.37, 0.45 and 0.43 Pa s, respectively.

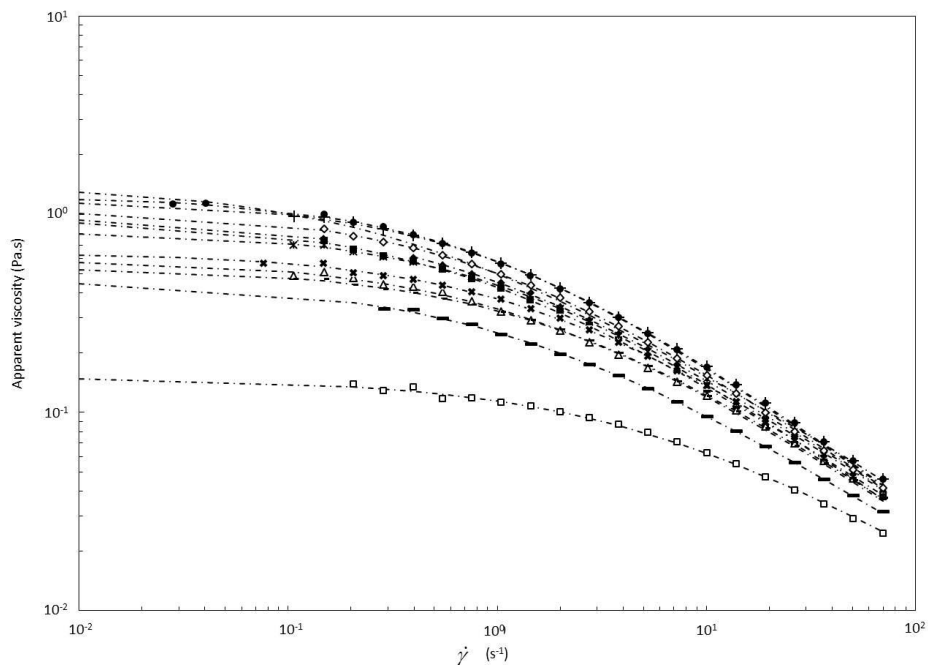


Figure 5.8 Effect of ionic strength NaCl (M) and pH on FucoPol's shear rate dependency on viscosity. (◆) 0.15M NaCl - pH 4.5; (■) 0.65 M NaCl - pH 4.5; (△) 0.15 M NaCl - pH 9.5; (×) 0.65 M NaCl - pH 9.5; (*) 0.40 M NaCl - pH 7.0; (●) 0.40 M NaCl - pH 7.0; (+) 0.40 M NaCl - pH 7.0; (+) 0.05M NaCl - pH 7.00; (▪) 0.75 M NaCl - pH 7.00; (◇) 0.40 M NaCl - pH 3.47; (□) 0.40 M NaCl - pH 10.54. Lines represent the fitted model.

RSM Modelling of Ionic Strength and pH Effect on zero-shear viscosity

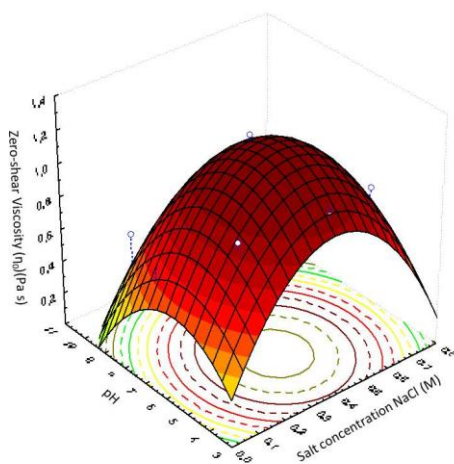
Statistical analysis was also used to evaluate the impact of ionic strength NaCl (M) and pH on the quadratic model for describing η_0 . ANOVA of the second order model (Masmoudi et al., 2008) showed a satisfactory fit ($R^2 = 0.85$) (according to Lundstedt et al., 1998), a sum of squares (SS) of 1.109, with 10 degrees of freedom, and an insignificant lack-of fit ($p = 0.120$) (Table 5.4).

Table 5.4 shows the linear (X_1 ; X_2), quadratic (X_1X_1 ; X_2X_2) and the interaction (X_1X_2) coefficients of ionic strength NaCl (M) (X_1) and pH (X_2) on η_0 . Linear pH and quadratic ionic strength are the factors which had a significant effect on η_0 , since $p < 0.05$.

Table 5.4 Analysis of variance of the second order model for parameter η_0 (zero shear viscosity from Cross model fitting)

Source of variation	η_0				
	Sum of squares	Df	Mean squared	F-values	p-value
X_1	0.001	1	0.001	0.018	0.899
X_2	0.384	1	0.384	9.344	0.038
X_1X_1	0.480	1	0.480	11.687	0.027
X_2X_2	0.265	1	0.265	6.446	0.064
X_1X_2	0.001	1	0.001	0.035	0.860
Lack-of-fit	0.163	2	0.054	37.209	0.120
Pure error	0.001	2	0.001		
Total (corr.)	1.109	10	0.123		
R^2	0.850				

The 3D response surface plot (Figure 5.9) evidenced the correlation between response and independent variables. The quadratic effect is represented by the parabola format on the 3D surface plot (Figure 5.9), which demonstrated that for the higher and lower ionic strength and pH (axial points) the zero-shear viscosity decreased. The zero-shear viscosity presented higher values for ionic strength and pH within 0.10 – 0.50 M NaCl and 3.0 – 8.0, respectively, corresponding to the ranges for which a higher intrinsic viscosity was observed (Figure 5.8).

**Figure 5.9** Response surface of zero-shear viscosity (η_0) as a function of pH and NaCl concentration.

Dynamic measurements

The mechanical spectra for the FucoPol solutions at different ionic strengths and pH (Figure 5.10) indicated liquid like solutions as in standard conditions, since the loss modulus (G'') is higher than the storage modulus (G') for all the solutions measured with a strong frequency dependence, indicating again samples of entangled polymer chains in aqueous media.

Whatever the pH and ionic strength values, the spectra were very similar, with a noticeable cross-over point for higher frequencies (above 1 Hz). The exception was the solution with 0.40 M NaCl and pH 10.5, for which the loss and storage modulus presented lower values. This result indicates that at higher pH values the interactions between polymer chains in solution are weakened, which is consistent with the lower apparent viscosity presented in Figure 5.8.

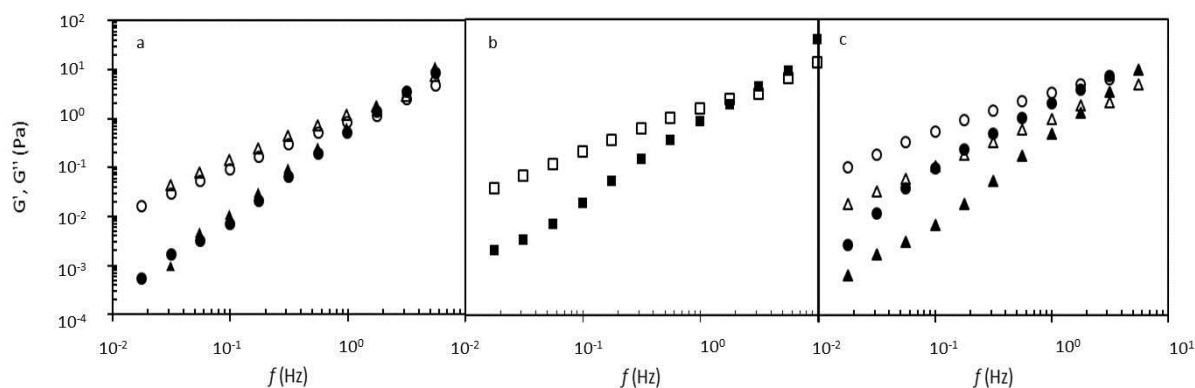


Figure 5.10 Mechanical spectra for FucoPol solutions with different ionic strength and pH values, G' (full symbols) and G'' (empty symbols). (a) (● and ○) 0.75 M NaCl – pH 7.00; (▲ and △) 0.05 M NaCl – pH 7.00; (b) (■ and □) 0.40 M NaCl – pH 7.00; (c) (● and ○) 0.40 M NaCl – pH 3.45; (▲ and △) 0.40 M NaCl – pH 10.54.

5.4.2.3 Temperature Effect (pH ~ 5.6)

Steady shear Measurements

A solution with a FucoPol concentration of 0.81 wt.% in deionised water was submitted to a shear rate range from 1 to 700 s^{-1} , at different temperatures (15, 25, 30, 45, 55 and 65 °C). The viscosity measurements showed a shear-thinning behaviour, since the apparent viscosity decreased as the shear rate increased, for all temperatures tested (Figure 5.11).

On the other hand, the apparent viscosity decreased with the temperature increase, showing the influence of this parameter on the polymer's rheological properties. It is notorious in Figure 5.11 that the shear rate corresponding to the transition from Newtonian to shear-thinning behaviour moves to higher values as the temperature increases, which means that for higher temperatures the formation of new interactions is faster. This behaviour is similar to that observed in works with other polysaccharides, such as for the galactose-rich EPS produced by *P. oleovorans* from glycerol byproduct (Alves et al., 2010).

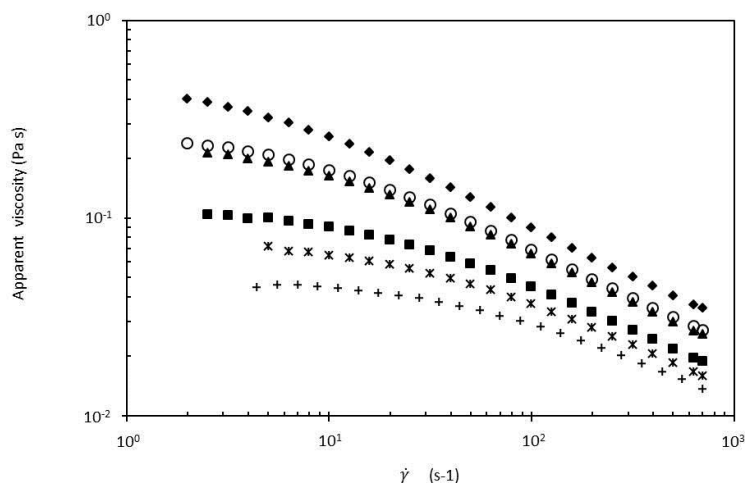


Figure 5.11 Flow curves for a 0.81 wt.% FucoPol solution at different temperatures: (◆) 15°C; (○) 25°C; (▲) 30°C; (■) 45°C; (*) 55°C; (+) 65°C.

The Carreau model Eq. 5.4 (Carreau, 1972) was used to describe the steady shear viscosity dependence with the shear rate, at different temperatures:

$$\eta_a = \eta_\infty \frac{\eta_0 + \eta_\infty}{[1 + (\lambda \dot{\gamma})^2]^N} \quad \text{Eq. 5.4}$$

where $\dot{\gamma}$ is the shear rate (s^{-1}), η_a is the apparent viscosity (Pa s), η_∞ is the infinite shear rate viscosity (Pa s), η_0 is the zero-shear rate viscosity (Pa s), λ is a time constant (s) and N is a dimensionless constant. Since the second Newtonian plateau was never approached, Eq. 5.4 was simplified assuming η_∞ much higher than η_0 and η_a . The model fitted quite well the experimental results, and the parameter values are presented in Table 5.5.

Table 5.5 Parameters of Carreau model for the range of temperatures studied

T (°C)	Carreau Model		
	η_0 (Pa s)	λ (s)	N
15	0.443±0.008	0.334±0.039	0.224±0.010
25	0.240±0.004	0.175±0.017	0.219±0.007
30	0.215±0.004	0.154±0.016	0.218±0.008
45	0.103±0.001	0.086±0.010	0.197±0.010
55	0.075±0.002	0.092±0.020	0.171±0.014
65	0.045±0.001	0.037±0.005	0.174±0.010

$$RE = \sum_{i=1}^n \frac{(|x_{exp,i} - x_{cal,i}|/x_{exp})}{n} \text{ was } 0.019 \leq RE \leq 0.039$$

As expected, η_0 and λ decreased with increasing temperature. The relaxation time constant (λ) decreased from 0.334 s^{-1} to 0.037 s^{-1} as the temperature increased from 15 to 65 °C, respectively. This fact indicates that less time is needed to form new interactions between polymer molecules at higher temperatures. Consequently, the transition from Newtonian plateau to shear-thinning regime is less notorious and moves to higher shear rate values.

Dynamic Measurements

Similarly to the previously studied conditions, the mechanical spectra for FucoPol solutions at 15 and 65 °C (Figure 5.12 a) indicated the presence of viscous samples of entangled polymer chains. At low frequencies ($f < \sim 3$ Hz), the loss modulus (G'') was higher than the storage modulus (G'), indicating a liquid-like behaviour for the polymer solution. At high frequencies, a cross-over was detected at 15 °C, after which the elastic contribution predominates. However, this behaviour was not observed at 65 °C. At lower temperatures, a higher viscosity was observed, i.e. 15° C had the highest viscosity while 65° C had the lowest (Figure 5.11). Hence, less energy is needed to transfer to those samples in order to store more energy than that dissipated, and perceive a G'' and G' cross-over. Figure 5.12 b shows the dynamic (η') and the out of phase (η'') viscosities, consisting of the viscous and elastic components of the complex viscosity ($\eta^* = \eta' - i\eta''$), respectively. Their behaviour is in agreement with that of dynamic moduli presented in Figure 5.12 a.

Frequency sweeps were performed before and after the steady state measurements and the obtained mechanical spectra were coincident for all temperatures studied. These results confirmed that FucoPol solutions do not have an organized internal structure that would suffer irreversible changes after being subjected to high shear rates, such as 700 s^{-1} . By the contrary, their viscoelastic properties were maintained.

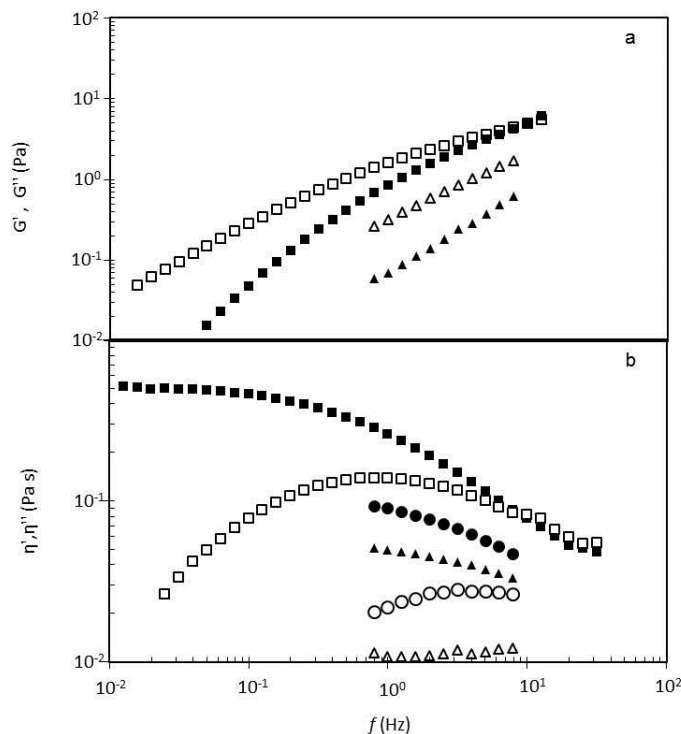


Figure 5.12 (a) Mechanical spectra of 0.81wt.% FucoPol solution at 15 °C (squares) and 65 °C (triangles), G' - full symbols; G'' - open symbols. (b) Dynamic viscosity η' (full symbols) and out of phase viscosity η'' (open symbols) as a function of the applied frequency for 15 °C (squares), 45 °C (bullets) and 65 °C (triangles).

Application of Time-Temperature Superposition (TTS) principle

TTS principle superposes oscillatory isothermal frequency data of viscoelastic variables into a single master curve using the temperature-dependent shift factor a_T to extend the frequency axis by several orders of magnitude (Nickerson et al., 2004). According to this principle, all contributions to the dynamic moduli should be proportional to $T\rho$ and all relaxation times should have the same temperature dependence. The change of temperature from T to T_0 (reference temperature) will change G' and G'' , corresponding to the multiplication by $T_0\rho_0/T\rho$ (temperature density ratio) defined as b_T (Ferry, 1980). This shift factor was necessary to have a good superposition of the measurements done at the different temperatures (Roth et al., 2004).

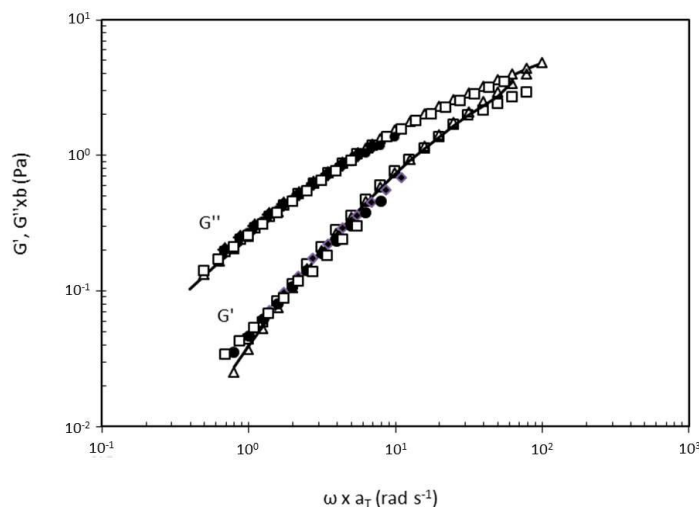


Figure 5.13 Frequency and temperature superposition of the loss (G'') and storage (G') moduli. The solid line represents the data for the reference temperature (25 °C) and the symbols correspond to the other temperatures: (\triangle) 15 °C; (\blacksquare) 30 °C; (\bullet) 45 °C; (\blacklozenge) 55 °C; (\square) 65 °C.

The TTS for both moduli is shown in Figure 5.13, and the respective shift factors are presented in Table 5.6. TTS principle was applied successfully, suggesting that FucoPol EPS solution is thermorheologically simple, with the relaxation times for all mechanisms changing identically with temperature (Nickerson et al., 2004). In addition, the range of frequencies was significantly enlarged for the lower temperatures, enabling the estimation of the dynamic moduli for frequency values outside the range measured by the rheometer.

Table 5.6 Shift factors of Time-Temperature Superposition

T °C	G''		G'	
	a_T	b_T	a_T	b_T
15	2.00	1.10	2.00	1.10
25	1.00	1.00	1.00	1.00
30	0.70	0.85	1.00	1.20
45	0.20	0.58	0.22	0.52
55	0.14	0.58	0.16	0.51
65	0.10	0.55	0.11	0.50

Temperature influence on rheological parameters

To determine the activation energy at a given concentration and shear rate, the apparent viscosity and the zero-shear rate viscosity were studied as a function of the temperature according to the Arrhenius law (Desbrieres, 2004):

$$\eta_i = A \exp\left(\frac{E_a}{RT}\right) \quad \text{Eq. 5.5}$$

where η_i (Pa s) represents the apparent viscosity or the zero-shear rate viscosity determined by the Carreau equation, A is the preexponential factor, E_a is the activation energy, R is the gas constant and T is the absolute temperature.

The variation of the activation energy with the apparent viscosity for two different shear rates (5 and 13 s⁻¹), and for the zero shear rate, is plotted in Figure 5.14. The Arrhenius equation fitted quite well the experimental data and, as can be seen, the activation energy decreased as the shear rate increased. For zero shear rate the activation energy was 36.8±5.2 kJ mol⁻¹ and for 13 s⁻¹ it was 25.7±3.1 kJ mol⁻¹. In fact, as the shear rate increases, molecular interactions have shorter lifetimes and less energy is needed to promote viscous flow.

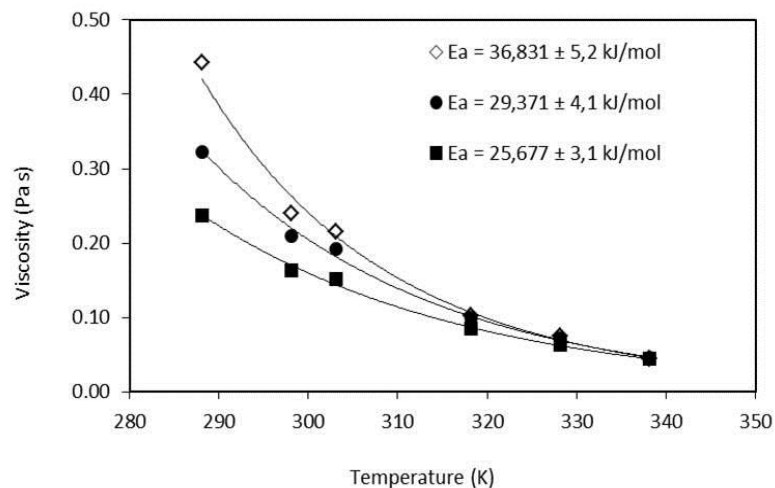


Figure 5.14 Temperature dependence of: apparent viscosity at shear rate 5 s^{-1} (●) and 13 s^{-1} (■); zero-shear rate viscosity estimated by the Carreau model (◇). The lines correspond to Arrhenius equation.

Consecutive temperature cycles were also performed, in which the same sample was subjected to different temperatures (from 25 to 80 °C) during 10 min. After each heating step, the temperature was reduced to 25 °C, where both oscillatory and steady-state tests were carried out. As can be seen in Figure 5.15 a, the flow curves were nearly concurrent. The same may be observed for the dynamic data presented in Figure 5.15 b (G' and G'') and c (η' and η''). Besides a small difference at low frequencies, before and after the temperature cycles, the mechanical spectra are rather similar, meaning that the polymer solution did not suffer significant alterations and its rheological properties were maintained. These results indicate that the polymer sample is quite stable under the tested temperature fluctuations. This is an interesting characteristic for certain industrial applications, in which thermal variations may occur (e.g. food processing).

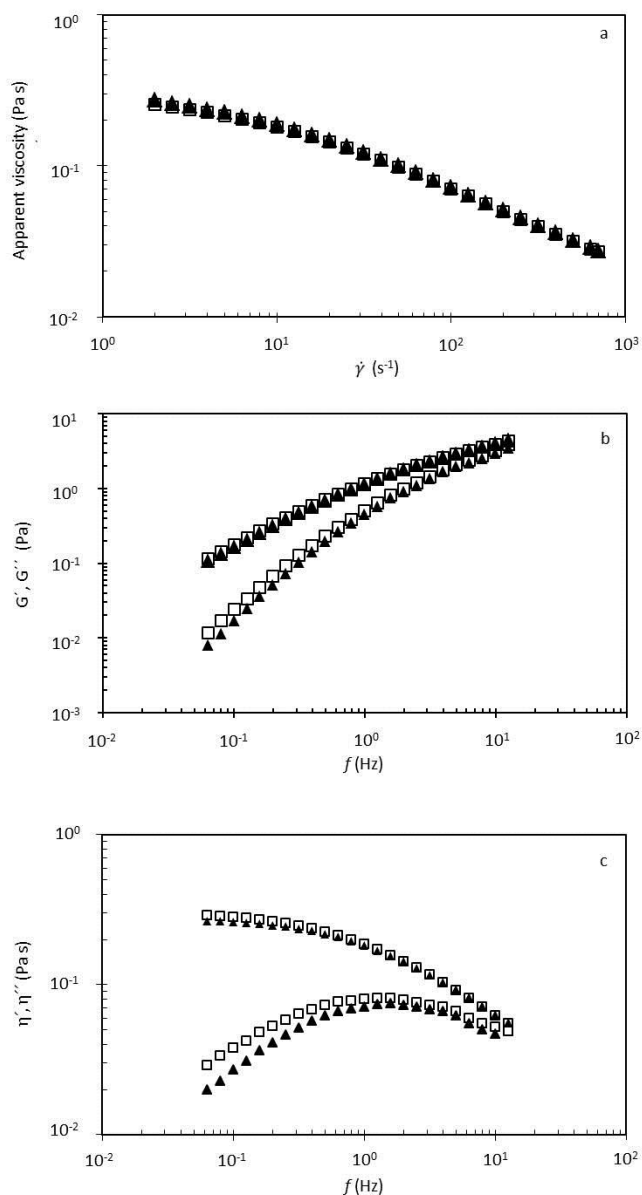


Figure 5.15 Data measured at 25 °C before (open symbols) and after (full symbols) the temperature cycles: (a) flow curves; (b) dynamic moduli and (c) dynamic (η') and out of phase (η'') viscosities.

Cox-Merz Rule

Figure 5.16 presents the apparent and complex viscosities as a function of the shear rate and angular frequency, respectively, for the present case-study. It can be seen that the Cox–Merz rule is valid for all temperatures tested. These results indicate a sample with simple rheological properties, without the formation of large aggregates,

hyperentanglements or gel-like structures, which is in agreement with the oscillatory data presented in Figure 5.12.

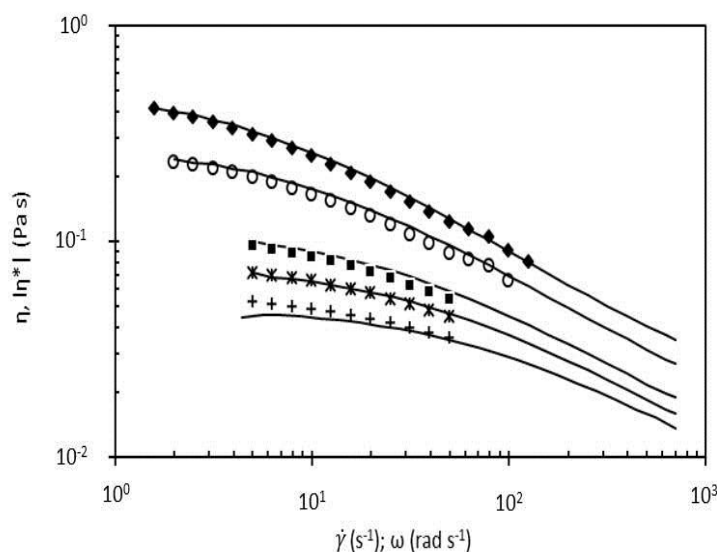


Figure 5.16 Apparent viscosity η (lines), and complex viscosity $|\eta^*|$ (symbols), as a function of the shear rate and angular frequency, respectively.

5.4.3. Concentration Regimes

The concentration dependence of zero shear-rate specific viscosity ($\eta_{sp,0}$) can be represented as the logarithmic of $\eta_{sp,0}$ as a function of biopolymer concentration. This standard procedure is based on approaches used by several authors (e.g. Morris et al., 1981; Lapasin and Pricl, 1995; Bohm and Kulicke, 1999; Arvidson et al., 2006; Wyatt and Liberatore, 2009). For concentration values below 0.1%wt, the $\eta_{sp,0}$ data was obtained by capillary viscometry, while for higher values a controlled stress rheometer was used. Figure 5.17 displays FucoPol behaviour. The curve has three distinct linear zones, characterized by different slopes, and separated by two critical concentrations (c^* and c^{**}). This type of correlation is analogous to the one exhibited by other high molecular weight microbial polysaccharide solutions, such as xanthan (Cuvelier and Launay, 1986), the galactose-rich

EPS produced by *Pseudomonas oleovorans* (Hilliou et al., 2009) and the exopolysaccharide produced by *P. acidi-propionici* (Gorret et al., 2003).

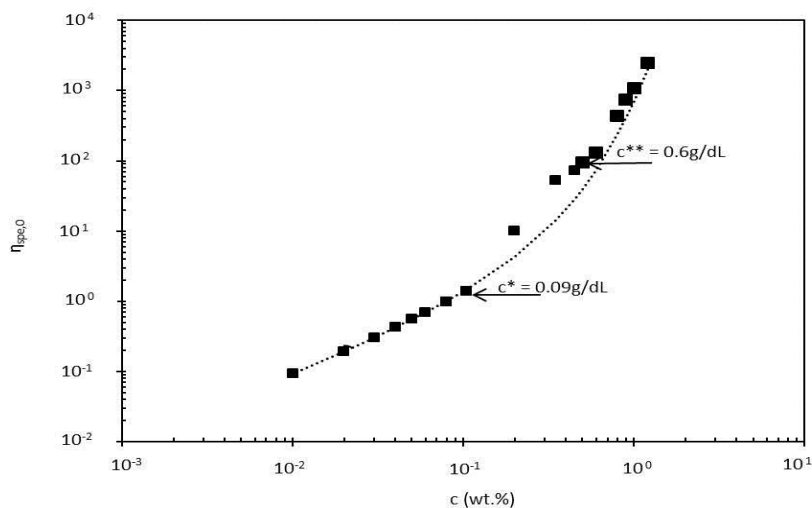


Figure 5.17 Concentration dependence of zero-shear specific viscosity for FucoPol samples. Dotted line: Martin model.

The dilute regime is characterized by isolated coils of polymer molecules with a free mobility and a negligible influence on each other. c^* set the dilute regime boundary, marking the onset of significant coil overlap (Gorret et al., 2003). The coil overlap parameter ($c^*[\eta]$), or space occupancy, was found to be approximately 0.8. With increasing concentration, polymer molecules start being directly affected by each other (Arvidson et al., 2006). This leads to a change from one stage to another, thus resulting in a significant increase of the slope. The intermediate concentration region has a slope of 2.43, with space occupancy between 0.8 and 5.34. c^{**} corresponds to the beginning of the entangled regime, where molecules interact intensively with each other (Lai and Yang, 2007). The estimated values ($c^* \sim 0.09$ wt.%, $c^{**} \sim 0.6$ wt.%) are higher than the ones obtained for xanthan at the same ionic strength ($c^* \sim 0.024$ wt.%, $c^{**} \sim 0.092$ wt.%) (Cuvelier and Launay, 1986). This result may be related to a smaller hydrodynamic volume of FucoPol, expressed by its lower intrinsic viscosity ($[\eta] \leq 8.54$ dL g⁻¹), when compared to that of xanthan ($[\eta] = 47.5$ dL g⁻¹). The slope above c^{**} (3.78) is in the range (3.3-4.0) presented for several

random coil polymers in the literature (alginate, xanthan, colanic acid, galactomannans) (Morris et al., 1981; Milas et al., 1990; Launay et al., 1997; Ren et al., 2003). The high value may indicate the existence of a large number of entanglements.

Martin (Eq. 5.6) equation was adjusted successfully to the data presented in Figure 5.17:

$$\eta_{sp,o} = c[\eta]_0 e^{K_M c [\eta]_0} \quad \text{Eq. 5.6}$$

where K_M is the Martin polymer-polymer interaction parameter. A good fit was obtained ($R^2 = 0.99$) for FucoPol with a K_M of 0.49 ($[\eta]_0 = 8.54 \text{ dL g}^{-1}$, 0.1M NaCl, 25°C). Cuvelier and Launay (1986) presented a similar value ($K_M = 0.42$) for xanthan ($[\eta]_0 = 51.5 \text{ dL g}^{-1}$, 0.1M NaCl, 25°C).

5.5. Conclusions

Fucopol intrinsic viscosity and shear flow was stable under a wide range of pH and ionic strength (3.5 – 8.0 and 0.05 – 0.50 M NaCl, respectively). The polymer produced viscous solutions with a shear-thinning behaviour. There was no hysteresis when the shear rate was decreased, after subjecting the polymer solution to shear rate values up to 700 s^{-1} . The flow curves were described successfully by the Cross model and the dependence of the estimated relaxation time with polymer concentration suggests a large degree of interaction between FucoPol molecules. Mechanical spectra and application of the Cox-Merz rule suggest the presence of entangled macromolecules in a viscous solution.

The Carreau model fitted quite well the steady state data at the different temperatures tested. The Arrhenius equation described adequately the temperature

dependence of η_0 and the apparent viscosity at different shear rates. As expected, a decrease of the activation energy was noticed with the increase of shear rate due to the lower resistance to viscous flow. FucoPol maintained its rheological properties at 25°C under consecutive temperature fluctuations, even after heated up to 80°C. This novel polysaccharide produces aqueous solutions that are thermorheologically simple and stable.

Chapter 6

FucoPol

Emulsifying and Flocculating Capacity

6.1. Summary

Some microbial polysaccharides possess the ability to emulsify and stabilize mixtures between water and hydrophobic compounds. Furthermore, polysaccharides may also have the capacity to separate solids from liquids in aqueous systems, acting as flocculating agents. In this chapter, FucoPol was tested for both properties. The emulsion forming and stabilizing capacity was evaluated for different hydrophobic compounds (e.g. food grade oils and hydrocarbons). Furthermore, FucoPol's emulsifying performance was also assessed at three different polymer concentrations and Oil/Water (O/W) ratios. On the other hand, FucoPol's flocculating activity was studied using kaolin clay as the suspended solids. For both studies, results were compared with other commercial emulsion forming and flocculating agents.

FucoPol has shown a good emulsion forming and stabilizing capacity for food grade oils (emulsification index, $E_{24} > 60\%$), similar to some commercial polysaccharides (xanthan and pectin). Given the high emulsification index obtained against sunflower oil (60%), it was chosen for the study of FucoPol's emulsifying capacity at different polymer concentrations and different O/W ratios. The most structured oil in water emulsion produced with sunflower oil was achieved for 1.5 wt.% polymer and a O/W ratio of 60/40, which presented the highest apparent viscosity and the highest dynamic moduli. Besides, the increase of polymer concentration, from 0.5 wt.% to 1.5 wt.%, resulted in an increase of the viscosity and of the dynamic moduli, for all O/W proportions tested.

Furthermore, FucoPol has demonstrated a similar flocculating capacity (28%), in the same range of some commercially available products (xanthan and carboxymethylcellulose).

These functional properties make FucoPol a promising alternative to many synthetic polymers, as well as other natural polysaccharides in several applications in the food, pharmaceutical, cosmetic, textile, paper and petroleum industries. Since FucoPol is probably biodegradable, harmless to human and environment and may have a lower cost.

6.2. Introduction

An emulsion is a dispersion of droplets of liquids that are not completely miscible (e.g. oil in water) and may exhibit structural changes in various ways depending on characteristics of the system and conditions it is under (Vianna-Filho et al., 2012). However, emulsions are thermodynamically unstable, where creaming, flocculation, coalescence or Ostwald ripening phenomena may occur (Calero et al., 2013). Surface-active ingredients adsorb at the newly formed oil/water interface during emulsion preparation, and protect them against immediate re-coalescence (Phillips and Williams, 2009). The emulsifying agents commonly used are proteins (e.g. those derived from milk or eggs) and small molecule-surfactants (Dickinson, 2003).

In addition, some polysaccharides have the ability to stabilize emulsion droplets as well, either by acting as interface stabilizers, or by increasing the viscosity of the aqueous continuous phase. Many microbial polysaccharides can find applications as bioemulsifiers due to their ability to stabilize emulsions between water and hydrophobic compounds (Freitas et al., 2009b).

Some examples include sodium hyaluronan, xanthan and Fucogel, which are used as additives in cosmetics as moisturizing agents (Phillips and Williams, 2009; Vianna-Filho et al., 2012). Moreover, polysaccharides may also be applied in several other industries, namely oil, water and soil bioremediation, detergents and laundry, pulp and paper processing, paints, pharmaceuticals, personal care products and food processing (Al-Araji et al., 2007).

Some microbial polysaccharides may be used as flocculating agents, to support solid–liquid separation in aqueous systems. In sedimentation processes, flocculants provide a significant increase in settlement rate and improvement in supernatant clarification (Singh et al., 2007).

Flocculants are frequently used in water treatment, food and fermentation industries, drinking water purification and downstream processes (Xiong et al., 2010). In general, flocculating agents are divided in three groups, namely: (i) inorganic flocculants, such as aluminum sulphate and polyaluminum chloride; (ii) organic synthetic flocculants, such as polyacrylamide derivatives and polyethylene amine; and (iii) naturally occurring flocculants, such as chitosan, sodium alginate, and microbial flocculants. Inorganic and organic synthetic flocculants are commonly used due to their strong flocculating activity and low cost. However, there is evidence that synthetic flocculating substances may cause health and environmental problems. Such as the case of the acrylamide monomer which is harmful to humans (e.g. neurotoxic and carcinogenic) and the environment (e.g. non-degradable in nature) (Xiong et al., 2010; Notembiso et al., 2011; Yang et al., 2012).

On the other hand, natural polysaccharide flocculants have advantages such as safety, strong effect, biodegradability and harmlessness to humans and the environment, which make them potentially suitable for the replacement of inorganic and organic synthetic flocculants. Hence, the search for new biodegradable bioflocculants, with strong flocculating activity, is attracting wide research interest (Xiong et al., 2010; Notembiso et al., 2011; Yang et al., 2012).

In this chapter, a preliminary study of FucoPol's emulsion forming and stabilizing capacity was assessed under several polymer concentrations and oil/water ratios. Besides, the polymer's flocculating activity was also evaluated. Results for both properties were compared to other commercially available polymers, namely, Fucogel, xanthan, guar gum, alginate, pectin and carboxymethylcellulose (CMC).

6.3. Material and Methods

6.3.1. Emulsion forming and stabilizing capacity

The standard assay for testing the emulsifying activity was based on the method described by Cooper and Goldenberg (1987). Briefly, a FucoPol aqueous solution (0.5 wt%) was mixed with different hydrophobic compounds (3:2 v/v ratio) and stirred in the vortex, and the emulsification index (E_{24} , %) was determined after 24 h, using the following equation:

$$E_{24} = \frac{h_e}{h_t} \times 100 \quad \text{Eq.6.1}$$

where h_e (mm) is the height of the emulsion layer and h_t (mm) is the overall height of the mixture. All tests were performed in duplicate. The tested hydrophobic compounds included hydrocarbons (hexane, Riedel de Haen; hexadecane, Sigma; toluene, Sigma; diethylether, Riedel de Haen; benzene, Riedel de Haen) and oils (corn oil, sunflower oil, rice bran oil and cedar wood oil, purchased at the local supermarket; and silicone oil, Wacker).

The same test procedure was also carried out for commercial polysaccharides: Fucogel (Solabia), xanthan gum (Fluka), citrus pectin (Riedel de Haen), guar gum (Fluka), sodium alginate (Sigma), carboxymethylcellulose (Aqualon, France) and Triton X100 (Riedel de Haen), with the same concentration in deionized water.

Further studies were performed in order to evaluate the effect of polymer concentration (0.50, 1.00, 1.50 wt.%) and oil/water (O/W) ratios (20/80, 40/60, 60/40 and 80/20). The oil used was sunflower oil. The emulsions were prepared by stirring at 13 500 rpm in an Ultra Turrax homogenizer for 5 minutes and stored at 4°C for 24h. The emulsification index (E_{24}) was evaluated and the steady shear and the viscoelastic

properties of the emulsions were measured using a controlled stress rheometer (HAAKE RS75, Germany) equipped with a cone and plate geometry (diameter 35 mm, angle 2°) at a temperature of 25°C. Stress sweeps were performed at a constant frequency ($f=1\text{Hz}$) in order to ensure that the frequency sweeps were performed within the linear viscoelastic region. A tension of 1 Pa was used in all frequency sweeps performed.

6.3.2. Flocculating activity

The flocculating activity was tested using kaolin clay (Fluka) as the suspended solid, following the procedure described by Kurane et al. (1986) and Gong et al. (2008). 2 mL of FucoPol solution (0.01 wt.%) and 2 mL CaCl_2 solution (1% w/v) were added to a kaolin suspension (5 g L^{-1} , pH 7.0). The mixture was stirred in a vortex (1 min) and left standing for 5 min. The absorbance of the upper layer was measured at 550 nm. A control was prepared using the same method but FucoPol was replaced by deionized water. The flocculating activity was calculated according to the following equation:

$$\text{Flocculating activity (\%)} = (A - B)/A \times 100 \quad \text{Eq. 6.2}$$

where A and B are the optical densities of the control and the sample, respectively.

The same test procedure was carried out using aqueous solutions of several commercial polysaccharides, namely, Fucogel (Solabia), xanthan gum (Fluka), citrus pectin (Riedel de Haen), guar gum (Fluka), sodium alginate (Sigma) and carboxymethylcellulose (CMC) (Aqualon, France). An inorganic flocculant, $\text{Al}_2(\text{SO}_4)_3$ (Riedel de Haen), was also tested. All tests were performed in duplicate.

6.4. Results and discussion

6.4.1. Emulsion forming and stabilizing capacity

A preliminary assessment of FucoPol's potential to be used as an emulsion forming and stabilizing agent was performed with the polymer in aqueous solution (0.5 wt.%). Several hydrophobic compounds, namely, food grade oils, mineral oils and hydrocarbons, were assayed (Table 6.1). For comparison, the same test procedure was performed with Triton X-100, which is a synthetic emulsifier, and other commercial polysaccharides reported to be able to stabilize emulsions, namely, xanthan, pectin and alginate (Leroux et al., 2003; Lim et al., 2007).

A measure to evaluate the emulsion forming and stabilizing capacity of an emulsifier consists on evaluating its ability to retain at least 50% of the original emulsion volume 24h after its preparation (Willumsen and Karlson, 1997). Considering this criterion, FucoPol has proven to possess high emulsion forming and stabilizing capacity for the food-grade oils tested, namely, sunflower oil, corn oil and rice bran oil, with emulsification indexes of 60, 64 and 80%, respectively. The ability of this biopolymer to stabilize emulsions with vegetable oils suggests its potential application as cleaning or emulsifying agent in the food industry. Cedar wood oil, though having lower emulsification index (20%), formed stable emulsions that did not break within the test period. Little emulsion-stabilizing capacity, with emulsions breaking up after only a few minutes, was observed for silicone oil.

FucoPol demonstrated to have a lower emulsion forming and stabilizing capacity for the tested hydrocarbons (Table 6.1). In fact, under the conditions tested, no emulsion was formed with xylene, diethylether, benzene or toluene, while low emulsification indexes (<10%) were obtained for decane and chloroform. Although stable emulsions were formed with hexadecane and hexane, their emulsification indexes were rather low (22 and 30%, respectively) (Table 6.1).

As shown in Table 6.1, FucoPol has demonstrated to have higher emulsification indexes than xanthan, alginate and pectin for most of the compounds tested. Also, the capacity of FucoPol to form and stabilize emulsions is specific for certain hydrophobic compounds, which is also a characteristic of the other commercial polysaccharides tested (Freitas et al., 2009a).

Table 6.1 Emulsification index (E_{24}) for FucoPol and commercially available emulsion forming and stabilizing agents against several hydrophobic compounds. All emulsions were prepared by mixing a 0.5wt% aqueous solution with each of the hydrophobic compound (3:2 v/v ratio) and left at room temperature for 24 h to determine E_{24}

E_{24} (%)	FucoPol	Xanthan	Alginate	Pectin	Triton X-100
<i>Oils</i>					
Cedarwood oil	20	30	10	40	80
Sunflower oil	60	40	56	20	80
Corn oil	64	90	40	60	82
Rice bran oil	80	50	50	60	90
<i>Hydrocarbons</i>					
Hexadecane	22	40	10	20	80
Hexane	30	40	10	30	70

Effect of different FucoPol concentrations and O/W ratios

Following the preliminary results showing the emulsion-forming capacity of FucoPol, further experiments were performed to test its performance in different oil/water (O/W) ratios, as well as in different polymer concentrations. These studies were performed with sunflower oil, which was one of the food-grade oils for which FucoPol had high emulsification index. The O/W proportions used and the different concentrations of FucoPol solution are presented in Table 6.2.

The emulsification index (E_{24}) obtained with a 0.5 wt.% FucoPol aqueous solution by blending the two phases (O/W ratio equal to 60/40, equivalent to a ratio of 3:2 v/v) with a high shear mixer (Ultra Turrax homogenizer) was quite similar to that obtained previously for the emulsions prepared by stirring at lower shear with the vortex ($E_{24} \sim 60\%$). For that

polymer concentration and O/W ratio, the shear applied did not influence the emulsion height after 24h.

When FucoPol concentrations of 1.0 wt.% and 1.5 wt.% were used, no phase separation was observed after 24h ($E_{24} = 100\%$) for all O/W ratios tested, except in the case of O/W=80/20, for which quite low E_{24} values were observed (14% and 23%, respectively). A different behaviour was observed when a polymer concentration of 0.5 wt.% was applied. In this case, even though a complete oil in water stabilization was never achieved, a higher E_{24} (71%) was determined for an O/W ratio of 80/20. This fact must be further investigated, by studying the effect of other factors besides polymer concentration (e.g. solution pH, ionic strength, as well as polymer composition and structure) on the emulsion forming and stabilization.

Table 6.2 Emulsification index (E_{24}) for FucoPol against sunflower oil and apparent viscosity at a shear rate 1 s^{-1} for FucoPol solutions and emulsions with different O/W proportions

FucoPol (wt.%)	O/W (v/v %)	E_{24} (%)	η FucoPol solution (Pa s)	η Emulsions (Pa s)
0.50	20/80	71	0.28	0.53
	40/60	57		1.89
	60/40	64		0.59
	80/20	71		0.06
1.00	20/80	100	0.68	1.37
	40/60	100		3.37
	60/40	100		3.80
	80/20	14		0.51
1.50	20/80	100	3.39	6.54
	40/60	100		15.70
	60/40	100		20.01
	80/20	23		2.53

Steady shear tests

The rheological properties of the emulsions formed were studied after maturation at 4 °C for 24h. The respective steady shear flow curves are presented in Figure 6.1. Most of the emulsions have shown a strong shear thinning behaviour, except the one prepared with 0.5 wt.% FucoPol solution and an O/W ratio of 80/20, which demonstrated a Newtonian behaviour. The shear thinning is attributed to the disentanglement of the polysaccharide chains in the aqueous phase, along with the deformation of the oil droplets into ellipsoidal shapes and with the breaking of agglomerates into their elements that start to form layers coincident with the shear plane (Brumer 2006, Tadros, 2011). The Newtonian behaviour of the 80/20 emulsion prepared with a 0.5 wt.% FucoPol solution may be caused by the lower concentration of FucoPol in the emulsion, which may have resulted in the formation of a thinner and much less concentrated polymer layer surrounding the oil droplets, imparting a lower resistance to flow, that was independent on the shear applied.

For the polymer concentrations of 1.5 wt.% and 1.0 wt.%, the O/W ratio of 60/40 was the one exhibiting a higher apparent viscosity at low shear rates, followed by the 40/60, 20/80 and 80/20 ratios (Table 6.2, Figure 6.1). However, when a 0.5 wt.% concentration was used there was a change in the behaviour and the O/W proportion of 40/60 was the one rendering an emulsion with a higher apparent viscosity. This fact is probably a consequence of the influence of the amount of FucoPol available to form and stabilize an emulsion, regarding to its overall oil content. As the oil content increases, a higher amount of polymer is needed in the aqueous phase to maintain the overall consistency of the droplets dispersion produced.

In general, the emulsions presented a higher apparent viscosity than the original FucoPol aqueous solutions. The exceptions were the emulsions formed with an O/W ratio of 80/20, for which a decrease of the apparent viscosity was observed. This fact may be attributed to a high oil droplets concentration in the emulsion, imparting a lower resistance to shear than the original polymer solution.

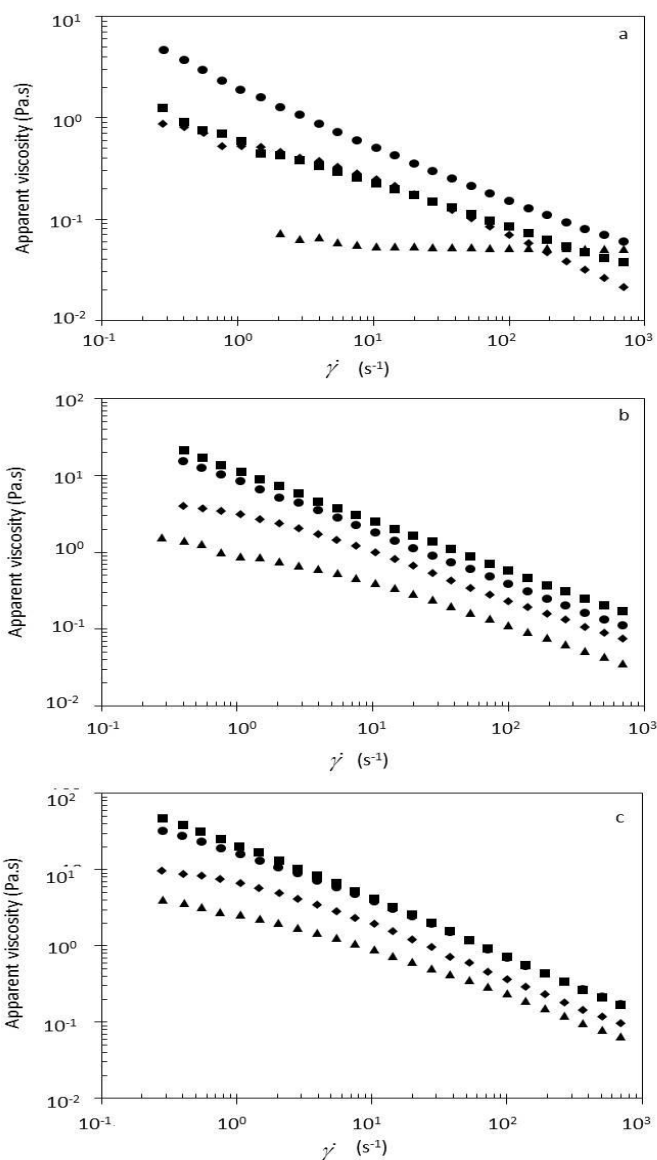


Figure 6.1 Flow curves of emulsions prepared with different polymer concentrations ((a) 0.50 wt.%; (b) 1.00 wt.% and (c) 1.50 wt.%) and different oil-water proportions: 20/80 (diamonds); 40/60 (bullets); 60/40 (squares); 80/20 (triangles).

For a fixed O/W proportion, the increase of FucoPol concentration in the aqueous phase led to an increase of the apparent viscosity of the resulting emulsions. This fact is attributed essentially to the increase of the polymer chain entanglements within the aqueous film surrounding the oil droplets, imparting a higher resistance to flow under steady shear. The same trend was observed by Calero et al., 2013 for emulsions formulated

with sunflower oil as disperse phase, potato protein as emulsifier and chitosan as stabilizer. The apparent viscosity of the emulsions after one day of maturation increased with the increase of the chitosan concentration used.

Oscillatory tests

Figure 6.2 shows the mechanical spectra of the O/W emulsions with different FucoPol concentrations. The variation of the dynamic moduli with the frequency was quite dependent on the O/W ratio for all FucoPol contents studied. This dependence was evaluated by the power law regression $G'(G'') = \alpha f^\beta$ (Valdez et al., 2006) and the exponent values β obtained are presented in Table 6.3.

Table 6.3 β values of the power law regression for the different emulsions

	0.5 wt.% FucoPol		1.0 wt.% FucoPol		1.5wt.% FucoPol	
	$\beta(G')$	$\beta(G'')$	$\beta(G')$	$\beta(G'')$	$\beta(G')$	$\beta(G'')$
20/80	2.05	0.91	0.90	0.55	0.50	0.29
40/60	0.77	0.51	0.48	0.46	0.40	0.27
60/40	1.72	0.87	0.74	0.47	0.33	0.15
80/20	1.75	1.13	1.40	0.76	0.83	0.51

For the emulsions with 1.5 wt.% FucoPol (Figure 6.2 a), the O/W ratio of 60/40 was the one that presented the highest dynamic moduli values and the lowest variation with frequency, $\beta(G') = 0.33$ and $\beta(G'') = 0.15$, with $G' > G''$ over the entire frequency range. This behaviour indicates that this emulsion was the most structured, which is in agreement with the steady shear data that has shown a higher apparent viscosity (Figure 6.1 a). In opposition, the O/W ratio of 80/20 formed an emulsion with the lowest dynamic moduli which have shown a higher variation with the frequency, $\beta(G') = 0.83$ and $\beta(G'') = 0.51$. In addition, G'' was higher than G' within most of the frequency range, with a crossover at high frequencies. The results show that the emulsions behaviour changes from that

generally attributed to a viscous solution with entangled polymer chains to that of a weak gel, when moving from O/W proportions of 60/40, to 40/60, 20/80 and 80/20.

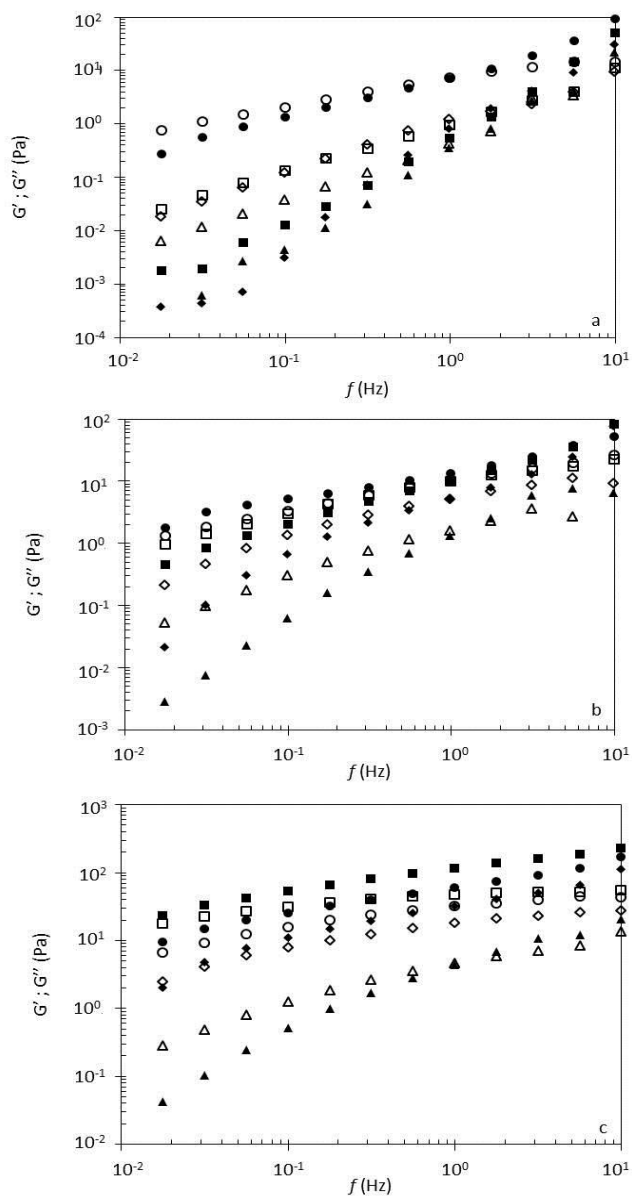


Figure 6.2 Mechanical spectra showing the frequency dependence of G' (full symbols) and G'' (open symbols). (a) 0.50 wt.% (b) 1.00 wt.% (c) 1.50 wt.%. O/W ratios: 20/80 (diamonds); 40/60 (bullets); 60/40 (squares); 80/20 (triangles).

As FucoPol's concentration used decreased to 1.0 wt.% and 0.5 wt.% (Figures 6.2 b and c), lower dynamic moduli were observed, along with a larger variation with the frequency, as can be confirmed by the increase of the respective β values. Furthermore, the O/W ratio that produced an emulsion with a stronger internal structure changed from 60/40 to 40/60. This fact was more evident for a 0.5% FucoPol concentration, which is in agreement with the higher apparent viscosity presented in Figure 6.1.

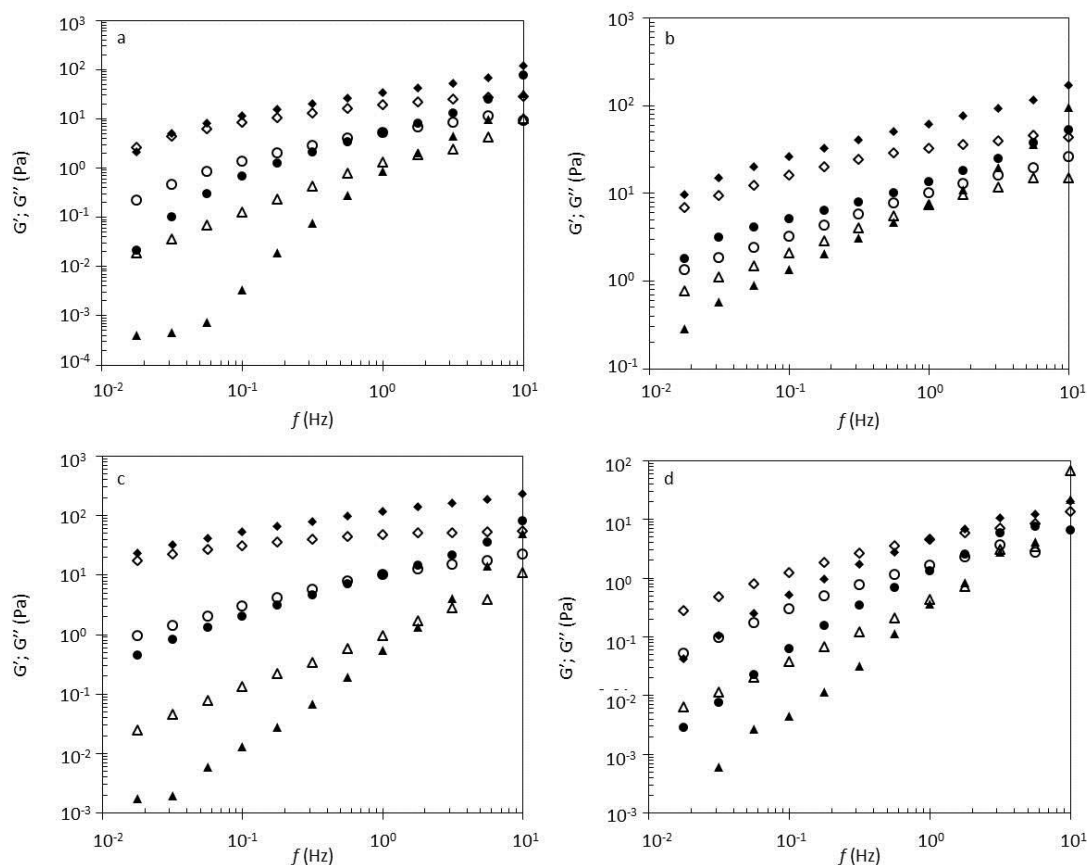


Figure 6.3 Mechanical spectra showing the frequency dependence of G' (full symbols) and G'' (open symbols). (a) 20/80 (b) 40/60 (c) 60/40 (d) 80/20. FucoPol wt.%: 0.5 (triangles); 1.0 (bullets); 1.5 (diamonds.).

Figure 6.3 shows the mechanical spectra for the emulsions studied arranged according to the O/W ratio. It can be observed more clearly the effect of FucoPol concentration on the dynamic moduli of the emulsions. For all O/W proportions tested, the increase of polymer concentration led to the increase of both G' and G'' and, simultaneously, to a decrease of their dependency with the frequency. This fact may be

attributed to a more effective stabilization of the oil-water interface along with the increase of the viscosity of the continuous phase.

6.4.2. Flocculating activity

A preliminary test of the flocculating activity of FucoPol was performed using a kaolin suspension and compared with commercial flocculants, namely, $\text{Al}_2(\text{SO}_4)_3$, alginate, xanthan, guar gum, chitosan and CMC (Figure 6.4). These preliminary tests were performed at room temperature and neutral pH, for flocculants concentration of 0.01wt%. As expected, $\text{Al}_2(\text{SO}_4)_3$ had the highest flocculating activity (30%), while CMC and xanthan had flocculating activities of 27 and 24%, respectively. Nevertheless, for the tested conditions, the EPS had similar flocculating activity (28%), which is a very promising result. Alginate, guar gum and chitosan had much lower flocculating activities (11, 8 and 6%, respectively) than the EPS (Figure 6.4).

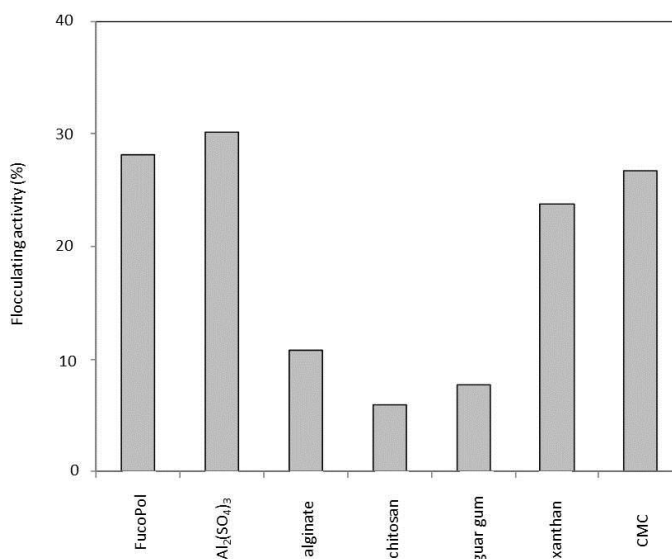


Figure 6.4 Flocculating activity of FucoPol in comparison with commercially available flocculants.

These results indicate that the polymer has high flocculating activity under the conditions tested, which envisages its potential use for colloid and cell aggregation in several applications, such as water treatment and food and mining industries. Inorganic (e.g. $\text{Al}_2(\text{SO}_4)_3$) and synthetic organic flocculating agents (e.g. polyacrylamide) are inexpensive products, but have a low biodegradability and are not shear resistant (Singh et al., 2007). On the other hand, some of them are dangerous for human health, namely polyacrylamides, whose monomers are neurotoxic, and poly(aluminum chloride) that induces Alzheimer disease. To overcome these environmental and public health problems, naturally occurring flocculants, including several polysaccharides have been suggested as safe alternatives (Freitas et al., 2009b; Lim et al., 2007; Yokoi et al., 2002). FucoPol produced by *Enterobacter* A47 may be included amongst these bioflocculants.

6.5. Conclusions

FucoPol has shown a good emulsion forming and stabilizing capacity for several hydrophobic compounds, including oils and hydrocarbons, similar to some commercial polysaccharides. FucoPol has shown to possess high emulsion forming and stabilizing capacity for the food grade oils tested ($E_{24} > 60\%$), namely sunflower oil, corn oil and rice oil. However, for the tested hydrocarbons (hexadecane and hexane) the polymer demonstrated a lower emulsion forming and stabilizing capacity ($< 30\%$).

Regarding the emulsions produced with sunflower oil, and for FucoPol aqueous solutions in concentrations above 1.0 wt.%, no phase separation after 24h was observed for most of the O/W ratios tested. Moreover, the emulsions presented a strong shear thinning behaviour, being the O/W ratio of 60/40 the one exhibiting a higher apparent viscosity at low shear rates.

Furthermore, the variation of the dynamic moduli with the frequency was quite dependent on the O/W ratio for all FucoPol concentrations studied. The polymer solution with 1.5 wt.% polymer concentration and the O/W ratio of 60/40 resulted in the most structured emulsion, which is in agreement with the steady shear data that has shown a higher apparent viscosity. Decreasing polymer concentration to 0.5 wt.% led to a change in the O/W ratio that produced an emulsion with a stronger internal structure from 60/40 to 40/60. For all O/W proportions tested, the increase of polymer concentration led to the increase of both G' and G'' and, simultaneously, to a decrease of their dependency with the frequency.

Under the conditions tested (i.e. room temperature, neutral pH and flocculant concentration of 0.01 wt.%), FucoPol showed a good flocculating activity (28%), similar to aluminium sulphate and xanthan.

FucoPol's emulsion forming and stabilizing capacity, and flocculating capacity, make it a promising alternative to commercial polysaccharides.

Chapter 7

General Conclusions and Future Work

7.1. General Conclusions

In this thesis the production and characterisation of a novel bacterial exopolysaccharide (FucoPol) using glycerol byproduct from the biodiesel industry was studied. FucoPol's producing bacterium was identified as *Enterobacter* A47 by biochemical and physiological identification and by 16S rRNA gene sequence determination.

FucoPol's standard bioprocess included an initial batch phase wherein *Enterobacter* A47 grew exponentially, followed by a fed-batch phase in which EPS synthesis was more pronounced. In a typical cultivation, *Enterobacter* A47 was able to produce 7.50 – 7.97 gEPS L⁻¹, within 3 – 4 days of cultivation, corresponding to volumetric productivities of 2.04 and 2.51 g L⁻¹ d⁻¹. FucoPol was composed of fucose (32 – 36 %mol), galactose (25 – 26 %mol), glucose (28 – 38 %mol), glucuronic acid (9 – 10 %mol) and acyl groups substituents (succinyl, pyruyl and acetyl) and presented a high molecular weight (4.19 – 5.0×10⁶).

Furthermore, *Enterobacter* A47 was able to grow and synthesize EPS under a wide range of temperatures and pH. However, FucoPol production and the macromolecular characteristics were considerably affected. The synthesis of high fucose content EPS was stable for wide temperature (25-35 °C) and pH (6.0 – 8.0) ranges, which make the bioprocess robust. The EPS with the highest fucose content (36 – 37 %mol) presented Mw around 4.0×10⁶.

The impact of using different glycerol and nitrogen concentrations were also evaluated. Once more, *Enterobacter* A47 was able to grow and produce EPS for all the initial glycerol and nitrogen concentrations. FucoPol production has shown to be stable within an initial glycerol and nitrogen concentrations of ~25 – 50 and 0.68 – 1.05 g L⁻¹, respectively, while for nitrogen concentrations above 1.05 g L⁻¹ the EPS production was severely impaired. Increasing glycerol concentration in the feeding solution from 200 to 400 g L⁻¹ and using 9 g L⁻¹ nitrogen resulted in the highest EPS synthesis (10.18 g L⁻¹), volumetric productivity (5.52 g L⁻¹ d⁻¹) and fucose content (41 %mol) of this study.

Regarding FucoPol's aqueous solutions properties, it presented an intrinsic viscosity of $\sim 8.00 \text{ dL g}^{-1}$ that was stable under a wide range of pH and ionic strength values (3.5 – 8.0 and 0.05 – 0.50 M NaCl, respectively). The polymer was able to produce viscous solutions with a shear-thinning behaviour, which were also stable under wide ranges of pH, ionic strength and temperatures. The mechanical spectra and the application of the Cox- Merz rule suggested the presence of entangled macromolecules in a viscous solution. Moreover, FucoPol maintained its rheological properties at 25°C under consecutive temperature fluctuations, even after heated up to 80°C.

FucoPol showed a good emulsion forming and stabilizing capacity ($E_{24} > 60 \%$) for several hydrophobic compounds, especially for food grade oils, similar to some commercial polysaccharides. Furthermore, under the conditions tested, FucoPol presented a high flocculating activity (28%), similar to xanthan and CMC and superior to other natural polysaccharides (e.g. alginate).

The main focus of this work was the rich-fucose polysaccharides due to their high market demand. However, the ability shown by the bacterium to synthesize EPS with different composition, as a result of the modification of cultivation conditions, is also remarkable. In view of this, such capability confers the bioprocess a great versatility, enabling to achieve different polymers, which can be used in different applications. Beyond the interesting physical characteristics observed, FucoPol's chemical composition may confer additional bioactive activity, since fucose-containing polysaccharides have been reported to have pharmacological and cosmetic properties. Taking into account the versatile properties presented, combined to the prospective lower production costs from using a low-cost carbon source, FucoPol has an enormous potential to be used on several industrial applications, namely in cosmetics, pharmaceuticals, detergents and paints, as well as in processes that require thermal stability (e.g. food processing and oil drilling fluids).

7.2. Future Work

The results obtained in this work may be improved and extended in diverse ways.

Firstly, FucoPol production can be further optimized in terms of medium composition, namely, micronutrients, such as phosphate, sulphate and magnesium. Moreover, operational parameters, such as dissolved oxygen concentration, aeration and stirring rate, can also affect cell growth and polymer synthesis by *Enterobacter* A47 and, hence, their effect should be studied. Other bioreactor operation modes (e.g. repeated fed-batch, continuous) may also be tested, as well as other feeding strategies (e.g. pulses).

The bioprocess can also be optimized in terms of the downstream procedure to yield high purity polymers in high yields, while taking into consideration possible industrial applications.

It is also important to study the *Enterobacter* A47 metabolic pathway in order to better understand the EPS synthesis process.

The potential development of FucoPol systems for high-value cosmetic, food and pharmaceutical applications is closely related to its performance in structures, such as hydrogels, emulsions, films and particles (micro/nanoparticles), as well as its ability to form viscous solutions. FucoPol emulsion forming and stabilizing capacity should be evaluated under diverse ionic strength and pH values. It may also be studied for other potential properties, such as gelling capacity and the polymer's ability to form films and particles (micro/nanoparticles), regarding the encapsulation and release of selected key substances (e.g. antioxidants, drugs, antimicrobials).

Taking into account some possible industrial applications (e.g. cosmetic, food, pharmaceutical) the safety of this biopolymer should be assessed by cytotoxic assays. The biological activity may also be evaluated, as well as the antioxidant properties, anti-inflammatory effect and antimicrobial activity.

Bibliography

Al-Araji, L., Rahman, R.N.Z.R.A., Basri, M., Salleh, A.B., 2007. Microbial surfactant. *Asia Pacific Journal of Molecular Biology and Biotechnology* 15, 99–105.

Al-Asheh, S., Abu-Jdayil, B., Abunasser, N., Barakat, A., 2002. Rheological characteristics of microbial suspensions of *Pseudomonas aeruginosa* and *Bacillus cereus*. *International Journal of Biological Macromolecules* 30, 67–74.

Albuquerque, M.G.E., Torres, C.A., Reis, M.A.M., 2010. Polyhydroxyalkanoate (PHA) production by a mixed microbial culture using sugar molasses: effect of the influent substrate concentration on culture selection. *Water Research* 44, 3419–3433.

Alvarez-Manceñido, F., Landin, M., Lacik, I., Martínez-Pacheco, R., 2008. Konjac glucomannan and konjac glucomannan/xanthan gum mixtures as excipients for controlled drug delivery systems. Diffusion of small drugs. *International Journal of Pharmaceutics* 349, 11–18.

Alves, V.D., Freitas, F., Costa, N., Carvalheira, M., Oliveira, R., Gonçalves, M.P., Reis, M.A.M., 2010. Effect of temperature on the dynamic and steady-shear rheology of a new microbial extracellular polysaccharide produced from glycerol byproduct. *Carbohydrate Polymers* 79, 981–988.

Appendini, P., Hotchkiss, J.H., 2002. Review of antimicrobial food packaging. *Innovative Food Science & Emerging Technologies* 3, 113–126.

Arvidson, S.A., Rinehart, B.T., Gadala-Maria, F., 2006. Concentration regimes of solutions of levan polysaccharide from *Bacillus* sp. *Carbohydrate Polymers* 65, 144–149.

Ashby, R.D., Solaiman, D.K.Y., Foglia, T.A., 2005. Synthesis of short-/medium-chain-length poly (hydroxyalkanoate) blends by mixed culture fermentation of glycerol. *Biomacromolecules* 6, 2106–2112.

Ashtaputre, A.A., Shah, A.K., 1995. Emulsifying property of a viscous exopolysaccharide from *Sphingomonas paucimobilis*. *World Journal of Microbiology and Biotechnology* 11, 219–222.

Badino Jr., A.C., Facciotti, M.C.R., Schmidell, W., 1999. Estimation of the rheology of glucoamylase fermentation broth from the biomass concentration and shear conditions. *Biotechnology Techniques* 13, 723–726.

Bae, I.Y., Oh, I.-K., Lee, S., Yoo, S.H., Lee, H.G., 2008. Rheological characterization of levan polysaccharides from *Microbacterium laevaniformans*. *International Journal of Biological Macromolecules* 42, 10–3.

Bajaj, I.B., Saudagar, P.S., Singhal, R.S., Pandey, A., 2006. Statistical approach to optimization of fermentative production of gellan gum from *Sphingomonas paucimobilis* ATCC 31461. *Journal of Bioscience and Bioengineering* 102, 150–6.

Bajaj, I.B., Survase, S.A., Saudagar, P.S., Singhal, R.S., 2007. Gellan gum: fermentative production, downstream processing and applications. *Food Technology and Biotechnology* 45, 341–354.

Bandaiphet, C., Prasertsan, P., 2006. Effect of aeration and agitation rates and scale-up on oxygen transfer coefficient, k_La in exopolysaccharide production from *Enterobacter cloacae* WD7. *Carbohydrate Polymers* 66, 216–228.

Banik, R.M., Santhiagu, A., 2006. Improvement in production and quality of gellan gum by *Sphingomonas paucimobilis* under high dissolved oxygen tension levels. *Biotechnology Letters* 28, 1347–50.

Banik, R.M., Santhiagu, A., Upadhyay, S.N., 2007. Optimization of nutrients for gellan gum production by *Sphingomonas paucimobilis* ATCC-31461 in molasses based medium using response surface methodology. *Bioresource Technology* 98, 792–7.

Ben Salah, R., Chaari, K., Besbes, S., Ktari, N., Blecker, C., Deroanne, C., Attia, H., 2010. Optimisation of xanthan gum production by palm date (*Phoenix dactylifera* L.) juice by-products using response surface methodology. *Food Chemistry* 121, 627–633.

Bohm, N., Kulicke, W.M., 1999. Rheological studies of barley (1–3)(1–4)-b-glucan in concentrated solution: investigation of the viscoelastic flow behaviour in the sol-state. *Carbohydrate Research* 315, 293–301.

Bonet, R., Simon-Pujol, M.D., Congregado, F., 1993. Effects of nutrients on exopolysaccharide production and surface properties of *Aeromonas salmonicida*. *Applied and Environmental Microbiology* 59, 2437–2441.

Brandl, H., Gross, R.A., Lenz, R.W., Fuller, R.C., 1988. *Pseudomonas oleovorans* as a source of poly(beta-hydroxyalkanoates) for potential applications as biodegradable polyesters. *Applied and Environmental Microbiology* 54, 1977–1982.

Brenner, D.J., McWhorter, A.C., Kai, A., Steigerwalt, A.G., Farmer III, J.J., 1986. *Enterobacter asburiae* sp. nov., a new species found in clinical specimens, and reassignment of *Erwinia dissolvens* and *Erwinia nimipressuralis* to the genus *Enterobacter* as *Enterobacter dissolvens* comb. nov. and *Enterobacter nimipressuralis* comb. nov. *Journal of Clinical Microbiology* 23, 1114–1120.

Brummer, R., 2006. *Rheology essentials of cosmetic and food emulsions*. Springer, Berlin, Germany.

Bueno, S.M., Garcia-Cruz, C.H., 2001. The influence of fermentation time and the presence of salts in the rheology of the fermentation broth of a polysaccharide-producing bacteria free of soil. *Journal of Food Engineering* 50, 41–46.

Burchard, W., 2001. Structure formation by polysaccharides in concentrated solution. *Biomacromolecules* 2, 342–353.

Básaca-Loya, A., Burboa, M.G., Valdez, M.A., Gámez, R., Goycoolea, F.M., Gutiérrez-Millán, L.E., 2008. Aggregation behavior and rheology of culture broths of *Rhodospirillum rubrum*. *Revista Mexicana de Física* 54, 119–126.

Calero, N., Muñoz, J., Cox, P.W., Heuer, A., Guerrero, A., 2013. Influence of chitosan concentration on the stability, microstructure and rheological properties of O/W emulsions

formulated with high-oleic sunflower oil and potato protein. *Food Hydrocolloids* 30, 152–162.

Calvo, C., Ferrer, M.R., Martínez-Checa, F., Bejar, V., Quesada, E., 1995. Some Rheological Properties of the Extracellular Polysaccharide Produced by *Volcaniella eurihalina* F2-7. *Applied Biochemistry and Biotechnology* 55, 45–54.

Candia, J.-L.F., Deckwer, W.-D., 1999. Effect of the nitrogen source on pyruvate content and rheological properties of xanthan. *Biotechnology Progress* 15, 446–452.

Canilha, L., Silva, D.D.V., Carvalho, W., Mancilha, I.M., 2005. Aditivos alimentares produzidos por via fermentativa. Parte 3: polissacarídeos e enzimas. *Revista Analytica* 20, 332–341.

Carreau, P.J., 1972. Rheological equations from molecular network theories. *Transactions of the Society of Rheology* 16, 99–127.

Casas, J.A., Santos, V.E., García-Ochoa, F., 2000. Xanthan gum production under several operational conditions: molecular structure and rheological properties. *Enzyme and Microbial Technology* 26, 282–291.

Cescutti, P., Kallioinen, A., Impallomeni, G., Toffanin, R., Pollesello, P., Leisola, M., Eerikäinen, T., 2005. Structure of the exopolysaccharide produced by *Enterobacter amnigenus*. *Carbohydrate Research* 340, 439–47.

Chaturvedi, P., Warren, C.D., Altaye, M., Morrow, A.L., Ruiz-Palacios, G., Pickering, L.K., Newburg, D.S., 2001. Fucosylated human milk oligosaccharides vary between individuals and over the course of lactation. *Glycobiology* 11, 365–72.

Chawla, P.R., Bajaj, I.B., Survase, S.A., Singhal, R.S., 2009. Microbial cellulose: fermentative production and applications. *Food Technology and Biotechnology* 47, 107–124.

Chenlo, F., Moreira, R., Silva, C., 2011. Steady-shear flow of semidilute guar gum solutions with sucrose, glucose and sodium chloride at different temperatures. *Journal of Food Engineering* 107, 234–240.

- Chung, Y.R., Brenner, D.J., Steigerwalt, A.G., Kim, B.S., Kim, H.T., Cho, K.Y., 1993. *Enterobacter pyrinus* sp. nov., an organism associated with brown leaf spot disease of pear trees. *International Journal of Systematic Bacteriology* 43, 157–161.
- Cooper, D.G., Goldenberg, B.G., 1987. Surface-active agents from two *Bacillus* species. *Applied and Environmental Microbiology* 53, 224–229.
- Coppa, G.V., Zampini, L., Galeazzi, T., Gabrielli, O., 2006. Prebiotics in human milk: a review. *Digestive and Liver Disease* 38, S291–S294.
- Cross, M.M., 1965. Rheology of non-Newtonian fluids: a new flow equation for pseudoplastic systems. *Journal of Colloid Science* 20, 417–437.
- Cuvelier, G., Launay, B., 1986. Concentration regimes in xanthan gum solutions deduced from flow and viscoelastic properties. *Carbohydrate Polymers* 6, 321–333.
- Dharmadi, Y., Murarka, A., Gonzales, R., 2006. Anaerobic fermentation of glycerol by *Escherichia coli*: a new platform for metabolic engineering. *Biotechnology and Bioengineering* 94, 821–829.
- Dias, J.M.L., Serafim, L.S., Lemos, P.C., Reis, M.A.M., Oliveira, R., 2005. Mathematical modelling of a mixed culture cultivation process for the production of polyhydroxybutyrate. *Biotechnology and Bioengineering* 92, 209–22.
- Dickinson, E., 2003. Hydrocolloids at interfaces and the influence on the properties of dispersed systems. *Food Hydrocolloids* 17, 25–39.
- Doi, M., Edwards, S., 1986. *The theory of polymer dynamics*. Clarendon Press, Oxford.
- Donot, F., Fontana, A., Baccou, J.C., Schorr-Galindo, S., 2012. Microbial exopolysaccharides: main examples of synthesis, excretion, genetics and extraction. *Carbohydrate Polymers* 87, 951–962.
- Elnashar, M., 2011. *Biotechnology of Biopolymers*. InTech, Rijeka.

Falcão, D.Q., Costa, E.R., Alviano, D.S., Alviano, C.S., Kuster, R.M., Menezes, F.S., 2006. Atividade antioxidante e antimicrobiana de *Calceolaria chelidonioides* Humb. Bonpl. & Kunth. *Brazilian Journal of Pharmacognosy* 16, 73–76.

Fariña, J.I., Santos, V.E., Perotti, N.I., Casas, J.A., Molina, O.E., García-Ochoa, F., 1999. Influence of the nitrogen source on the production and rheological properties of scleroglucan produced by *Sclerotium rolfsii* ATCC 201126. *World Journal of Microbiology and Biotechnology* 15, 309–316.

Ferry, J.D., 1980. *Viscoelastic properties of polymers*. John Wiley & Sons, Ltd, New York.

Fialho, A.M., Martins, L.O., Donval, M.-L., Leitao, J.H., Ridout, M.J., Jay, A.J., Morris, V.J., Sá-Correia, I., 1999. Structures and properties of gellan polymers produced by *Sphingomonas paucimobilis* ATCC 31461 from lactose compared with those produced from glucose and from cheese whey. *Applied and Environmental Microbiology* 65, 2485–91.

Freitas, F., Alves, V.D., Carvalheira, M., Costa, N., Oliveira, R., Reis, M.A.M., 2009. Emulsifying behaviour and rheological properties of the extracellular polysaccharide produced by *Pseudomonas oleovorans* grown on glycerol byproduct. *Carbohydrate Polymers* 78, 549–556.

Freitas, F., Alves, V.D., Pais, J., Costa, N., Oliveira, C., Mafra, L., Hilliou, L., Oliveira, R., Reis, M.A.M., 2009. Characterization of an extracellular polysaccharide produced by a *Pseudomonas* strain grown on glycerol. *Bioresource Technology* 100, 859–65.

Freitas, F., Alves, V.D., Reis, M.A.M., 2011. Advances in bacterial exopolysaccharides: from production to biotechnological applications. *Trends in Biotechnology* 29, 388–98.

Furuse, H., Amari, T., Miyawaki, O., Asakura, T., Toda, K., 2002. Characteristic behavior of viscosity and viscoelasticity of *Aureobasidium pullulans* culture fluid. *Journal of Bioscience and Bioengineering* 93, 411–415.

Furuta, H., Maeda, H., 1999. Rheological properties of water-soluble soybean polysaccharides extracted under weak acidic condition. *Food Hydrocolloids* 13, 267–274.

- García-Ochoa, F., Santos, V.E., Casas, J.A., Gómez, E., 2000. Xanthan gum: production, recovery, and properties. *Biotechnology Advances* 18, 549–79.
- Gennes, P.G. de, 1979. *Scaling concepts in polymer physics*. Cornell University Press, New York.
- Goh, K.K.T., Matia-Merino, L., Hall, C.E., Moughan, P.J., Singh, H., 2007. Complex rheological properties of a water-soluble extract from the fronds of the black tree fern, *Cyathea medullaris*. *Biomacromolecules* 8, 3414–21.
- Gong, W.-X., Wang, S.-G., Sun, X.-F., Liu, X.-W., Yue, Q.-Y., Gao, B.-Y., 2008. Bioflocculant production by culture of *Serratia ficaria* and its application in wastewater treatment. *Bioresource Technology* 99, 4668–4674.
- Gorret, N., Renard, C.M.G.C., Famelart, M.H., Maubois, J.L., Doublier, J.L., 2003. Rheological characterization of the EPS produced by *P. acidi-propionici* on milk microfiltrate. *Carbohydrate Polymers* 51, 149–158.
- Graessley, W.W., 1974. The entanglement concept in polymer rheology. *Advances in Polymer Science* 16, 1–179.
- Grant, W.D., Sutherland, I.W., Wilkinson, J.F., 1969. Exopolysaccharide colanic acid and its occurrence in the *Enterobacteriaceae*. *Journal of Bacteriology* 100, 1187–93.
- Guetta, O., Mazeau, K., Auzely, R., Milas, M., Rinaudo, M., 2003. Structure and properties of a bacterial polysaccharide named Fucogel. *Biomacromolecules* 4, 1362–71.
- Hahn, M.W., Lünsdorf, H., Janke, L., 2004. Exopolymer production and microcolony formation by planktonic freshwater bacteria: defence against protistan grazing. *Aquatic Microbial Ecology* 35, 297–308.
- Harris, L.S., Oriel, P.J., 1989. Heteropolysaccharide produced by *Enterobacter sakazakii*.
- Hilliou, L., Freitas, F., Oliveira, R., Reis, M.A.M., Lespineux, D., Grandfils, C., Alves, V.D., 2009. Solution properties of an exopolysaccharide from a *Pseudomonas* strain obtained using glycerol as sole carbon source. *Carbohydrate Polymers* 78, 526–532.

Hoffmann, H., Stindl, S., Ludwig, W., Stumpf, A., Mehlen, A., Monget, D., Pierard, D., Ziesing, S., Heesemann, J., Roggenkamp, A., Schleifer, K.H., 2005. *Enterobacter hormaechei* subsp. *oharae* subsp. nov., *E. hormaechei* subsp. *hormaechei* comb. nov., and *E. hormaechei* subsp. *steigerwaltii* subsp. nov., three new subspecies of clinical importance. *Journal of Clinical Microbiology* 43, 3297–3303.

lagher, F., Reicher, F., Ganter, J.L.M.S., 2002. Structural and rheological properties of polysaccharides from mango (*Mangifera indica* L.) pulp. *International Journal of Biological Macromolecules* 31, 9–17.

Imeson, A., 2010. Food stabilisers, thickeners and gelling agents. Blackwell Publishing Ltd, Oxford.

Janda, J.M., Abbott, S.L., 2007. 16S rRNA gene sequencing for bacterial identification in the diagnostic laboratory: pluses, perils, and pitfalls. *Journal of Clinical Microbiology* 45, 2761–4.

Jang, J.-H., Bae, S.-K., Lim, D.J., Kim, B.-J., Kong, J.-Y., 2002. Rheological properties of polysaccharides produced by a *Zoogloea* sp. *Biotechnology Letters* 24, 297–301.

Jiang, L., 2010. Optimization of fermentation conditions for pullulan production by *Aureobasidium pullulan* using response surface methodology. *Carbohydrate Polymers* 79, 414–417.

Jukes, T.H., Cantor, C.R., 1969. Evolution of protein molecules. Academic Press, New York.

Kalogiannis, S., Iakovidou, G., Liakopoulou-Kyriakides, M., Kyriakidis, D.A., Skaracis, G.N., 2003. Optimization of xanthan gum production by *Xanthomonas campestris* grown in molasses. *Process Biochemistry* 39, 249–256.

Kanari, B., Banik, R.R., Upadhyay, S.N., 2002. Effect of environmental factors and carbohydrate on gellan gum production. *Applied Biochemistry and Biotechnology* 102-103, 129–40.

Kaplan, D.L., 1998. Biopolymers from renewable resources. Springer-Verlag, Heidelberg.

Karinen, R.S., Krause, A.O.I., 2006. New biocomponents from glycerol. *Applied Catalysis A:General* 306, 128–133.

- Krishnan, S., Raj, C.J., Robert, R., Ramanand, A., Das, S.J., 2007. Growth and characterization of succinic acid single crystals. *Crystal Research and Technology* 42, 1087–1090.
- Kumar, A.S., Mody, K., Jha, B., 2007. Bacterial exopolysaccharides--a perception. *Journal of Basic Microbiology* 47, 103–17.
- Kurane, R., Takeda, K., Suzuki, T., 1986. Screening for and characteristics of microbial flocculants. *Agricultural and Biological Chemistry* 50, 2301–2307.
- Kämpfer, P., Ruppel, S., Remus, R., 2005. *Enterobacter radicincitans* sp. nov., a plant growth promoting species of the family *Enterobacteriaceae*. *Systematic and Applied Microbiology* 28, 213–221.
- Lai, L.S., Yang, D.H., 2007. Rheological properties of the hot-water extracted polysaccharides in Ling-Zhi (*Ganoderma lucidum*). *Food Hydrocolloids* 21, 739–746.
- Landon, R.S., Law, R.C.S., Webb, C., 1993. Fermentation broth rheology during dextran production by *Leuconostoc mesenteroides* BS12 (F) as a possible tool for control. *Applied Microbiology and Biotechnology* 40, 251–257.
- Lapasin, R., Priel, S., 1995. Rheology of industrial polysaccharides: theory and applications. Blackie Academic and Professional, Glasgow.
- Lapasin, R., Priel, S., Graziosi, M., Molteni, G., 1988. Rheological properties of polysaccharide solutions and derived printing pastes in continuous and oscillatory flow conditions. *Industrial & Engineering Chemistry Research* 27, 1802–1806.
- Launay, B., Cuvelier, G., Martinez-Reyes, S., 1997. Viscosity of locust bean, guar and xanthan gum solutions in the Newtonian domain: a critical examination of the $\log(\eta_{sp})_o - \log c[\eta]_o$ master curves. *Carbohydrate Polymers* 34, 385–395.
- Lawson, C.J., Sutherland, I.W., 1978. Economic microbiology, Primary Products of Metabolism. Academic Press, London.
- Lee, C.H., An, D.S., Lee, S.C., Park, H.J., Lee, D.S., 2004. A coating for use as an antimicrobial and antioxidative packaging material incorporating nisin and α -tocopherol. *Journal of Food Engineering* 62, 323–329.

Leroux, J., Langendorff, V., Schick, G., Vaishnav, V., Mazoyer, J., 2003. Emulsion stabilizing properties of pectin. *Food Hydrocolloids* 17, 455–462.

Lim, D.J., Kim, J.D., Kim, M.Y., Yoo, S.H., Kong, J.Y., 2007. Physicochemical properties of the exopolysaccharides produced by marine bacterium *Zoogloea* sp. KCCM10036. *Journal of Microbiology and Biotechnology* 17, 979–984.

Lim, J.S., Kim, J.H., Kim, C., Kim, S.W., 2002. Morphological and rheological properties of culture broth of *Cephalosporium acremonium* M25. *Korea-Australia Rheology Journal* 14, 11–16.

Lin, E.C.C., 1976. Glycerol dissimilation and its regulation in bacteria. *Annual Review of Microbiology* 30, 535–578.

Linton, J.D., 1991. Metabolite production and growth efficiency. *Antonie van Leeuwenhoek* 60, 293–311.

Liu, L., Du, G., Chen, J., Zhu, Y., Wang, M., Sun, J., 2009. Microbial production of low molecular weight hyaluronic acid by adding hydrogen peroxide and ascorbate in batch culture of *Streptococcus zooepidemicus*. *Bioresource Technology* 100, 362–367.

Liu, S.B., Qiao, L.P., He, H.L., Zhang, Q., Chen, X.L., Zhou, W.Z., Zhou, B.C., Zhang, Y.Z., 2011. Optimization of fermentation conditions and rheological properties of exopolysaccharide produced by deep-sea bacterium *Zunongwangia profunda* SM-A87. *PloS One* 6.

Lo, Y.-M., Yang, S.-T., Min, D.B., 1997. Effects of yeast extract and glucose on xanthan production and cell growth in batch culture of *Xanthomonas campestris*. *Applied Microbiology and Biotechnology* 47, 689–694.

Lue, A., Zhang, L., 2009. Rheological behaviors in the regimes from dilute to concentrated in cellulose solutions dissolved at low temperature. *Macromolecular Bioscience* 9, 488–96.

Lundstedt, T., Seifert, E., Abramo, L., Thelin, B., Nyström, Å., Pettersen, J., Bergman, R., 1998. Experimental design and optimization. *Chemometrics and Intelligent Laboratory Systems* 42, 3–40.

Maidak, B.L., Cole, J.R., Parker, C.T., Garrity, G.M., Larsen, N., Li, B., Lilburn, T.G., McCaughey, M.J., Olsen, G.J., Overbeek, R., Pramanik, S., Schmidt, T.M., Tiedje, J.M., Woese, C.R., 1999. A new version of the RDP (Ribosomal Database Project). *Nucleic Acids Research* 27, 171–3.

Majumder, A., Singh, A., Goyal, A., 2009. Application of response surface methodology for glucan production from *Leuconostoc dextranicum* and its structural characterization. *Carbohydrate Polymers* 75, 150–156.

Masmoudi, M., Besbes, S., Chaabouni, M., Robert, C., Paquot, M., Blecker, C., Attia, H., 2008. Optimization of pectin extraction from lemon by-product with acidified date juice using response surface methodology. *Carbohydrate Polymers* 74, 185–192.

Milas, M., Rinaudo, M., Knipper, M., Schuppiser, J.L., 1990. Flow and viscoelastic properties of xanthan gum solutions. *Macromolecules* 23, 2506–2511.

Mitchell, J.R., Ledward, D.A., 1985. *Functional properties of food macromolecules*. Elsevier Applied Sciences Publishers, Ltd, Essex.

Moosavi-Nasab, M., Pashangeh, S., Rafsanjani, M., 2010. Effect of fermentation time on xanthan gum production from sugar beet molasses. *World Academy of Science, Engineering and Technology* 44, 1244–1247.

Moreno, J., Vargas, M.A., Olivares, H., Rivas, J., Guerrero, M.G., 1998. Exopolysaccharide production by the cyanobacterium *Anabaena* sp. ATCC 33047 in batch and continuous culture. *Journal of Biotechnology* 60, 175–182.

Morris, E.R., 1990. Shear-thinning of “random coil” polysaccharides: Characterisation by two parameters from a simple linear plot. *Carbohydrate Polymers* 13, 85–96.

Morris, E.R., Cutler, A.N., Ross-Murphy, S.B., Rees, D., Price, J., 1981. Concentration and shear rate dependence of viscosity in random coil polysaccharide solutions. *Carbohydrate Polymers* 1, 5–21.

Moshaf, S., Hamidi-Esfahani, Z., Azizi, M.H., 2011. Optimization of conditions for xanthan gum production from waste date in submerged fermentation. *World Academy of Science, Engineering and Technology* 81, 521–524.

Müller, J.M., Monte Alegre, R., 2006. Alginate production by *Pseudomonas mendocina* in a stirred draft fermenter. *World Journal of Microbiology and Biotechnology* 23, 691–695.

Narayan, M.S., Manoj, G.P., Vatcharavelu, K., Bhagyalakshmi, N., Mahadevaswamy, M., 2005. Utilization of glycerol as carbon source on the growth, pigment and lipid production in *Spirulina platensis*. *International Journal of Food Sciences & Nutrition* 56, 521–528.

Nickerson, M.T., Paulson, A.T., Speers, R.A., 2004. Time–temperature studies of gellan polysaccharide gelation in the presence of low, intermediate and high levels of co-solutes. *Food Hydrocolloids* 18, 783–794.

Nontembiso, P., Sekelwa, C., Leonard, M.V., Anthony, O.I., 2011. Assessment of biofloculant production by *Bacillus* sp. *Gilbert*, a marine bacterium isolated from the bottom sediment of Algoa Bay. *Marine Drugs* 9, 1232–1242.

Oba, T., Higashimura, M., Iwasaki, T., Matser, A.M., Steeneken, P.A.M., Robijn, G.W., Sikkema, J., 1999. Viscoelastic properties of aqueous solutions of the phosphopolysaccharide “villian” from *Lactococcus lactis* subsp. *cremoris* SBT 0495. *Carbohydrate Polymers* 39, 275–281.

O’Hara, C.M., Steigerwalt, A.G., Hill, B.C., Farmer III, J.J., Fanning, G.R., Brenner, D.J., 1989. *Enterobacter hormaechei*, a new species of the family *Enterobacteriaceae* formerly known as enteric group 75. *Journal of Clinical Microbiology* 27, 2046–9.

Pamboukian, C.R.D., Facciotti, M.C.R., 2005. Rheological and morphological characterization of *Streptomyces olindensis* growing in batch and fed-batch fermentations. *Brazilian Journal of Chemical Engineering* 22, 31–40.

Papanikolaou, S., Aggelis, G., 2002. Lipid production by *Yarrowia lipolytica* growing on industrial glycerol in a single-stage continuous culture. *Bioresource Technology* 82, 43–49.

- Paul, F.M.B., Perry, D.F., Monsan, P.F., 1999. Strain of *Klebsiella pneumoniae*, subsp. *pneumoniae*, and a process for the production of a polysaccharide containing L-fucose.
- Pawlicki-Jullian, N., Courtois, B., Pillon, M., Lesur, D., Le Flèche-Mateos, A., Laberche, J.-C., Goncharova, N., Courtois, J., 2010. Exopolysaccharide production by nitrogen-fixing bacteria within nodules of Medicago plants exposed to chronic radiation in the Chernobyl exclusion zone. *Research in Microbiology* 161, 101–108.
- Pelletier, E., Viebke, C., Meadows, J., Williams, P.A., 2001. Solution rheology of kappa-carrageenan in the ordered and disordered conformations. *Biomacromolecules* 2, 946–51.
- Peña, C., Trujillo-Roldán, M.A., Galindo, E., 2000. Influence of dissolved oxygen tension and agitation speed on alginate production and its molecular weight in cultures of *Azotobacter vinelandii*. *Enzyme and microbial technology* 27, 390–398.
- Philbe, J.L., 2002. Nouveau microorganisme de la famille des *Enterobacteriaceae*.
- Phillips, G.O., Williams, P.A., 2009. Handbook of hydrocolloids. Woodhead Publishing Ltd, Cambridge.
- Prasertsan, P., Dermlim, W., Doelle, H., Kennedy, J.F., 2006. Screening, characterization and flocculating property of carbohydrate polymer from newly isolated *Enterobacter cloacae* WD7. *Carbohydrate Polymers* 66, 289–297.
- Prasertsan, P., Wichienchot, S., Doelle, H., Kennedy, J., 2008. Optimization for biopolymer production by *Enterobacter cloacae* WD7. *Carbohydrate Polymers* 71, 468–475.
- Pruesse, E., Quast, C., Knittel, K., Fuchs, B.M., Ludwig, W., Peplies, J., Glöckner, F.O., 2007. SILVA: a comprehensive online resource for quality checked and aligned ribosomal RNA sequence data compatible with ARB. *Nucleic Acids Research* 35, 7188–96.
- Péterszegi, G., Fodil-Bourahla, I., Robert, A.M., Robert, L., 2003. Pharmacological properties of fucose. Applications in age-related modifications of connective tissues. *Biomedicine & Pharmacotherapy* 57, 240–245.

Qader, S.A.U., Iqbal, L., Aman, A., Shireen, E., Azhar, A., 2005. Production of dextran by newly isolated strains of *Leuconostoc mesenteroides* PCSIR-4 and PCSIR-9. Turkish Journal of Biochemistry 31, 21–26.

Rainey, F.A., Ward-Rainey, N., Kroppenstedt, R.M., Stackbrandt, E., 1996. The genus *Nocardiopsis* represents a phylogenetically coherent taxon and a distinct actinomycete lineage: Proposal of *Nocardiopsaceae* fam. nov. International Journal of Systematic Bacteriology 46, 1088–1092.

Rao, M.A., 1999. Rheology of fluids and semisolid foods: Principles and applications. Aspen Publishers, Inc., Gaithersburg.

Ratnam, B.V.V., Rao, M.N., Rao, M.D., Rao, S.S., Ayyanna, C., 2003. Optimization of fermentation conditions for the production of ethanol from sago starch using response surface methodology. World Journal of Microbiology and Biotechnology 19, 523–526.

Rehm, B.H.A., 2010. Bacterial polymers: biosynthesis, modifications and applications. Nature Reviews Microbiology 8, 578–592.

Reis, M.A.M., Oliveira, R., Freitas, F., Alves, V.D., 2011. Fucose-containing bacterial biopolymer, WO 2011/073874 A2.

Reis, M.A.M., Oliveira, R., Oliveira, C., Freitas, F., Alves, V.D., Pais, J., 2008. Galactose-rich polysaccharide, process for the production of the polymer and applications, WO 2008/127134 A1.

Ren, Y., Ellis, P.R., Ross-Murphy, S.B., Wang, Q., Wood, P.J., 2003. Dilute and semi-dilute solution properties of (1→3), (1→4)-β-D-glucan, the endosperm cell wall polysaccharide of oats (*Avena sativa* L.). Carbohydrate Polymers 53, 401–408.

Ren, Y., Ellis, P.R., Sutherland, I.W., Ross-Murphy, S.B., 2003. Dilute and semi-dilute solution properties of an exopolysaccharide from *Escherichia coli* strain S61. Carbohydrate Polymers 52, 189–195.

Reyes, C., 2003. Reproducing shake flasks performance in stirred fermentors: production of alginates by *Azotobacter vinelandii*. Journal of Biotechnology 105, 189–198.

- Rinaudo, M., 2004. Role of substituents on the properties of some polysaccharides. *Biomacromolecules* 5, 1155–65.
- Rinaudo, M., 2008. Main properties and current applications of some polysaccharides as biomaterials. *Polymer International* 57, 397–430.
- Robijn, G.W., Wienk, H.L.J., van den Berg, D.J., Haas, H., Kamerling, J.P., Vliegthart, J.F.G., 1996. Structural studies of the exopolysaccharide produced by *Lactobacillus paracasei* 34-1. *Carbohydrate Research* 285, 129–139.
- Roca, C., Chagas, B., Farinha, I., Freitas, F., Mafra, L., Aguiar, F., Oliveira, R., Reis, M.A.M., 2012. Production of yeast chitin-glucan complex from biodiesel industry byproduct. *Process Biochemistry*, In Press.
- Rocheffort, W.E., Middleman, S., 1987. Rheology of xanthan gum: salt, temperature, and strain effects in oscillatory and steady shear experiments. *Journal of Rheology* 31, 337–369.
- Rodríguez-Monroy, M., Galindo, E., 1999. Broth rheology, growth and metabolite production of *Beta vulgaris* suspension culture: a comparative study between cultures grown in shake flasks and in a stirred tank. *Enzyme and Microbial Technology* 24, 687–693.
- Romeo, J., Nova, E., Wärnberg, J., Gómez-Martínez, S., Ligia, L.E.D., Marcos, A., 2010. Immunomodulatory effect of fibres , probiotics and synbiotics in different life-stages. *Nutrición Hospitalaria* 25, 341–349.
- Rosalam, S., England, R., 2006. Review of xanthan gum production from unmodified starches by *Xanthomonas compestris* sp. *Enzyme and Microbial Technology* 39, 197–207.
- Rottava, I., Batesini, G., Silva, M.F., Lerin, L., de Oliveira, D., Padilha, F.F., Toniazzo, G., Mossi, A., Cansian, R.L., Di Luccio, M., Treichel, H., 2009. Xanthan gum production and rheological behavior using different strains of *Xanthomonas* sp. *Carbohydrate Polymers* 77, 65–71.
- Rättö, M., Verhoef, R., Suihko, M.-L., Blanco, A., Schols, H.A., Voragen, A.G.J., Wilting, R., Siika-Aho, M., Buchert, J., 2006. Colanic acid is an exopolysaccharide common to many

enterobacteria isolated from paper-machine slimes. *Journal of Industrial Microbiology & Biotechnology* 33, 359–67.

Saitou, N., Nei, M., 1987. The neighbor-joining method: a new method for reconstructing phylogenetic trees. *Molecular Biology and Evolution* 4, 406–25.

Sandford, P.A., Cottrell, I.W., Pettitt, D.J., 1984. Microbial polysaccharides: new products and their commercial applications. *Pure and Applied Chemistry* 56, 879–892.

Silva, M.F., Fornari, R.C.G., Mazutti, M.A., de Oliveira, D., Padilha, F.F., Cichoski, A.J., Cansian, R.L., Di Luccio, M., Treichel, H., 2009. Production and characterization of xanthan gum by *Xanthomonas campestris* using cheese whey as sole carbon source. *Journal of Food Engineering* 90, 119–123.

Simsek, S., Mert, B., Campanella, O.H., Reuhs, B., 2009. Chemical and rheological properties of bacterial succinoglycan with distinct structural characteristics. *Carbohydrate Polymers* 76, 320–324.

Singh, R.P., Tripathy, T., Karmakar, G.P., Rath, S.K., Karmakar, N.C., Pandey, S.R., Kannan, K., Jain, S.K., Lan, N.T., 2000. Novel biodegradable flocculants based on polysaccharides. *Current Science* 78, 7–12.

Sittikijyothin, W., Torres, D., Gonçalves, M.P., 2005. Modelling the rheological behaviour of galactomannan aqueous solutions. *Carbohydrate Polymers* 59, 339–350.

Sousa, A.M.M., Alves, V.D., Morais, S., Delerue-Matos, C., Gonçalves, M.P., 2010. Agar extraction from integrated multitrophic aquacultured *Gracilaria vermiculophylla*: evaluation of a microwave-assisted process using response surface methodology. *Bioresource technology* 101, 3258–67.

Staudt, A.K., Wolfe, L.G., Shrout, J.D., 2011. Variations in exopolysaccharide production by *Rhizobium tropici*. *Archives of Microbiology* 194, 197–206.

Sun, S., Song, Y., Zheng, Q., 2008. pH-induced rheological changes for semi-dilute solutions of wheat gliadins. *Food Hydrocolloids* 22, 1090–1096.

- Sutherland, I.W., 1982. Biosynthesis of microbial exopolysaccharides. *Advances in Microbial Physiology* 23, 79–150.
- Sutherland, I.W., 1990. *Biotechnology of microbial exopolysaccharides*, Cambridge Studies in Biotechnology. Cambridge University Press, Cambridge, New York.
- Sutherland, I.W., 1998. Novel and established applications of microbial polysaccharides. *Trends in Biotechnology* 16, 41–46.
- Sutherland, I.W., 2001. Microbial polysaccharides from Gram-negative bacteria. *International Dairy Journal* 11, 663–674.
- Sutherland, I.W., 2002. A sticky business. Microbial polysaccharides: current products and future trends. *Microbiology Today* 29, 70-71.
- Synytsya, A., Copiková, J., Matejka, P., Machovic, V., 2003. Fourier transform Raman and infrared spectroscopy of pectins. *Carbohydrate Polymers* 54, 97–106.
- Sánchez, M.J., Jiménez-Aparicio, A., López, G.G., Tapia, G.T., Rodríguez-Monroy, M., 2002. Broth rheology of *Beta vulgaris* cultures growing in an air lift bioreactor. *Biochemical Engineering Journal* 12, 37–41.
- Tadros, T., 2011. Interparticle interactions in concentrated suspensions and their bulk (Rheological) properties. *Advances in Colloid and Interface Science* 168, 263–277.
- Tait, M.I., Sutherland, I.W., Clarke-Sturman, A.J., 1986. Effect of growth conditions on the production, composition and viscosity of *Xanthomonas campestris* exopolysaccharide. *Journal of General Microbiology* 132, 1483–1492.
- Temudo, M.F., Poldermans, R., Kleerebezem, R., van Loosdrecht, M.C., 2008. Glycerol fermentation by (open) mixed cultures: a chemostat study. *Biotechnology and Bioengineering* 100, 1088–1098.
- Thompson, J.C., He, B.B., 2006. Characterization of crude glycerol from biodiesel production from multiple feedstocks. *Applied Engineering in Agriculture* 22, 261–265.

Togrul, H., Arslan, N., 2003. Flow properties of sugar beet pulp cellulose and intrinsic viscosity–molecular weight relationship. *Carbohydrate Polymers* 54, 63–71.

Toledo, F.L., Gonzalez-Lopez, J., Calvo, C., 2008. Production of bioemulsifier by *Bacillus subtilis*, *Alcaligenes faecalis* and *Enterobacter* species in liquid culture. *Bioresource Technology* 99, 8470–5.

Tosh, S.M., Wood, P.J., Wang, Q., Weisz, J., 2004. Structural characteristics and rheological properties of partially hydrolyzed oat β -glucan: the effects of molecular weight and hydrolysis method. *Carbohydrate Polymers* 55, 425–436.

Tuinier, R., Zoon, P., Stuart, M.A.C., Fler, G.J., Kruij, C.G. de, 1999. Concentration and shear-rate dependence of the viscosity of an exocellular polysaccharide. *Biopolymers* 50, 641–646.

Valdez, M.A., Acedo-Carrillo, J.I., Rosas-Durazo, A., Lizardi, J., Rinaudo, M., Goycoolea, F.M., 2006. Small-deformation rheology of mesquite gum stabilized oil in water emulsions. *Carbohydrate Polymers* 64, 205–211.

Vanhooren, P.T., Vandamme, E.J., 1999. L-Fucose: occurrence, physiological role, chemical, enzymatic and microbial synthesis. *Journal of Chemical Technology and Biotechnology* 74, 479–497.

Vermeiren, L., Devlieghere, F., van Beest, M., de Kruij, N., Debevere, J., 1999. Developments in the active packaging of foods. *Trends in Food Science & Technology* 10, 77–86.

Vianna-Filho, R.P., Petkowicz, C.L.O., Silveira, J.L.M., 2012. Rheological characterization of O/W emulsions incorporated with neutral and charged polysaccharides. *Carbohydrate Polymers*, In Press.

Walter, R.H., 1998. Polysaccharide dispersions: chemistry and technology in food. Academic Press, New York.

Williams, A.G., Wimpenny, J.W.T., 1978. Exopolysaccharide production by *Pseudomonas* NCIB11264 grown in continuous culture. *Journal of General Microbiology* 104, 47–57.

- Williams, P.A., 2007. Handbook of industrial water soluble polymers, North. Wiley Online Library, Oxford.
- Willumsen, P.A., Karlson, U., 1997. Screening of bacteria, isolated from PAH-contaminated soils, for production of biosurfactants and bioemulsifiers. *Biodegradation* 7, 415–423.
- Wyatt, N.B., Liberatore, M.W., 2009. Rheology and viscosity scaling of the polyelectrolyte xanthan gum. *Journal of Applied Polymer Science* 114, 4076–4084.
- Xiong, Y., Wang, Y., Yu, Y., Li, Q., Wang, H., Chen, R., He, N., 2010. Production and characterization of a novel bioflocculant from *Bacillus licheniformis*. *Applied and Environmental Microbiology* 76, 2778–2782.
- Xu, C., Willför, S., Holmlund, P., Holmbom, B., 2009. Rheological properties of water-soluble spruce O-acetyl galactoglucomannans. *Carbohydrate Polymers* 75, 498–504.
- Xu, X., Liu, W., Zhang, L., 2006. Rheological behavior of *Aeromonas* gum in aqueous solutions. *Food Hydrocolloids* 20, 723–729.
- Yang, Q., Luo, K., Liao, D., Li, X., Wang, D., Liu, X., Zeng, G., Li, X., 2012. A novel bioflocculant produced by *Klebsiella* sp. and its application to sludge dewatering. *Water and Environment Journal*.
- Yang, Y.L., 2002. Novel microorganism isolated from chinese elm (*ulmus* sp.) and process for preparing exopolysaccharides by employing the microorganism, US 2002/0115158 A1.
- Yang, Z., Huttunen, E., Staaf, M., Widmalm, K., Tenhu, H., 1999. Separation, purification and characterisation of extracellular polysaccharides produced by slime-forming *Lactococcus lactis* ssp. *cremoris* strains. *International Dairy Journal* 9, 631–638.
- Yim, J.H., Kim, S.J., Aan, S.H., Lee, H.K., 2004. Physicochemical and rheological properties of a novel emulsifier, EPS-R, produced by marine bacterium *Hahella vhejuensis*. *Biotechnology and Bioprocess Engineering* 9, 405–413.
- Yokoi, H., Aratake, T., Hirose, J., Hayashi, S., Takasaki, Y., 2001. Simultaneous production of hydrogen and bioflocculant by *Enterobacter* sp. BY-29. *World Journal of Microbiology and Biotechnology* 17, 609–613.

Yokoi, H., Obita, T., Hirose, J., Hayashi, S., Takasaki, Y., 2002. Flocculation properties of pectin in various suspensions. *Bioresource Technology* 84, 287–290.

Zhang, Z., Chen, H., 2010. Fermentation performance and structure characteristics of xanthan produced by *Xanthomonas campestris* with a glucose/xylose mixture. *Applied Biochemistry and Biotechnology* 160, 1653–63.

van den Bulk, R.W., Zevenhuizen, L.P.T.M., Cordewener, J.H.G., Dons, J.J.M., 1991. Characterization of the extracellular polysaccharide produced by *Clavibacter michiganensis* subsp. *michiganensis*. *The American Phytopathological Society* 81, 619–623.

Çelik, E., Ozbay, N., Oktar, N., Çalik, P., 2008. Use of biodiesel byproduct crude glycerol as the carbon source for fermentation processes by recombinant *Pichia pastoris*. *Industrial & Engineering Chemistry Research* 47, 2985–2990.